

**DOT/FAA/TC-16/9**

Federal Aviation Administration  
William J. Hughes Technical Center  
Aviation Research Division  
Atlantic City International Airport  
New Jersey 08405

# **Preliminary Comparison of Agricultural and Single-Engine Air Tanker Operational Loads**

December 2016

Final Report

This document is available to the U.S. public through the National Technical Information Services (NTIS), Springfield, Virginia 22161.

This document is also available from the Federal Aviation Administration William J. Hughes Technical Center at [actlibrary.tc.faa.gov](http://actlibrary.tc.faa.gov).



U.S. Department of Transportation  
**Federal Aviation Administration**

## **NOTICE**

This document is disseminated under the sponsorship of the U.S. Department of Transportation in the interest of information exchange. The U.S. Government assumes no liability for the contents or use thereof. The U.S. Government does not endorse products or manufacturers. Trade or manufacturers' names appear herein solely because they are considered essential to the objective of this report. The findings and conclusions in this report are those of the author(s) and do not necessarily represent the views of the funding agency. This document does not constitute FAA policy. Consult the FAA sponsoring organization listed on the Technical Documentation page as to its use.

This report is available at the Federal Aviation Administration William J. Hughes Technical Center's Full-Text Technical Reports page: [actlibrary.tc.faa.gov](http://actlibrary.tc.faa.gov) in Adobe Acrobat portable document format (PDF).

1. Report No. DOT/FAA/TC-16/9		2. Government Accession No.		3. Recipient's Catalog No.	
4. Title and Subtitle PRELIMINARY COMPARISON OF AGRICULTURAL AND SINGLE-ENGINE AIR TANKER OPERATIONAL LOADS				5. Report Date December 2016	
				6. Performing Organization Code	
7. Author(s) Kamran Rokhsaz and Linda K. Kliment				8. Performing Organization Report No.	
9. Performing Organization Name and Address Wichita State University 1845 Fairmount Street Wichita, KS 67260-0044				10. Work Unit No. (TRAIS)	
				11. Contract or Grant No. 09-G-014	
12. Sponsoring Agency Name and Address U.S. Department of Transportation Federal Aviation Administration Air Traffic Organization NextGen & Operations Planning Office of Research and Technology Development Washington, DC 20591				13. Type of Report and Period Covered Final Report	
				14. Sponsoring Agency Code ANM-210L	
15. Supplementary Notes The Federal Aviation Administration Airport and Aircraft Safety R&D Division Technical Monitor was Dr. Sohrob Mottaghi.					
16. Abstract This investigation was carried out as part of the FAA's Operational Loads Monitoring program. Wichita State University undertook the task of comparing operational flight loads of aircraft flown for agricultural applications with those flown as single-engine air tankers (SEAT). The primary goal of this investigation was to assess the dependence of the load factors exerted on these airframes on the type of operation through comparison of the two. The objectives of this program were to evaluate typical operational in-service data and compare the results between the two types of operations. The scope of this investigation included: 1) identifying operators willing to implement the data acquisition system on their aircraft, 2) installing digital flight data recorders on the airframes, 3) post-processing the acquired data and examining it for data integrity, 4) developing ground-air-ground information and presenting it statistically, and 5) developing exceedance spectra for each aircraft. The statistical data formats used in this report allow thorough examination of various parameters related to the life cycle of these aircraft.  For this research, data were collected from two Air Tractor AT-802A aircraft, two PZL M18 airframes, and one Ayres Thrush S2R-T45. Basic flight parameters—such as airspeed, altitude, flight duration, and bank and pitch angles—are shown in statistical format. SEAT flights are divided into five airborne phases consisting of cruise out, entry into the drop zone, drop, exit from the drop zone, and return to base. Agricultural flights are divided into four airborne phases: cruise out, chemical release, turns in between successive releases, and return to base. Gust and maneuver loads are determined for various phases and presented graphically as cumulative occurrences. The vertical load spectra revealed distinct differences between the two types of operations. SEAT aircraft experienced relatively large load factors during the drop phases once or twice a mission, whereas spray aircraft were subjected to less severe load factors but many more times per mission. This research also revealed that the load factor alone may not be the proper indicator of the stresses exerted on the airframe. In these operations, because up to half of the takeoff weight can be released during a mission, the instantaneous weight of the aircraft has to be taken into account as well.  This preliminary report pertains to the analysis of the data collected from one season and is, therefore, very limited in range. A total of 454.5 hours of SEAT operation were compared with 104 hours of agricultural spraying. The intent of this program is to continue collecting data for several seasons and present the results in a more comprehensive final report in the future. It is speculated that additional data will reduce some of the scatter present in the current results.					
17. Key Words Flight profiles, Flight loads spectrum, Statistical loads data, Agricultural Aircraft, Single-Engine Air Tanker			18. Distribution Statement This document is available to the U.S. public through the National Technical Information Service (NTIS), Springfield, Virginia 22161. This document is also available from the Federal Aviation Administration William J. Hughes Technical Center at <a href="http://actlibrary.tc.faa.gov">actlibrary.tc.faa.gov</a> .		
19. Security Classif. (of this report) Unclassified		20. Security Classif. (of this page) Unclassified		21. No. of Pages 102	22. Price

## ACKNOWLEDGEMENTS

The work reported in this document was performed by the Flight Loads Group within the Department of Aerospace Engineering of the College of Engineering at Wichita State University (WSU). This effort was funded by the FAA under grant number 09-G-014. The principal investigators at WSU were Dr. Kamran Rokhsaz and Dr. Linda K. Kliment. The format used for presentation of the statistical data was adopted from the work previously performed by the principal investigators and the University of Dayton Research Institute. The program manager for the FAA William J. Hughes Technical Center was Dr. Edward Weinstein. David Rathfelder, of the FAA's Los Angeles Aircraft Certification Office, provided technical guidance.

## TABLE OF CONTENTS

	Page
EXECUTIVE SUMMARY	ix
1. INTRODUCTION	1
2. AIRCRAFT AND DATA DESCRIPTION	2
2.1 AIRCRAFT DESCRIPTION	2
2.2 RECORDED FLIGHT DATA	2
2.3 STRAIN GAUGES	2
3. DATA REDUCTION	4
3.1 INITIAL PROCESSING	4
3.2 DERIVED PARAMETERS	4
3.2.1 Liftoff and Touchdown	4
3.2.2 Altitude and Rate of Climb	4
3.2.3 Air Density	5
3.2.4 True and Equivalent Airspeeds	5
3.2.5 Flight Distance	5
3.3 WEIGHT ESTIMATION	6
3.3.1 Fuel Consumption	6
3.3.2 SEAT and Spray Missions	6
3.3.3 Ferry Missions	7
3.4 LOADS AND GUST OCCURRENCES	8
3.4.1 Sign Convention	8
3.4.2 Load Counts	9
3.4.3 Bending Moment Counts	9
3.4.4 Separation of Maneuver and Gust Load Factors	9
3.4.5 Normalizing of Vertical Load Factor	9
3.4.6 Correlation of Vertical Load Factor and Bending Moment	11
3.4.7 Altitude Bands	11
3.5 FLIGHT PHASE SEPARATION	15
3.5.1 SEAT Missions	15
3.5.2 Agricultural Application Missions	16
4. USAGE DATA PRESENTATION	20

4.1	OVERALL USAGE	20
4.2	PHASE-SPECIFIC USAGE	21
4.2.1	Cruise 1, Cruise 2, and Ferry	21
4.2.2	Entry, Drop, Exit, and Turn	22
5.	LOADS DATA PRESENTATION	26
5.1	OVERALL LOADS	26
5.1.1	Gust and Maneuver Load Factors	26
5.1.2	Bending Moment	29
5.2	PHASE-SPECIFIC LOADS	29
5.2.1	Gust and Maneuver Load Factors	29
5.2.2	Bending Moment	30
6.	SUMMARY	31
7.	CONCLUSIONS AND RECOMMENDATIONS	33
8.	REFERENCES	34
	APPENDIX A—USAGE DATA	A-1
	APPENDIX B—LOADS DATA	B-1

## LIST OF FIGURES

Figure		Page
1	Variation of weight and airspeed for two consecutive spray missions–Aircraft 4	8
2	Sign convention for airplane accelerations	8
3	Peaks-between-means classification of loads	9
4	Maximum bending moment and coincident vertical load factor	12
5	Bending moment and coincident maximum vertical load factor	13
6	Correlation of bending moment and normalized vertical load factor–Aircraft 1	14
7	Flight phases of SEAT missions	15
8	Time history of altitude for two flights with one drop each–Aircraft 1	16
9	Normal probability of entry and exit phase durations	17
10	Typical altitude time history from a spray mission–Aircraft 4	18
11	Flight path of the spray mission of figure 7–Aircraft 4	19
12	Time history of vertical load factor during a SEAT drop–Aircraft 1	24
13	Time history of vertical load factor during a spray operation–Aircraft 4	25

## LIST OF TABLES

Table		Page
1	Aircraft descriptions	2
2	Data collected by Appareo Systems	3
3	Summary of the data used in this report	3
4	Flight phase separation criteria SEAT missions	17
5	Flight phase separation criteria agricultural applications	19
6	Statistical formats and usage data	20
7	Statistical formats and flight loads	27

## LIST OF ACRONYMS

AGL	Above ground level
DFDR	Digital flight data recorder
GPS	Global positioning system
KIAS	Knots indicated airspeed
MSL	Mean sea level
MTOW	Maximum takeoff weight
NED	National Elevation Dataset
OLM	Operational loads monitoring
SEAT	Single-engine air tanker
SFC	Specific fuel consumption
USFS	United States Forest Service
WSU	Wichita State University

## EXECUTIVE SUMMARY

Wichita State University (WSU) investigated flight loads from a fleet of single-engine air tankers (SEATs) for comparison with their agricultural use. The FAA funded this investigation as an element of its Operational Loads Monitoring program.

Under this program, digital flight data recorders were installed on four aircraft. The recorded data from these aircraft were sent to WSU for post-processing and further analysis. Data were also acquired and stored from a fifth aircraft by the United States Forest Service (USFS) and made available to WSU.

The four aircraft instrumented under the present program consisted of two Air Tractor AT-802As and two PZL M18s. One of the latter airframes was used exclusively for agricultural spraying. The fifth aircraft, instrumented by the USFS, was an Ayres Thrush S2R-T45. All five aircraft were powered by turboprops and their takeoff gross weights ranged from 10,000–16,000 pounds.

Basic flight parameters—such as airspeed, altitude, flight duration, and bank and pitch angles—were extracted and shown in statistical formats consistent with previous reports in this area. Flights were divided into various phases, and the results were obtained for each phase and the entire mission. Load factors were separated for each phase into gust and maneuver loads using the 2-second rule. Exceedance charts were constructed for each phase and for the entire flights. In addition, load factors were normalized based on estimated instantaneous aircraft weight and used to develop a second set of exceedance charts. All five aircraft had a strain gauge mounted somewhere on the main spar, although data from only three of the airframes were useful. Attempts were also made to correlate the strain gauge outputs with the recorded normal load factors.

The statistical formats used in this study are those developed previously by the principal investigators and by the University of Dayton Research Institute. The data presented in these formats allow easy comparison of the design criteria with actual usage data, thereby providing the aircraft operators with a better understanding of those factors that influence the structural integrity of these aircraft. These data could also be used by the original equipment manufacturers for better understanding of the actual airframe usage and loads. Finally, this information can be used to refine the regulations concerning the design of these aircraft.

This preliminary report pertains to the analysis of the data collected from one season and is, therefore, very limited in scope. A total of 454.5 hours of SEAT operations were compared with 104 hours of agricultural spraying. The intent of this program is to continue collecting data for several seasons and present the results in a more comprehensive final report in the future. It is speculated additional data will reduce some of the scatter present in the current results.

## 1. INTRODUCTION

The FAA has had an active Operational Loads Monitoring (OLM) program for a few decades. Under this program, aircraft flight loads and usage information are collected and analyzed for better understanding of the factors that impact airframe fatigue and aging. As part of this program, a number of aircraft have been investigated, a sample of which can be found in references 1–5.

Little comparable information is available on more recent models of aircraft used for agricultural spraying and flown as single-engine air tankers (SEATs). These aircraft vary in maximum takeoff weight (MTOW), from 2,500–20,000 pounds. Especially absent in the literature are comparisons of the operational loads experienced by these aircraft from the two types of missions. Some data on aircraft used for agricultural applications are presented by Locke et al. [6]. However, the aircraft studied in this report ranged in MTOW from 2,900–8,600 pounds. Conversely, an FAA report by Hall [7] shows flight load spectra of a lightweight SEAT with an MTOW of 26,300 pounds. The difference in the MTOW makes the comparison of the flight loads of the two mission types difficult at best.

Since 2009, Wichita State University (WSU) has been engaged in the process of analyzing the flight data recorded on aircraft designed for agricultural operations and used as SEAT. Under this program, four aircraft were fitted with digital flight data recorders (DFDR) to collect basic inertial and air data from operations in the field for comparison and better understanding of the factors affecting the lift cycle of these airframes. The collected data also included output from one strain gauge mounted on the upper side of the lower spar cap on each airframe. Using in-service recorded flight data, the authors intended to highlight the differences between the usage and flight loads of the two types of operation.

The scope of this program was limited to the following:

- The data collected would contain vertical, longitudinal, and lateral accelerations as well as sufficient information to allow accurate calculation of airspeeds.
- WSU would examine the data for integrity and completeness and store the files in separate groups according to their usefulness.
- Ground-air-ground aircraft usage information for the fleet would be extracted by WSU and analyzed statistically.
- Normal accelerations would be divided into gust loads and maneuver loads by WSU and presented in exceedance charts.
- Normal accelerations recorded by accelerometers would be correlated with strain gauge output, when possible, to better understand the level of the loads carried by the wing structure.

The authors aimed to present the results in formats that would allow an objective examination of these parameters—thereby affording the regulators, manufacturers, and operators better understanding and control of those factors that influence the structural integrity of these aircraft.

## 2. AIRCRAFT AND DATA DESCRIPTION

### 2.1 AIRCRAFT DESCRIPTION

Under this program, four airframes were instrumented, and data were acquired from them over one operational season. These data were added to an older set, collected on a different airframe, but with the same recording system. Of the five airframes, one was exclusively flown as an agricultural aircraft for spraying operations that could be used as a baseline for comparison. These aircraft are listed in table 1.

**Table 1. Aircraft descriptions**

No.	Aircraft	Engine	Power (hp)	MTOW (lb)	Empty Weight (lb)	Hopper/Tank (gallons)
1	AT-802A	PT6A-67AG	1,350	16,000	7,214	800
2	AT-802A	TPE 331-14	1,650	16,000	7,542	800
3	PZL M18	TPE 331U	1,000	11,700	5,918	500
4	PZL M18*	TPE 331U	1,000	11,700	5,862	500
5	S2R-T45	PT6A	800	10,000	4,800	510

\* Used exclusively for agricultural applications

Aircraft 1 and 2 had the same basic airframe, but the latter was modified with a 1650-hp Garrett engine for better short-field operations and shorter spool-up time. This modification also increased the empty weight by approximately 300 pounds, without affecting the MTOW.

### 2.2 RECORDED FLIGHT DATA

Since 2006, the United States Forest Service (USFS) has collected a large amount of data from various aircraft. By studying various recording systems, Appareo Systems' GAU 2000 DFDR [8] emerged as the preferred recording device. This system, although limited in the number of channels, combines the robustness and simplicity needed for field operations. To be on par with the USFS OLM program, the same recorder was used for the present study. The data shown in table 2 was recorded at 8 Hz. The total number of flights and associated durations and distances are summarized in table 3.

### 2.3 STRAIN GAUGES

Each aircraft was equipped with one strain gauge mounted somewhere on the wing and calibrated to allow estimating the wing bending moment at that location. On Aircraft 1 and 2, the strain gauge was located on the upper side of the front lower spar cap, 43" from the centerline. On Aircraft 3 and 4, they were located 121" from the centerline on the upper side of the lower spar cap. The strain gauge location for Aircraft 5 was not known. Aircraft 2 and 5 had faulty strain gauge signals that could not be used for estimating the wing bending moments.

**Table 2. Data collected by Appareo Systems**

Parameter	Units
Line number	–
Elapsed time	Seconds
GPS* latitude and longitude	Degrees
GPS elevation	Feet
Pitch	Degrees
Roll	Degrees
GPS speed	Knots
Vertical speed	Feet per minute
Heading	Degrees
Pitch, roll, and yaw rate	Degrees per second
Longitudinal, lateral, and normal acceleration	g
True airspeed**	Knots
Equivalent airspeed**	Knots
Indicated airspeed	Knots
Course direction	Degrees
Pitot pressure	Inches of Mercury
Static pressure	Inches of Mercury
Outside air temperature	Degrees Celsius
Horizontal and vertical accuracy	Millimeter
Bay door status (chemical/retardant release trigger signal)	Binary
Strain gauge output	Volts

\* Global positioning system

\*\* Data obtained through post-processing

**Table 3. Summary of the data used in this report**

Aircraft	Number of Files	Number of Useful Files	Number of Flights	Total Time (hours)	Total Distance (nm)
1	156	111	634	146.4	19,838
2	93	84	516	139.3	20,922
3	161	45	103	67.3	7,829
4*	44	34	302	99.6	10,978
5	144	133	145	47.5	5,792
SEAT	554	373	1,398	454.5	54,381
Spray	44	34	302	99.6	10,978

\* Used exclusively for agricultural spraying

During the installation process, strain gauges were calibrated for known applied forces at specific locations on the wing while the aircraft was on the ground. On Aircraft 1 and 2, loads were applied at 217.5" outboard of the centerline, with 950 pounds of fuel in the wing. The zero bending moment corresponded to the zero externally applied calibration force with the aircraft resting on the landing gears. On Aircraft 3 and 4, calibration loads were applied at 154" outboard of the centerline, with no fuel in the wing. Again, the zero bending moment was associated with zero calibration force and the aircraft being on the ground.

Due to this calibration method, the values of the bending moment presented in this report can only be used for comparison of various cases and are not to be taken as total values.

### 3. DATA REDUCTION

#### 3.1 INITIAL PROCESSING

The GAU 2000 stored the information on Secure Digital cards. The operator then periodically sent the cards to WSU, where the raw data stored on the cards were processed by software provided by Appareo Systems. This software separated the flights and generated comma-separated flight files. Each flight file started when the aircraft master switch was turned on and ended when the system was turned off. Therefore, a flight file could contain multiple flights that required separation.

A separate code was used to estimate the ground elevation along the flight path using the National Elevation Dataset (NED) and instantaneous latitude and longitude. The NED is maintained by the United States Geological Survey and consists of input from various sources. The resolution of the data stored in NED depended on the location in the country. Further information regarding NED can be found on their website [9].

#### 3.2 DERIVED PARAMETERS

##### 3.2.1 Liftoff and Touchdown

In the absence of a squat switch signal, airspeed was used to separate individual flights within a flight file. Conservative estimates were used for airspeed to avoid inclusion of the loads from any of the ground phases.

##### 3.2.2 Altitude and Rate of Climb

Pressure altitude contained some noise; when it was differentiated, it resulted in unacceptable fluctuations of the rate of climb. Therefore, the pressure altitude was filtered using a 2-second running average. In those cases in which altitude above ground level (AGL) was of interest, the local ground elevation was subtracted from the filtered pressure altitude.

### 3.2.3 Air Density

Recorded values of static pressure and outside air temperature were used in the equation of state of an ideal gas to find the air density:

$$\rho = p / RT \quad (1)$$

where,

$$\begin{aligned} \rho &= \text{local air density, slug/ft}^3 \\ p &= \text{absolute local static pressure, lbf/ft}^2 \\ R &= \text{specific gas constant of air, 1716.2 ft-lbf/slug-}^\circ\text{R} \\ T &= \text{local temperature, }^\circ\text{R} \end{aligned}$$

Reference sea level air density,  $\rho_s$ , of 0.002377 slug/ft<sup>3</sup> was used for the calculation of true airspeed. No corrections were possible to account for humidity.

### 3.2.4 True and Equivalent Airspeeds

As all flights were in the low-speed range, true airspeed was estimated from indicated airspeed using:

$$V_t = V_i \sqrt{\frac{\rho_s}{\rho}} \quad (2)$$

where,

$$\begin{aligned} V_i &= \text{indicated airspeed, ft/s} \\ V_t &= \text{true airspeed, ft/s} \end{aligned}$$

The results were checked against the values in the flight files, which were calculated by the Appareo Systems software during the initial post-processing.

### 3.2.5 Flight Distance

Flight distance was determined by integrating true airspeed between takeoff and landing:

$$D = \sum_{t_{start}}^{t_{end}} V_t \Delta t \quad (3)$$

where,

$$\begin{aligned} D &= \text{distance, ft} \\ \Delta t &= \text{time step size, seconds} \end{aligned}$$

### 3.3 WEIGHT ESTIMATION

Aircraft weight was not a recorded parameter, but the chemicals or retardant aboard constituted a significant part of the takeoff weight. Therefore, a running estimate of the weight was developed during each mission. The specific method used for estimating the takeoff weight and other changes in the weight depended on the aircraft and mission.

#### 3.3.1 Fuel Consumption

Regardless of the nature of the mission, the total weight was continuously reduced during flight to account for fuel consumption. Fuel burn rates were established using the engine's specific fuel consumption (SFC) and assuming continuous operation at 80% maximum power. Information about engine torque and propeller revolutions per minute was not available.

#### 3.3.2 SEAT and Spray Missions

MTOW was assumed at the start of each flight to be consisted of the empty weight, the maximum allowable chemical or retardant, the pilot weight, and the fuel weight. Therefore, fuel weight at the start was estimated from:

$$W_{Fuel} = MTOW - W_{empty} - W_{Load} - W_{Pilot} \quad (4)$$

In this expression, "Load" refers to the retardant or chemical weight. For each mission, drop durations were summed. Drop rates were assumed to be constant and determined by dividing the total load weight by the total drop duration. During each drop, the weight was reduced by the amount of the load released during each drop. At every landing, fuel and the load were assumed to be replenished. An example case for two short spray flights is shown in figure 1. In figure 1(a), it appears that the first drop of the second flight (at approximately 1062 seconds into the flight) was missed (i.e., the bay door opened, but the weight did not change). However, examination of the corresponding time history of altitude would reveal that the aircraft was on the ground at that time. The actual first drop of the second flight started at 1165 seconds into the file. It is noteworthy that this case was unusual among agricultural application missions in that they could consist of more than 50 drops per flight. An equally important point is that the airspeeds in this report are in nautical miles per hour, as opposed to statute miles per hour as shown on the aircraft airspeed indicator.

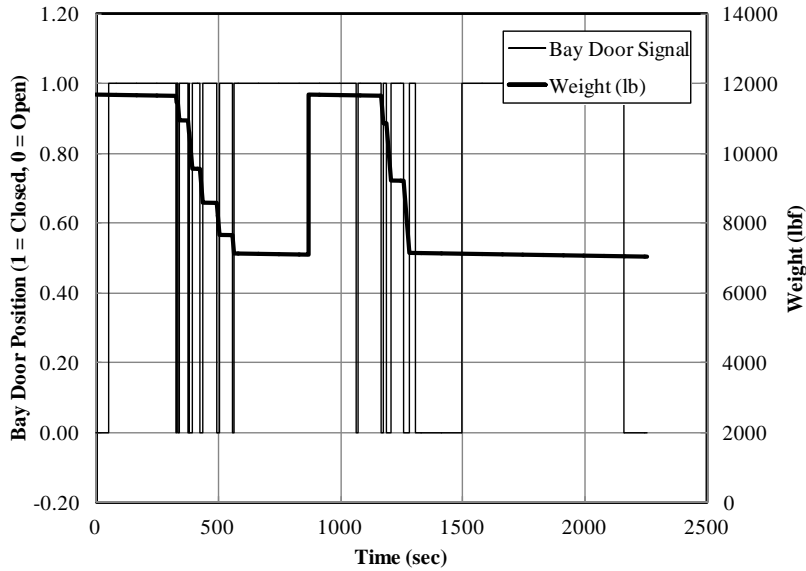
During spray missions, it was common for the release trigger signal to remain in the on position for some time after the last drop. As drops were detected by toggling of this switch, this resulted in artificially long total drop durations and, therefore, underestimated drop rates. Consequently, drops lasting longer than 1.5 minutes were eliminated as not being real. At typical spray flight speeds of roughly 100 knots indicated airspeed (KIAS), the aircraft traveled 2.5 nautical miles in 1.5 minutes, which was deemed to be longer than most spray runs.

### 3.3.3 Ferry Missions

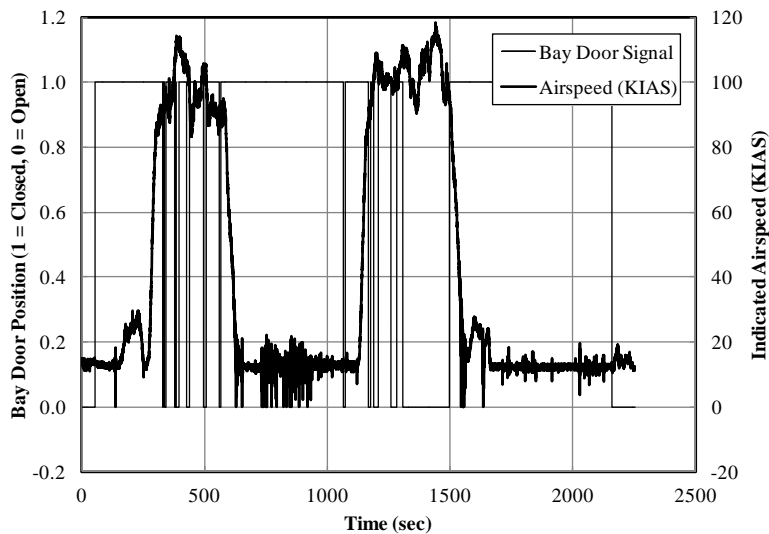
Takeoff weight was estimated from the empty weight and the maximum fuel weight, without any load. Therefore,

$$W_{TO} = W_{empty} + W_{Pilot} + W_{Fuel} < MTOW \quad (5)$$

Again, the weight was reduced as the mission progressed, based on SFC and assuming flight at an average of 80% maximum power.



(a) Time history of bay door position and total weight



(b) Time history of bay door position and indicated airspeed

**Figure 1. Variation of weight and airspeed for two consecutive spray missions–Aircraft 4**

### 3.4 LOADS AND GUST OCCURRENCES

#### 3.4.1 Sign Convention

The accelerations were recorded in three directions: normal ( $z$ ), longitudinal ( $x$ ), and lateral ( $y$ ). As shown in figure 2, the positive  $z$  direction was up and the positive  $x$  direction was forward. Because the longitudinal acceleration was very sensitive to the aircraft pitch attitude, not enough meaningful information could be extracted from it for the airborne phases.

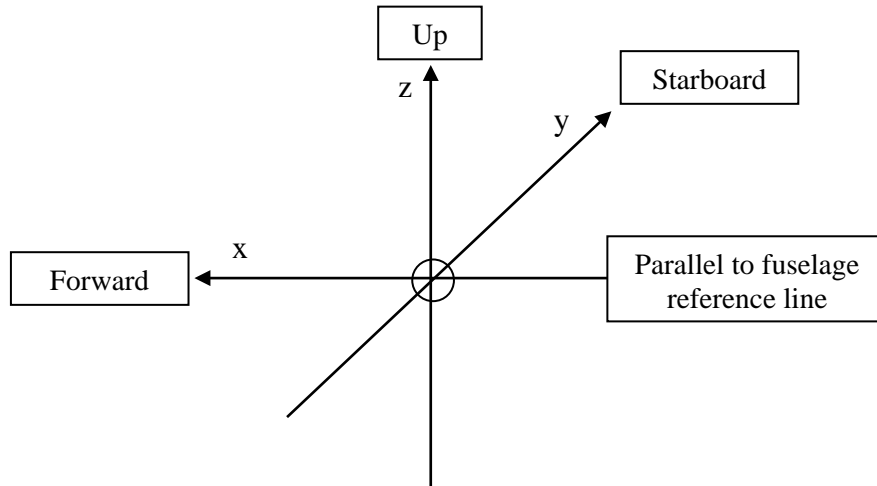


**Figure 2. Sign convention for airplane accelerations**

#### 3.4.2 Load Counts

The method of peaks-between-means [10] was used for counting the peaks and valleys in the incremental vertical acceleration. This method is consistent with past practices and can be applied regardless of whether the accelerations resulted from gusts or maneuvers. In this method, only one peak or valley is counted between two successive crossings of the mean. A threshold zone (i.e., dead band) is used in the data reduction to filter out the noise around the mean, as shown in figure 3. For vertical load factors, the dead band width of  $\pm 0.05$  g was used.

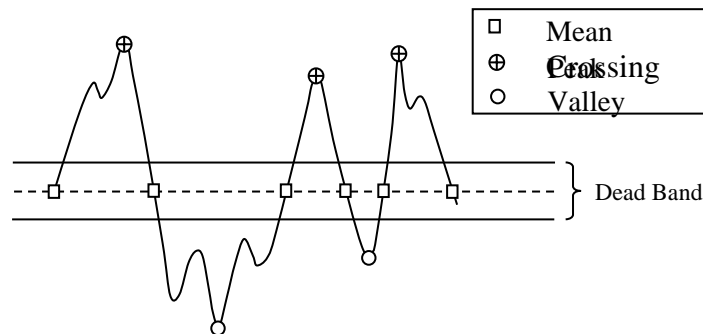


**Figure 3. Peaks-between-means classification of loads**

### 3.4.3 Bending Moment Counts

The method of peaks-between-means could not be used for counting the occurrences of wing bending moments. As the aircraft weight changed during flight, the average wing bending moment also changed, making it appear as a drift in its mean. This effect was magnified during the release of retardant or chemicals. Furthermore, there was significant noise in the wing bending moment signal that was caused by extracting very large values of this parameter from very small fluctuations of the strain gauge voltage. Therefore, certain thresholds were established for wing bending moment and cumulative time exceeding these thresholds per 1000 hours and per nautical mile were determined.

### 3.4.4 Separation of Maneuver and Gust Load Factors

The incremental vertical accelerations can be the result of gusts or maneuvers. To separate the loads into the two categories, Rustenburg et al. [10] recommended a 2-second cycle duration to be used for categorizing the incremental vertical accelerations. Therefore, accelerations lasting longer than 2 seconds were assumed to be due to maneuvers.

The cumulative occurrences of incremental load factors were determined as cumulative counts per 1000 hours and cumulative counts per nautical mile.

### 3.4.5 Normalizing of Vertical Load Factor

The aircraft weight changed significantly during spraying and firefighting missions. Consequently, the raw load factor was not a good indicator of the loads carried by the wing. It was reasoned that the same load factor would cause much larger stresses in the airframe at gross weight than it would at half that weight. Therefore, a normalized vertical load factor was devised to account for this effect. This parameter was defined as:

$$(n_z)_{normalized} = n_z \left( \frac{W}{MTOW} \right) \quad (6)$$

where,

$W$  = instantaneous aircraft weight, lb  
 $MTOW$  = maximum takeoff weight, lb

Cumulative occurrences of both vertical load factors for overall flights are presented in the report. It is important to realize that normalizing the load factors in this manner is valid only for loads carried by the wing. The load factors imposed on other parts of the airframe, such as engine mounts and empennage, are independent of the aircraft weight.

### 3.4.6 Correlation of Vertical Load Factor and Bending Moment

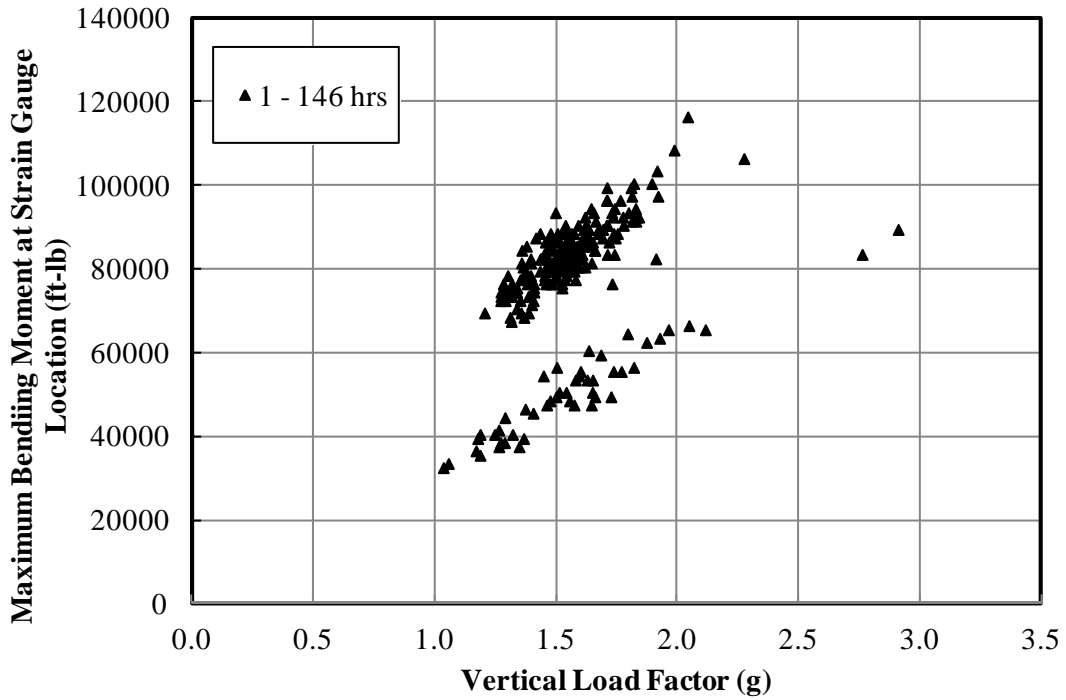
A great deal of noise was present in the values of the bending moment at the strain gauge locations. This was mostly attributed to the conversion of very small changes in the strain gauge voltage to very large values for the bending moment. Consequently, the vertical load factor and bending moment could not be correlated easily; figures 4 and 5 are used to show this fact. In figure 4, the maximum bending moment is plotted versus the coincident vertical load factor from the airframes with reliable strain gauge output, from one flight for each. The results from Aircraft 1 and Aircrafts 3 and 4 are presented in separate parts mainly because of the differences in the magnitudes caused by different gross weights and moment arms. Figure 5 shows the maximum vertical load factor and coincident bending moment. Ideally, these figures should be identical. However, it is clear from these figures that the latter data show lower levels of maximum bending moment for the same load factor.

Another factor influencing the bending moment was the instantaneous weight, of which only an estimate was available. Nonetheless, normalizing the load factor with the estimated aircraft weight resulted in somewhat better correlation between the two parameters. Figure 6 serves to show this point for one flight from Aircraft 1. In figure 6(a), the bending moment and coincident vertical load factor are shown during one SEAT mission. Each point in this plot corresponds to one line of data. It is clear from this figure that the data are grouped according to aircraft weight. As expected, before the drop, wing bending moments are much higher for the same load factor than after the drop. However, once the vertical load factors are normalized by the estimated instantaneous aircraft weight, they correlate much better with the bending moments, as shown in figure 6(b). The authors speculate that a better estimate of the instantaneous aircraft weight would result in even better correlation with much less scatter.

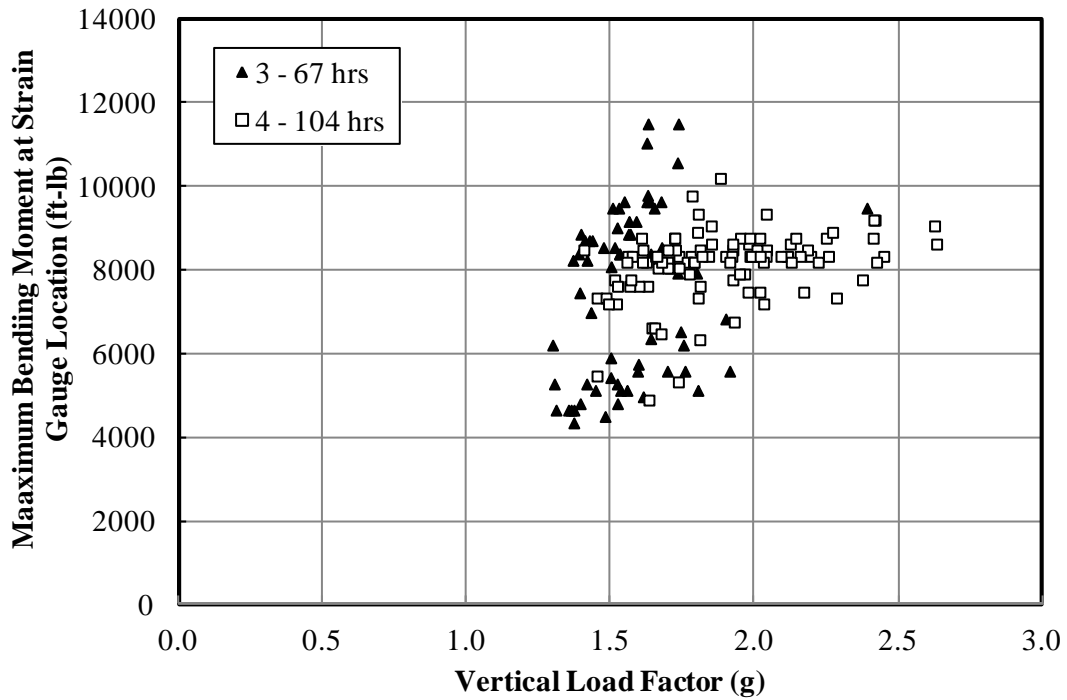
The conclusion drawn from this discussion is that neither parameter alone should be used as a measure of the loads exerted on the structure. The values of the bending moment alone contain too much uncertainty due to noise, whereas the load factor alone does not represent the effect of aircraft weight. Therefore, both parameters should be used side by side to arrive at more reliable conclusions.

### 3.4.7 Altitude Bands

All flights took place at relatively low AGL altitudes, especially during agricultural spraying and firefighting. Therefore, no attempt was made to categorize the loads according to altitude.

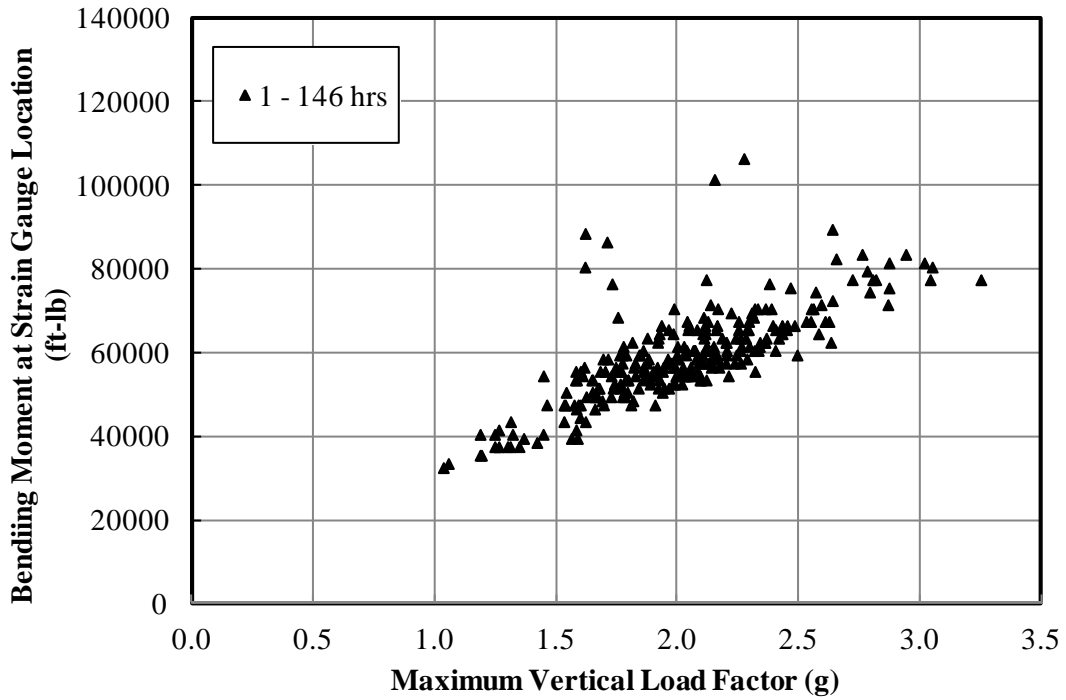


(a) Aircraft 1

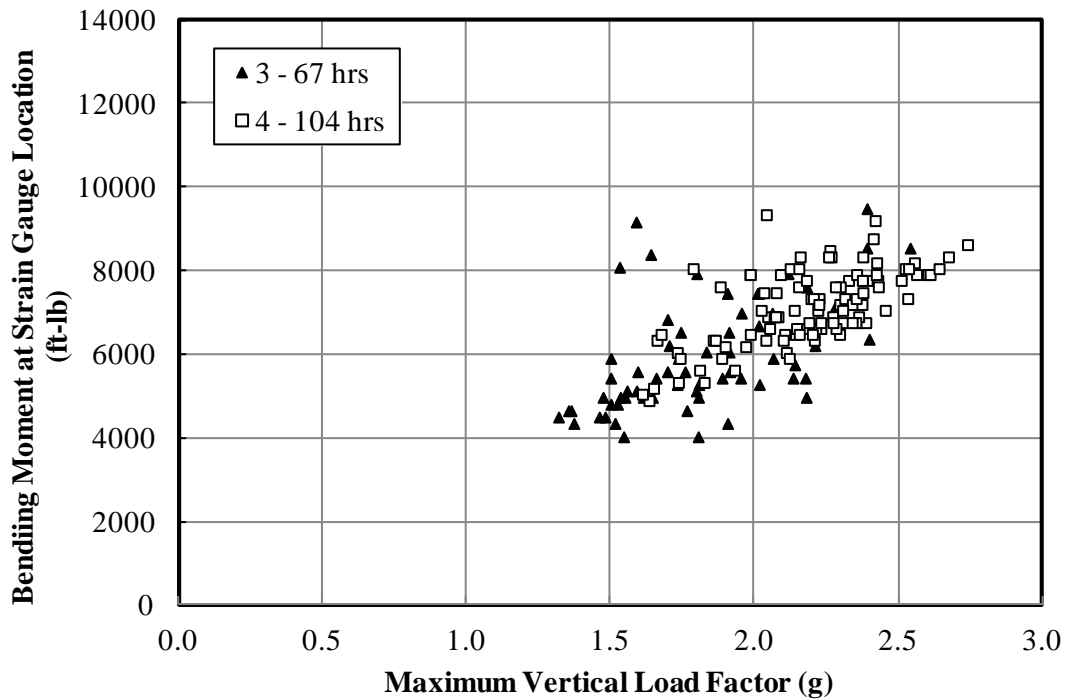


(b) Aircraft 3 and 4

**Figure 4. Maximum bending moment and coincident vertical load factor**

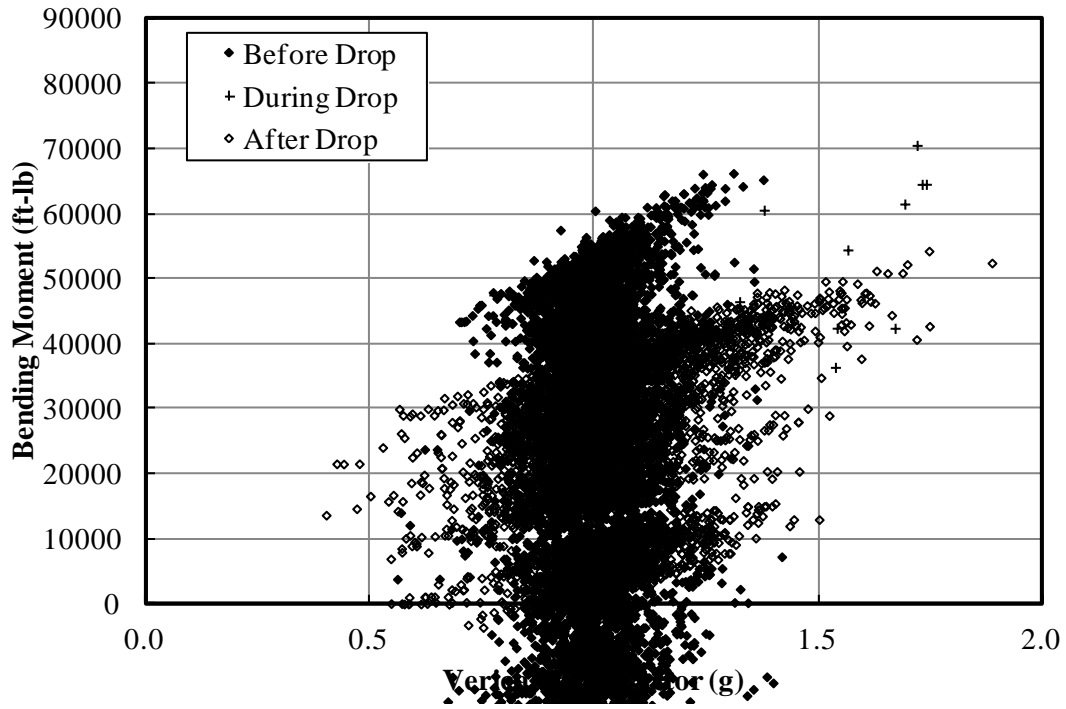


(a) Aircraft 1

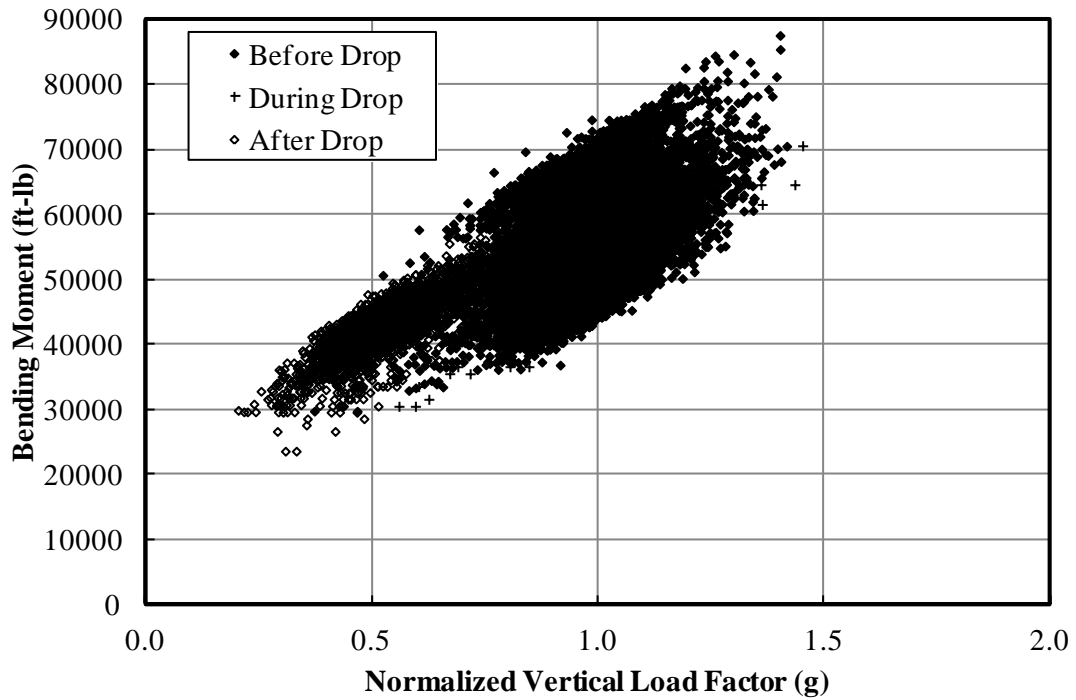


(b) Aircraft 3 and 4

**Figure 5. Bending moment and coincident maximum vertical load factor**



(a) Recorded vertical load factor



(b) Normalized vertical load factor

**Figure 6. Correlation of bending moment and normalized vertical load factor–Aircraft 1**

### 3.5 FLIGHT PHASE SEPARATION

Flights were divided into discrete phases for loads analysis. Only airborne phases were considered, and every effort was made to exclude any ground loads. Most missions were flown at relatively low altitudes. Therefore, only cruise- and mission-related phases (e.g., drops) were considered. Likewise, the data were not categorized into altitude bands. As a result, ferry missions consisted of one flight phase from takeoff to landing. Firefighting and spraying missions were divided into separate types of phases.

#### 3.5.1 SEAT Missions

Flight phases of SEAT missions were very similar to those of heavy air tankers, described by Rokhsaz et al. [11] and shown schematically in figure 7. Figure 8 shows the time history of one mission consisting of two flights with one drop each.

Each flight was divided into five phases, shown in table 4, which consisted of:

1. Cruise 1—Climb to altitude and cruise to the drop zone
2. Entry—Preparation for drop, including brief loiter and descent into the drop site
3. Drop—The actual time the retardant leaves the aircraft
4. Exit—Climb out to cruise altitude immediately following the drop
5. Cruise 2—Depart from the drop zone for the return trip and descent for landing

Each entry, drop, and exit phase was considered when a flight contained more than one drop. However, only one Cruise 1 and one Cruise 2 phase were associated with each flight.

In general, drops were recognized from the bay door signal. However, in the case of Aircraft 2, the bay door signal did not record properly. Therefore, aircraft AGL altitude and airspeed were used to recognize the drops. If minimum AGL altitude was less than 250 feet, and if the airspeed was above the assigned takeoff airspeed 1 minute before and 1 minute after reaching said altitude, a drop was assumed. In this case, the drop length was assumed to be 5 seconds, with 2.5 seconds preceding and following the point of minimum AGL altitude. The value of the minimum altitude was determined by visual inspection of a number of flights. Drop duration was based on the average of drop lengths found for other aircraft.

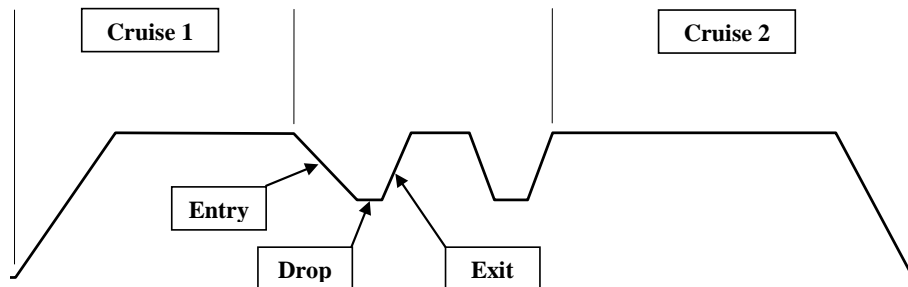


**Figure 7. Flight phases of SEAT missions**

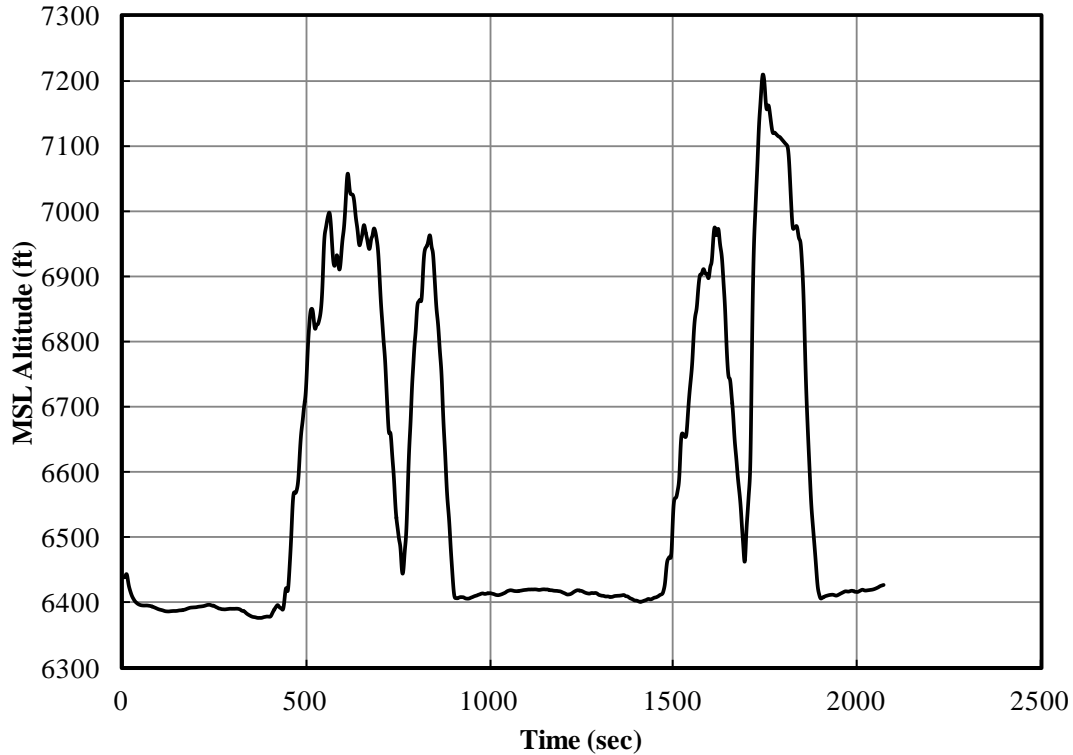


**Figure 8. Time history of altitude for two flights with one drop each–Aircraft 1**

In the absence of other indicators, entry and drop phases were assumed to last 1 minute each. This duration was established from visual examination of approximately 100 missions where the start and end of these phases could be estimated from a number of other parameters, such as airspeed and AGL altitude. Normal probabilities of entry and exit durations for these cases are shown in figure 9. While the average was closer to 50 seconds, a 1-minute duration was believed sufficient to capture the salient features of these phases. A longer period could cause overlapping of consecutive drop phases, whereas a shorter period, especially in comparison with heavy tanker operations, would not contain all the loads associated with entry and exit.

As stated earlier, Cruise 1 spanned between takeoff and 1 minute before the start of the first entry, and Cruise 2 covered the period from 1 minute past the end of the last exit and landing. In general, these two phases were remarkably short compared with heavy air tankers.

### 3.5.2 Agricultural Application Missions

These missions were very similar to those of the SEAT, except they entailed many more drops per flight. The time history of altitude for one mission is shown in figure 10. These flights were divided into the following four phases:

1. Cruise 1–Climb to altitude and cruise to the application site
2. Drop–The actual time the chemicals leave the aircraft
3. Turn–Flight segment between every two consecutive drops
4. Cruise 2–Depart from the application site for the return trip

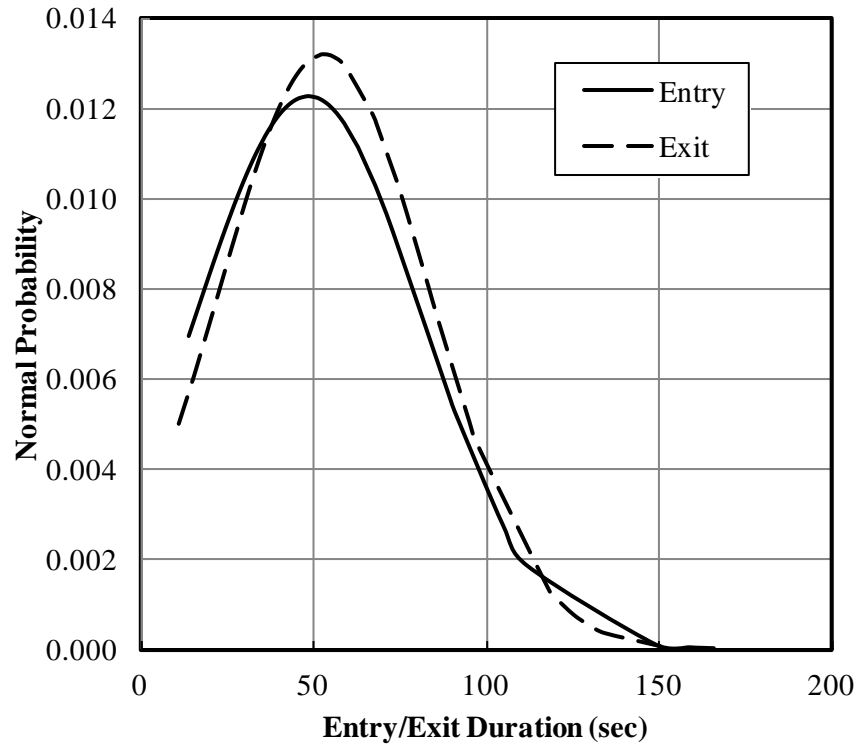


**Figure 9. Normal probability of entry and exit phase durations**

**Table 4. Flight phase separation criteria SEAT missions**

Flight Phase	Start Time ( $t_1$ ) Identification	Stop Time ( $t_2$ ) Identification
Cruise 1	Airspeed greater than takeoff value	One minute before the start of the first entry phase
Entry	One minute before the opening of the bay door	Opening of the bay door
Drop	Opening of the bay door	Closing of the bay door plus 0.5 seconds
Exit	End of the drop phase	One minute past the end of the drop phase
Cruise 2	One minute past the end of the last exit phase	Airspeed below takeoff speed

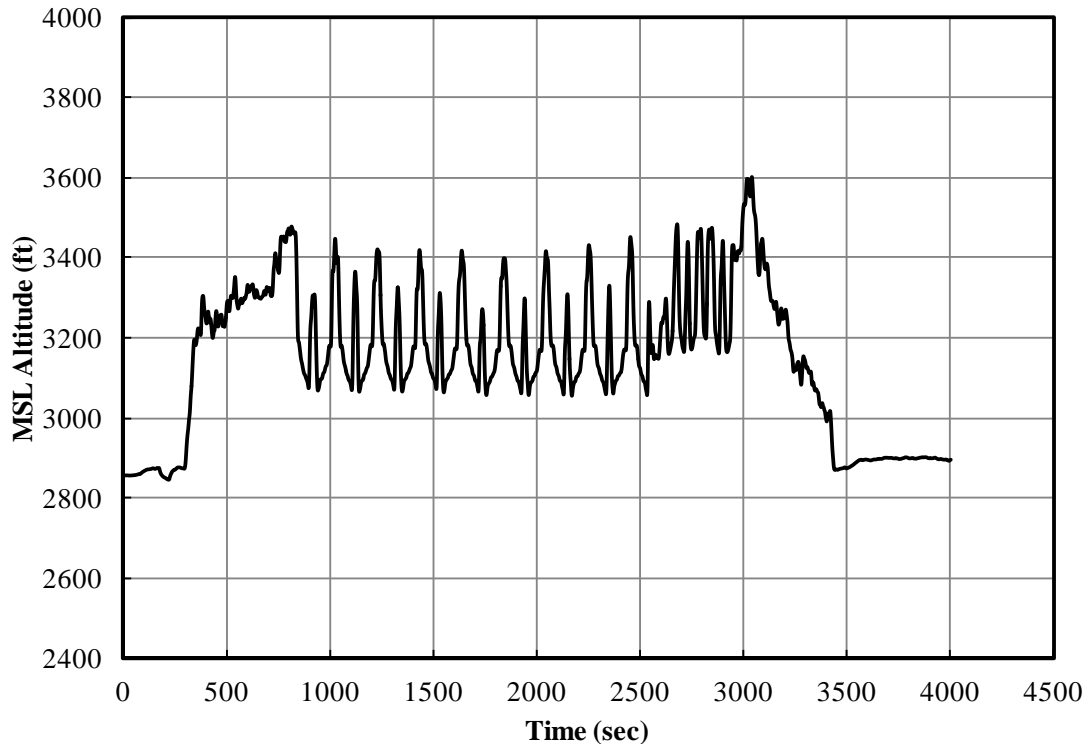


**Figure 10. Typical altitude time history from a spray mission–Aircraft 4**

In the case shown in figure 10, the aircraft was flown to a larger field first, where 17 drops took place, followed by it spraying a smaller adjacent field with five passes before returning to base. This can be seen more clearly from the flight path shown in figure 11.

The drops were identified from the release trigger signal. However, in this case, the drop was assumed to stop once the release trigger signal changed. While spraying, the flight path resembled a racetrack. Therefore, drops were separated by relatively steep turns, omitting the turns associated with entry into the field and exit from it. For example, in the case shown in figures 10 and 11, there were a total of 22 drops, 21 turns, and one Cruise 1 and one Cruise 2. Cruise 1 spanned between takeoff and 1 minute before the start of the first drop. Cruise 2 started 1 minute past the end of the last drop and ended at landing. Because of the nature of the operation, these two phases were remarkably short and flown at low AGL altitudes. Flight phase separation criteria for these missions are summarized in table 5.

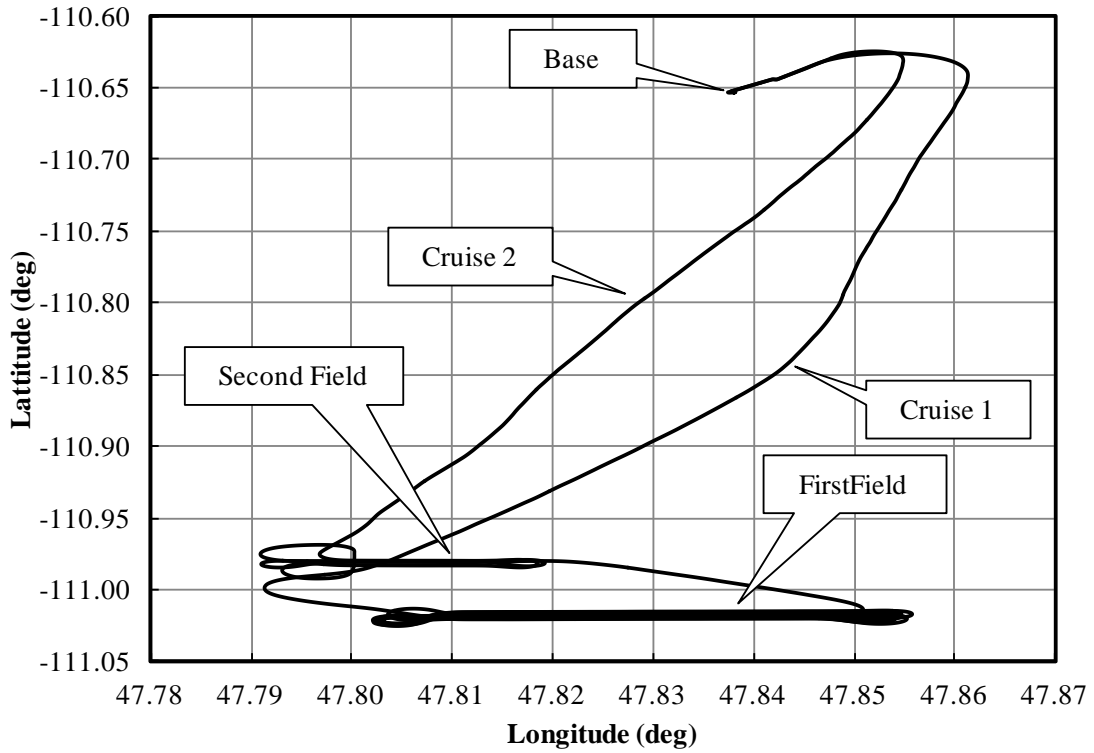


**Figure 11. Flight path of the spray mission of figure 7–Aircraft 4**

**Table 5. Flight phase separation criteria agricultural applications**

Flight Phase	Start Time ( $t_1$ ) Identification	Stop Time ( $t_2$ ) Identification
Cruise 1	Airspeed greater than takeoff value	One minute before the start of the first drop phase
Drop	Release trigger signal on	Release trigger signal off
Turn	End of a drop phase	Start of the next drop
Cruise 2	One minute past the end of the last drop phase	Airspeed below takeoff speed

#### 4. USAGE DATA PRESENTATION

This section explores the results associated with aircraft usage. Overall usage is presented first, followed by the discussion of the individual airborne phases. The list of figures pertaining to this section is given in table 6. The figures listed in this table and discussed in this section are presented in appendix A.

**Table 6. Statistical formats and usage data**

Aircraft Usage Data	Figure
<b>OVERALL FLIGHT</b>	
Maximum altitude and coincident indicated airspeed—all phases	A-1
Comparison of maximum MSL* and AGL altitudes—Aircraft 2	A-2
Maximum indicated airspeed and coincident MSL altitude—all phases	A-3
Percentage of flights based on duration—all phases	A-4
Vertical load factor and coincident indicated airspeed—all phases	A-5
Maximum and minimum pitch angle—all phases	A-6
Maximum and minimum roll angle—all phases	A-7
<b>CRUISE 1, CRUISE 2, FERRY</b>	
Average duration and distance for cruise and ferry flights	A-8
Maximum indicated airspeed and coincident MSL altitude	A-9
Maximum vertical load factor and coincident indicated airspeed	A-10
<b>ENTRY, DROP, EXIT, TURN</b>	
Average duration and distance for drops and turns	A-11
Maximum indicated airspeed and coincident MSL altitude—SEATs	A-12
Maximum indicated airspeed and coincident MSL altitude—agricultural application	A-13
Maximum vertical load factor and coincident indicated airspeed—SEATs	A-14
Maximum vertical load factor and coincident indicated airspeed—agricultural applications	A-15

\*Mean sea level

#### 4.1 OVERALL USAGE

Maximum mean sea level (MSL) altitude and coincident airspeed are shown in figure A-1 for all aircraft. Although the maximum altitudes appeared to be equally distributed between sea level and 16,000 feet, in reality, most of these cases corresponded with much lower AGL altitudes. This trend can be seen more clearly in figure A-2, in which the maximum MSL and AGL altitudes are compared for Aircraft 2. While the MSL altitudes were mostly grouped roughly between 8,000 and 12,000 feet, the AGL altitudes were grouped between 2,000 and 6,000 feet. In fact, in this case, the average MSL and AGL altitudes were 10,400 and 5,300 feet, respectively. Based on this observation, no attempt was made to categorize any of the data according to altitude.

Maximum indicated airspeed and coincident MSL altitude are shown in figure A-3. This figure also shows the never-exceed airspeeds for AT-802A and PZL M18 aircraft. This quantity could not be determined clearly for Aircraft 5. Understandably, Aircraft 1 and 2, with the larger engines, could reach higher maximum airspeeds. Furthermore, Aircraft 2, which was equipped with the 1650-hp Garrett engine, achieved the highest maximum airspeeds. The higher airspeeds were also associated with SEAT missions and travelling to and from the Fire Traffic Area. Based on the examination of the data, most chemical or retardant releases took place at airspeeds ranging from 80–130 KIAS.

The majority of the flights lasted between 30 and 60 minutes, as indicated in figure A-4. The exception was Aircraft 5, which was the lightest of all five airframes. Generally, flights lasting longer than 2 hours were to ferry the aircraft. On average, flights for agricultural applications lasted longer than SEAT missions, as expected.

Maximum vertical load factors and coincident indicated airspeeds are shown in figure A-5. The loads from each airframe are shown in a separate part of this figure for clarity. Also, in each part of this figure, the legend indicates the aircraft number and number of hours flown. Comparing various parts of this figure, it is evident that the maximum vertical load factors occurred during firefighting missions; although in no case did the load factor exceed +3.5 g. The majority of the larger load factors on the SEAT aircraft were one-time events associated with the retardant drop. The accelerations shown in these figures are simply those recorded by the accelerometers and were not normalized for changing aircraft weight.

Figures A-6 and A-7 show the maximum and minimum pitch and roll angles per flight. In these figures, the abscissa shows the aircraft number, and each pair of points (i.e., one maximum and one minimum) is associated with each flight. The recorded pitch and roll angles on Aircraft 2 were erroneous and omitted in these figures. It is obvious from these figures that the largest pitch and roll angles were associated with agricultural applications. Nonetheless, maximum load factors were much smaller than those of firefighting missions, as indicated in figure A-5.

## 4.2 PHASE-SPECIFIC USAGE

### 4.2.1 Cruise 1, Cruise 2, and Ferry

Results from these three phases are presented side by side because of their similarities in the nature of flying. All three cases involve minimal maneuvering and, for the most part, relatively constant altitudes and airspeeds.

Average duration and distance for these phases are shown in figure A-8. In every case, the Cruise 2 phase was slightly shorter than Cruise 1. In addition, both the Cruise 1 and Cruise 2 phases were much shorter than those from heavy air tankers. It was not surprising that both of these phases were much shorter for the agricultural applications. In most cases, these operations involve flights from temporary bases set up very close to the fields that are being sprayed. Notably, the data from Aircraft 4 also contained only one ferry flight. Therefore, no meaningful statistical information could be extracted for this case.

Maximum indicated airspeed and coincident MSL altitudes are shown in figure A-9. Various parts of this figure also show the duration of each phase for each aircraft. Comparison of the

cruise phases shows that the aircraft were flown at slightly higher airspeed on the return trips. This could be a direct result of the weight difference between Cruise 1 and Cruise 2 phases. Coupled with the longer average durations shown in figure A-8, this resulted in availability of 25–45% more data from the former phase. The number of hours flown in ferry missions was comparable with Cruise 1 and Cruise 2. Data from only one ferry flight were available from Aircraft 4, shown as a single point in figure A-9(c).

Maximum vertical load factor and coincident indicated airspeeds are presented in figure A-10. The load factors from the three phases were comparable, with slightly higher values for Cruise 2 at approximately 100 KIAS. In all likelihood, this behavior was caused by the considerably lower wing loadings on the return trips. In two cases, the maximum load factor from ferry flights exceeded +2.5 g, which was unexpected.

#### 4.2.2 Entry, Drop, Exit, and Turn

These phases were grouped together because they all involve maneuvering flight. Average durations and distances for the drop and the turn phases are shown in figure A-11. The reader is reminded that the Turn phase was unique to the agricultural application flights. Also, in the absence of other indicators, entry and exit phases for SEAT flights were assumed to last one minute each. Therefore, they were not included in this summary. Furthermore, because of a malfunctioning bay door signal on Aircraft 2, its drop durations were set to 5 seconds. It is evident from figure A-11 that, compared to other SEAT missions, this duration was quite reasonable. Finally, as expected, the average drop duration during agricultural spraying was considerably longer than it was for firefighting missions.

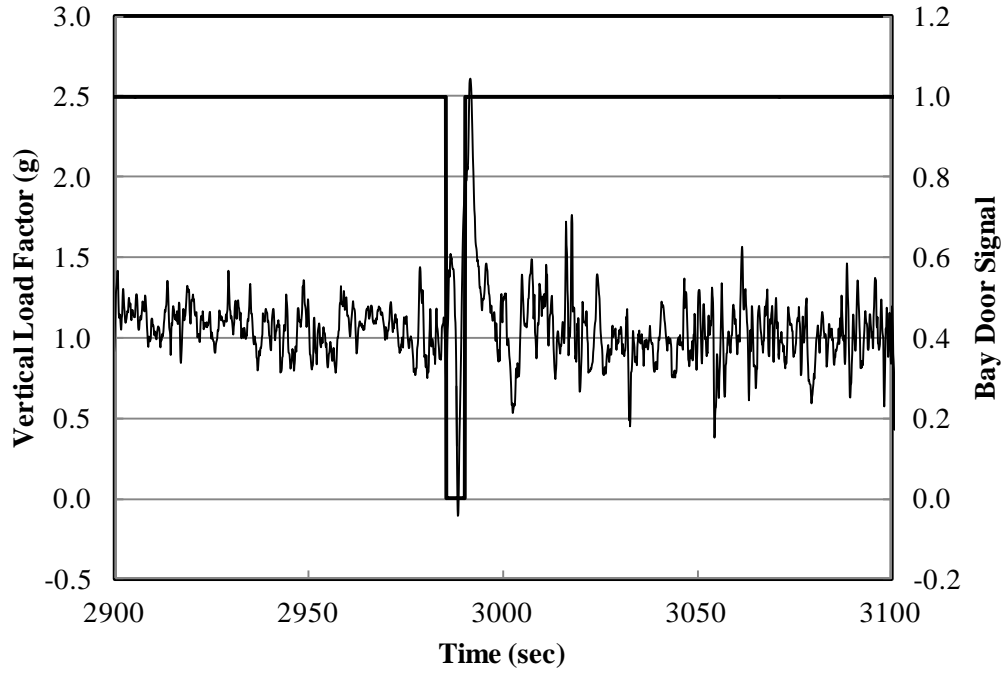
Maximum indicated airspeeds and coincident altitudes are shown in figures A-12 and A-13. The results for Aircraft 4 are shown separately because, for this aircraft, phases were slightly different from those of the SEAT, and the number of occurrences of each phase was much larger than comparable phases of SEAT. However, the same scale is used for both sets of figures to allow for easier comparison of the results. The total duration of each phase for each aircraft is also shown in these figures.

It is clear from these results that the maximum airspeeds were grouped predominantly around 110–130 KIAS. SEATs were flown over a variety of sites. Therefore, even though drops were performed close to the ground, the corresponding MSL altitudes covered a wide range of values. Conversely, Aircraft 4 was flown in one part of the country, which explains the smaller variations in its altitudes. Obviously, the drops were cumulatively the shortest of the phases for the SEAT aircraft—resulting in insufficient data, in some cases, for definitive analysis.

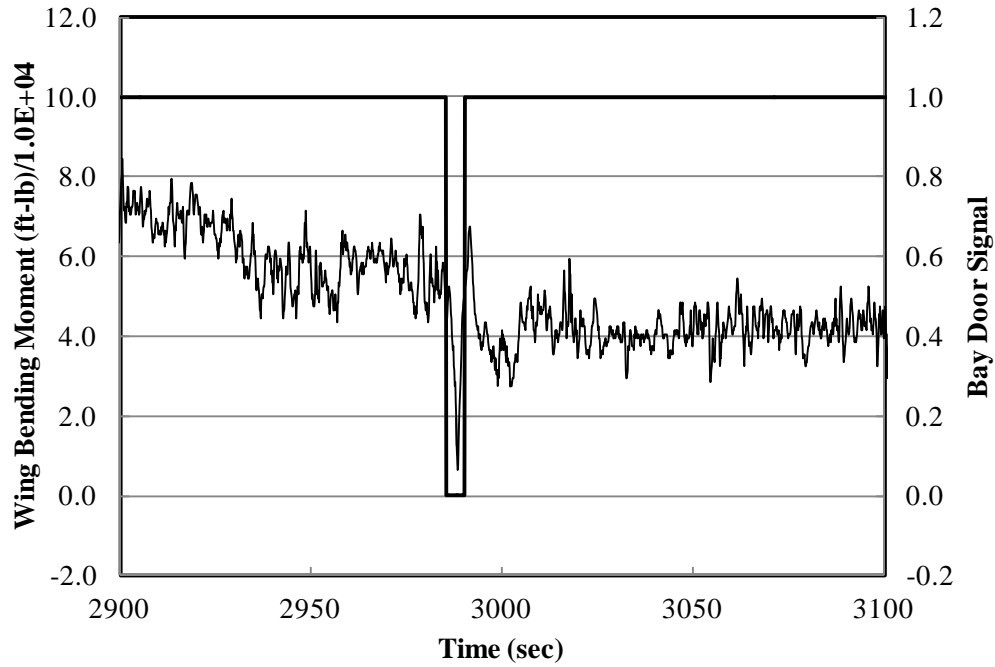
Maximum vertical load factor and coincident indicated airspeed are given in figures A-14 and A-15. Again, the results for the SEAT and agricultural applications are shown separately for the purpose of clarity. For the SEAT, the maximum variation in load factor was during the drop phase. This phase was generally accompanied by a large positive load factor, approaching +3 g. In most cases, the peak load factor was accompanied by a relatively large unloading of the structure, sometimes following the peak and at other times preceding it. A typical example is shown in figure 12. The authors speculate that most of the positive load factors were caused by the rapid loss of aircraft weight during the drop, whereas the unloading of the structure was

driven by the pilot. The latter can also be seen in the time history of the wing bending moment, which does not peak as high at the end of the drop when the aircraft weight has been reduced to almost half.

Whereas the maximum vertical load factors were spread over a wide range of values for the SEAT aircraft, they were closely grouped for agricultural missions. Also, the maximum load factors for the Turn phases were slightly larger than those for the drop phases. As mentioned earlier, in these cases the maximum load factors were not as large but occurred more frequently during a mission. A somewhat typical time history of the load factor is shown in figure 13. In this figure, the change in the strain gauge signal is also shown to demonstrate the reduction in the stress as the aircraft became lighter, despite the fact that the peak values of the positive load factor increased as the mission proceeded.

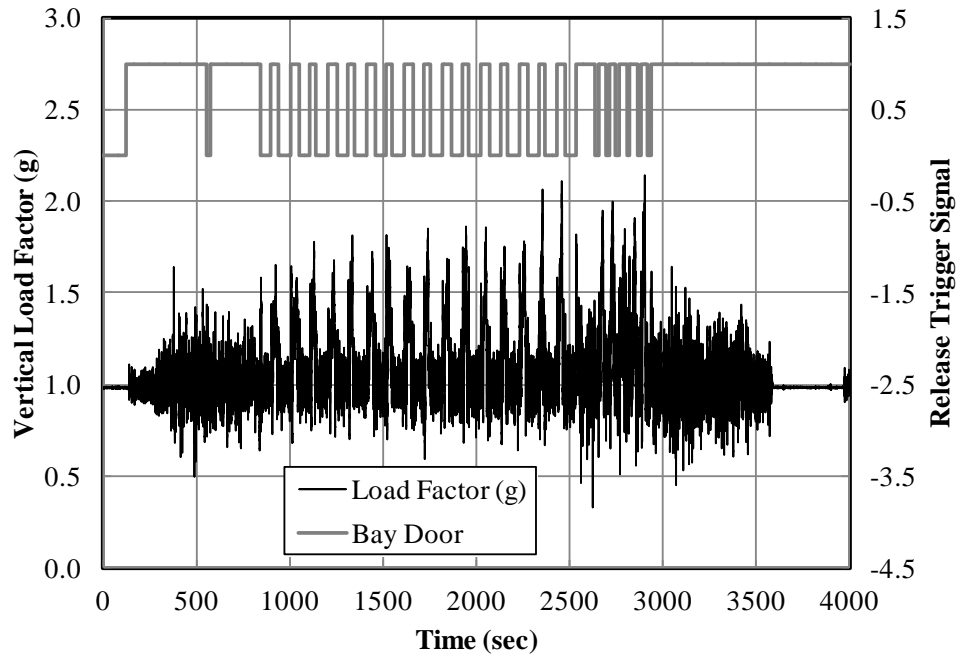


(a) Vertical load factor

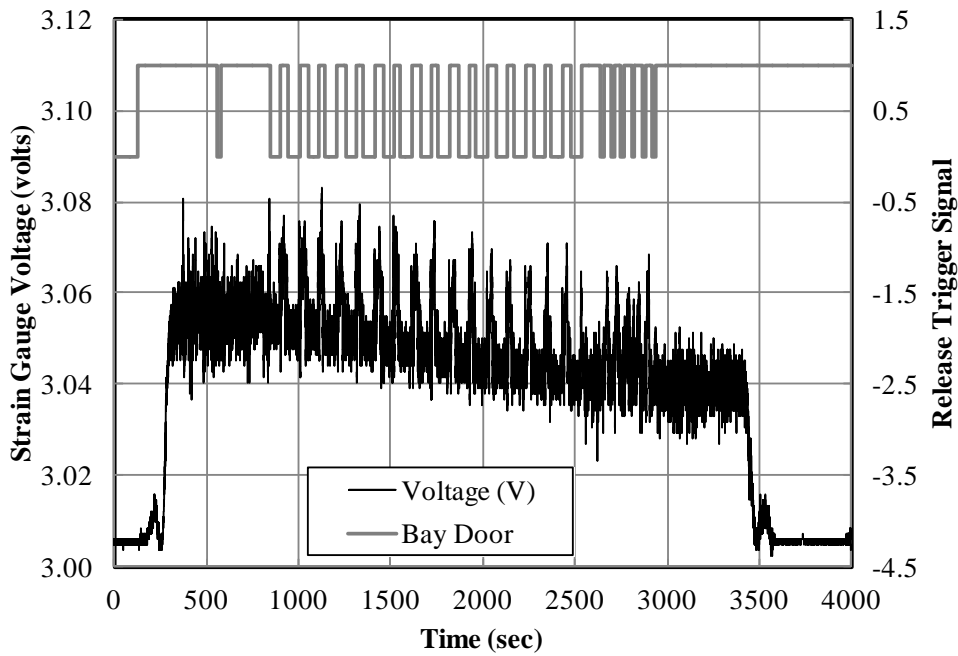


(b) Wing bending moment

**Figure 12. Time history of vertical load factor during a SEAT drop–Aircraft 1**



(a) Vertical load factor



(b) Strain Gauge Voltage

**Figure 13. Time history of vertical load factor during a spray operation–Aircraft 4**

## 5. LOADS DATA PRESENTATION

This section explores the load factors and measured bending moments. The reader is reminded that the bending moments represent the values at the strain gauge locations and can only be used while taking into account the strain gauge calibration processes. The figures associated with this section are summarized in table 7.

### 5.1 OVERALL LOADS

#### 5.1.1 Gust and Maneuver Load Factors

In this section, flight loads and the wing bending moment for the entire flight (overall) are discussed. These include the results from all phases combined, although the data from each aircraft are presented separately for ease of comparison. A summary of the total duration and distance for each aircraft is shown in figure B-1 (found in appendix B along with the other figures mentioned in this section). The data from Aircraft 3 and 5 were rather limited because the former was out of service for part of the season, and the data collection from the latter was terminated by the USFS.

Cumulative occurrences of incremental gust vertical load factor are shown in figures B-2 to B-6. In these figures, flight load data from all missions are compared with those of ferry missions, which formed a small subset of the total data for each aircraft. Data from Aircraft 4 contained only one ferry mission, which could not be used to arrive at realistic exceedance plots.

A comparison of the results from various aircraft shows a great deal of agreement among them for incremental vertical load factors between +1 g and -1 g. Also, within this range of load factors, there was little difference between the results from all missions and those limited to ferry missions. In general, the larger volume of data from all missions allowed extension of the plots to positive load factors beyond  $\pm 1$  g. Furthermore, the larger load factors, associated with drop phases, contributed to the differences between ferry missions and all flights for incremental load factors larger than +1 g. In only one case did the incremental gust load factor exceed +2 g.

Figures B-7–B-11 allow comparison of the cumulative occurrences of incremental maneuver vertical load factors. These figures also show the results presented in reference 7 for SEAT aircraft, the heaviest of which had a MTOW of 8200 pounds.

In almost every case, there was a noticeable difference between the cumulative occurrences of maneuver load factors from all missions and those of ferry missions—in magnitude and in frequency. However, these differences were mostly in positive load factors, in which incremental values reached and exceeded +2 g frequently. Finally, the results from Aircraft 4, which was used exclusively for agricultural applications, behaved differently from those of SEAT aircraft. Load factors between +0.5 g and +1.5 g occurred over one order of magnitude more frequently, but values exceeding +1.5 g were scarce. The results from Aircraft 3 and 4, which had similar airframes, are superimposed in figure B-12 to highlight these differences. Whereas the cumulative occurrences of gust load factors are very close, the positive maneuver load factors differ significantly. This can only be due to the difference in the nature of the missions. SEAT aircraft experience a rather large factor during the drop, which occurs once or twice per mission.

Conversely, during agricultural applications, while the load factors are modest, they occur at much larger frequencies.

**Table 7. Statistical formats and flight loads**

Flight Loads Data	Figure
<b>OVERALL FLIGHT</b>	
Summary of overall duration and distance	B-1
Cumulative occurrence of incremental gust vertical load factor–Aircraft 1	B-2
Cumulative occurrence of incremental gust vertical load factor–Aircraft 2	B-3
Cumulative occurrence of incremental gust vertical load factor–Aircraft 3	B-4
Cumulative occurrence of incremental gust vertical load factor–Aircraft 4	B-5
Cumulative occurrence of incremental gust vertical load factor–Aircraft 5	B-6
Cumulative occurrence of incremental maneuver vertical load factor–Aircraft 1	B-7
Cumulative occurrence of incremental maneuver vertical load factor–Aircraft 2	B-8
Cumulative occurrence of incremental maneuver vertical load factor–Aircraft 3	B-9
Cumulative occurrence of incremental maneuver vertical load factor–Aircraft 4	B-10
Cumulative occurrence of incremental maneuver vertical load factor–Aircraft 5	B-11
Comparison of the results from Aircraft 3 and 4	B-12
Impact of weight on overall cumulative occurrence of incremental gust vertical load factor–Aircraft 1	B-13
Impact of weight on overall cumulative occurrence of incremental gust vertical load factor–Aircraft 2	B-14
Impact of weight on overall cumulative occurrence of incremental gust vertical load factor–Aircraft 3	B-15
Impact of weight on overall cumulative occurrence of incremental gust vertical load factor–Aircraft 4	B-16
Impact of weight on overall cumulative occurrence of incremental gust vertical load factor–Aircraft 5	B-17
Impact of weight on overall cumulative occurrence of incremental maneuver vertical load factor–Aircraft 1	B-18
Impact of weight on overall cumulative occurrence of incremental maneuver vertical load factor–Aircraft 2	B-19
Impact of weight on overall cumulative occurrence of incremental maneuver vertical load factor–Aircraft 3	B-20
Impact of weight on overall cumulative occurrence of incremental maneuver vertical load factor–Aircraft 4	B-21
Impact of weight on overall cumulative occurrence of incremental maneuver vertical load factor–Aircraft 5	B-22
Exceedance in seconds of maximum bending moment per 1000 hours–linear scale	B-23

**Table 7. Statistical formats and flight loads (continued)**

Exceedance in seconds of maximum bending moment per 1000 hours–semi-log scale	B-24
Exceedance in seconds of maximum bending moment per nautical mile–linear scale	B-25
Exceedance in seconds of maximum bending moment per nautical mile–semi-log scale	B-26
Duration and distance flown in each phase	B-27
Cumulative occurrence of incremental gust vertical load factor–Aircraft 1	B-28
Cumulative occurrence of incremental gust vertical load factor–Aircraft 2	B-29
Cumulative occurrence of incremental gust vertical load factor–Aircraft 3	B-30
Cumulative occurrence of incremental gust vertical load factor–Aircraft 4	B-31
Cumulative occurrence of incremental gust vertical load factor–Aircraft 5	B-32
Cumulative occurrence of incremental maneuver vertical load factor–Aircraft 1	B-33
Cumulative occurrence of incremental maneuver vertical load factor–Aircraft 2	B-34
Cumulative occurrence of incremental maneuver vertical load factor–Aircraft 3	B-35
Cumulative occurrence of incremental maneuver vertical load factor–Aircraft 4	B-36
Cumulative occurrence of incremental maneuver vertical load factor–Aircraft 5	B-37
Exceedance in seconds of maximum bending moment per 1000 hours–Aircraft 1	B-38
Exceedance in seconds of maximum bending moment per nautical mile–Aircraft 1	B-39
Exceedance in seconds of maximum bending moment per 1000 hours–Aircraft 3	B-40
Exceedance in seconds of maximum bending moment per nautical mile–Aircraft 3	B-41
Exceedance in seconds of maximum bending moment per 1000 hours–Aircraft 4	B-42
Exceedance in seconds of maximum bending moment per nautical mile–Aircraft 4	B-43

In almost every case, the frequency of occurrence of negative incremental maneuver load factors for SEAT aircraft agreed well with those of Hall’s FAA report [7]. However, for positive values, there was significant disagreement with the results shown in this document, especially at higher load factors. The source of these differences is unclear, but similar disagreements were also shown in the FAA report by Rokhsaz et al. [11].

Cumulative occurrences of weight-normalized incremental gust vertical load factor are shown in figures B-13–B-17. As a reminder, weight-normalized values are equivalent load factors acting on the airframe at MTOW. When the weight reduction due to retardant or chemical release, or fuel consumption, was taken into account, it resulted in a lower equivalent vertical load factor. As indicated in these figures, the impact of normalization on the gust load factors was evident more in their frequencies of occurrence. However, the effect on the maneuver load factors was significant, as shown in figures B-18–B-22. In every case, normalizing the loads resulted in reduction of the load factor or shifting of the entire curve to the left. While positive load factors became less severe, the negative load factors became more severe. The authors find the reduction in the positive loads reasonable. However, consistent with the underlying concept, perhaps the negative load factors should have been normalized differently. After all, if the reduction in the

aircraft weight reduces the stresses on the airframe due to positive load factors, it should have the same effect in the case of negative load factors.

### 5.1.2 Bending Moment

Exceedance in seconds of maximum bending moments at strain gauge locations are shown in figures B-23–B-26, per 1000 hours and per nautical mile, respectively. In each case, the results are shown on a linear scale first, followed by the same information on a semi-logarithmic scale. Each type of scale offers its own advantages in allowing visualization of the results. Only three of the five aircraft had useable strain gauge outputs. Also, because of the differences in gross weights, strain gauge locations, and the internal structural arrangement, the bending moments for the AT-802A and PZL M18 differed by one order of magnitude. The reader is reminded of the earlier discussion regarding the fidelity of the bending moment data and the caveats associated with the calibration of the strain gauges.

Despite the limited number of hours, the differences between the SEAT (Aircraft 3) and agricultural operations (Aircraft 4) are clear from part (b) of these figures. In general, as the aircraft weight decreased, so did the bending moment. Therefore, the abscissa in these figures can be thought of as time in the reverse order (i.e., mission progressing from right to left along this axis). Both airframes were subjected to the same bending moments at gross weight. However, on the agricultural aircraft, the bending moment was relieved gradually over time, whereas on the SEAT aircraft this happened suddenly, highlighted by the inflection in the curve at approximately 60,000 in-lb. Therefore, the latter airframe was subjected to the larger bending moment over a longer time period. The details of this behavior could be seen more clearly when the data was separated by phases. Figures B-25 and B-26 convey the same information, but per nautical miles.

## 5.2 PHASE-SPECIFIC LOADS

Durations and distances flown in each phase are shown in figure B-27 for all aircraft. This figure also shows the overall time and distance flown. The reader is cautioned that, because of the gaps between individual phases, the sums of the times and distances for various phases do not add up to those of the overall values.

### 5.2.1 Gust and Maneuver Load Factors

Cumulative occurrences of incremental gust vertical load factor are shown in figures B-28–B-32. Examination of the figures pertaining to SEATs shows that the frequency of occurrence of the loads during the drop phase far exceeded those of other phases. However, the reader is reminded that this phase did not last more than a few seconds per flight. The frequencies of occurrence of vertical gust load factor during other phases were comparable, with the exit phase roughly exceeding the others. However, it should be noted that because the aircraft weighed significantly less during the exit phase than during the entry, the higher load factors of the former phase do not translate directly into higher structural stresses. Also, in every case, the slightly larger gust load factors during Cruise 2, compared with Cruise 1, are the result of lower wing loading associated with the former.

The results for Aircraft 4, shown in figure B-31, differed from those of the SEATs in that the gust loads from all flight phases showed frequencies of occurrence that were much closer to each other. This can be attributed to two factors. First, agricultural spraying takes place at quite low altitudes, regardless of the phase. Therefore, the aircraft is mostly operated inside the boundary layer on the ground. Secondly, these aircraft are not subject to the same level of atmospheric convective activity as it presents in the vicinity of a fire zone. As a result, while the gust load factors for the drop phase were slightly larger than those of the other phases, the differences were not as large as those for the SEAT. Again, the load factors were slightly higher during Cruise 2 than during Cruise 1 due to the difference in the wing loadings between these two phases.

Cumulative occurrences of the incremental maneuver load factors are presented in figures B-33–B-37. The largest number of hours of data was available from Aircraft 1. Therefore, the plots for this aircraft show the least amount of scatter. On the other hand, the least amount of data was associated from Aircraft 3. Consequently, it is the hardest to establish clear trends from the results of its data.

In general, the results from the SEAT aircraft showed the highest incremental maneuver loads to be associated with drop, exit, and entry phases—in that order. This was expected in that most drop phases lasted for several seconds. Therefore, the load factors generated in this phase as the result of retardant release were associated with maneuvers. Also, drops are generally followed by rather aggressive maneuvering, turns, or pull-ups to exit the area. This was assumed to be the contributor to the larger maneuver load factors in this phase. Again, the differences between Cruise 1 and Cruise 2 phases could be attributed to the difference in the weight between them.

The results from agricultural applications showed the largest loads to be associated with the turns, although no incremental load factors above +1.6 g were detected. Therefore, even though these loads appear to be higher, they are actually just more frequent. The fact that the loads from the drop phase were less severe than the turns was expected in that the former is flown very close to the ground, with little necessity for aggressive maneuvering.

It is noteworthy that the occurrences of maneuver load factors were approximately one order of magnitude fewer than those of gust-induced loads. This is in contrast with the results shown in Hall's FAA report [7]. Also, positive and negative gust load factors occurred with roughly the same frequency, but positive maneuver load factors were detected about 10 times more frequently than negative load factors.

### 5.2.2 Bending Moment

As a reminder, these results were available from only three of the airframes. Also, the method of obtaining these exceedance charts, and the conditions under which the strain gauges were calibrated, have to be taken into account in the process of interpreting these results. Finally, because each format offered a different perspective of the bending moment behavior, both linear and semi-logarithmic formats are presented in the following material.

For Aircraft 1, exceedances in seconds per 1000 hours and per nautical mile are shown in figures B-38 and B-39. These figures show that the bending moment was the largest for Cruise 1 and entry phases because the aircraft was near gross weight during these phases. The next most

severe case was that of the drop phase, which lasted only a few seconds. While these three phases appear to resemble each other closely on the semi-logarithmic scale, the linear scale shows that the bending moments were not as severe during the drop phase. Similarly, the semi-logarithmic scale shows a difference of almost two orders of magnitude at higher values of bending moment for the exit and Cruise 2 phases. However, the linear scale shows the two cases almost matching.

These trends differ somewhat from those of maneuver loads in which the drop case was always the most severe, followed by the exit phase. The differences in the trends can only be attributed to the effect of the aircraft weight, which was not included in the normal accelerations but was present in bending moments. Because of the inherent noise in the strain gauge signal, it was not possible to separate the effect of the aircraft weight from the loads imposed by gusts and maneuvers.

Similar trends can also be seen in the results from Aircraft 3, which are shown in figures B-40 and B-41. It is noteworthy that the scale of the abscissa in these figures is one order of magnitude different from those of the previous figures because of the differences in weight and strain gauge locations.

Although the trends are consistent with those of Aircraft 1, the results from various phases are farther apart in this case. The authors attribute this to the scarcity of the data, which resulted from this aircraft being taken out of service in mid-season (146 hours for Aircraft 1 versus 44 hours for Aircraft 3).

Finally, the bending moments from Aircraft 4 are presented in figures B-42 and B-43. These results can be compared with those of Aircraft 3 because of their similar airframes and strain gauge locations. It is obvious from these figures that the largest bending moments were associated with the turn phase. If one interprets the abscissa as the inverse of time, these figures show that the fully loaded aircraft performing turns would result in the largest bending moments, as expected. However, as the aircraft weight decreases with time, the severity of the bending moments, per 1000 hours or nautical mile, would decrease below that of the Cruise 1 phase. The drop phase showed the third largest bending moments. These results are not in agreement with those from the maneuver load factors because the latter did not include the effect of the aircraft weight.

## 6. SUMMARY

Operational data recorded from five agricultural aircraft were used to compare their usage and flight loads. The fleet consisted of two Air Tractor AT-802As, two PZL M18s, and one Ayres Thrush S2R-T45 aircraft. One AT-802A was fitted with a 1650-hp Garrett engine, but the modification did not alter its MTOW. Four of the airframes were used as SEAT, and the fifth was flown exclusively for agricultural applications. The data collectively consisted of 354 hours of flight time on the SEAT and 104 hours of the agricultural operation.

Missions were divided into five airborne phases for the SEAT aircraft and four phases for agricultural applications. Some of the information extracted from these data pertained to airframe

usage, but the emphasis was placed on flight loads. The information about loads was presented as exceedance charts, for the overall flight, and for individual phases.

The majority of the SEAT missions were shown to last less than 1 hour. Also, most missions were flown at relatively low AGL altitudes. Maximum airspeed and coincident altitudes were determined and shown to be well within the aircraft limitations. Likewise, *V-n* diagrams of individual airframes showed that at no time were any of the limit load factors exceeded. Examination of the pitch and roll angles showed their extreme values to be associated with agricultural missions.

For each aircraft, individual flight phases were examined and compared. Average distance and duration of each phase were determined as well as the maximum altitude and indicated airspeeds. *V-n* diagrams were generated for each phase and aircraft. Because of the similarities in the type of flying, Cruise 1, Cruise 2, and ferry missions were compared and shown to have similar loads. In the case of SEAT aircraft, drop phases showed the largest maximum load factors, although they remained below the maximum allowable limits.

Gust and maneuver vertical load factors were separated using the 2-second rule, and their cumulative occurrences were presented per 1000 hours and per nautical mile. Overall gust and maneuver loads for all missions were compared with those of ferry flights, when available. Comparison was also made of the cumulative occurrences of maneuver load factors with other sources. Cumulative occurrences of gust loads for the three types of mission (i.e., firefighting, agricultural, and ferry missions) were shown to be very similar. Because of the availability of more SEAT data, their exceedance charts could be extended to slightly higher load factors. However, comparison of the maneuver load factors showed a great deal of difference between the ferry and firefighting missions, with the latter indicating more aggressive maneuvering and load factors that extended to larger values. The majority of the larger load factors are believed to be associated with the drop phase, in which the retardant release produced relatively large load factors. In addition, while the gust load factors were similar between agricultural and firefighting missions, the maneuver load factors were not, at least in the positive range. In the case of agricultural missions, the positive load factors did not reach very high values, but they occurred at much larger frequency than those of the SEAT missions.

Weight-normalized overall vertical load factors were compared with the recorded values. As expected, the reduction in aircraft weight also reduced the severity of the gust load factors. However, normalizing resulted in overall shifting of the maneuver loads to lower values. While the effect of normalizing on the gust loads was as expected, the impact on the maneuver load factors was not and, as a result, deserves further scrutiny.

All five aircraft were equipped with a single strain gauge mounted on the upper side of a lower spar cap. However, useable data was available from only three airframes. Cumulative exceedance of wing bending moments in seconds, at strain gauge locations, and subject to the constraints of the calibration process were determined for overall flights. The results were presented on a linear scale and a semi-logarithmic scale for clarity and adherence to tradition.

Cumulative occurrences of gust and maneuver load factors were determined for individual phases. Both gust and maneuver load factors associated with the drop phase were shown to be

the most severe, followed by the exit phase. However, a comparison of these results with the bending moment behavior showed that while the accelerations were higher during the exit phase, the wing bending moments were larger during the entry phase. The disagreement appears to be due to the difference in aircraft weight between the entry and exit phases.

## 7. CONCLUSIONS AND RECOMMENDATIONS

The objectives of this program were met. Considering that the data were not collected in a controlled laboratory setting, their overall quality was quite good. However, due to the limited number of flight hours, especially from agricultural operations, it is difficult to draw broad conclusions and arrive at statistically significant findings. Nonetheless, the results presented here should be useful to the FAA, aircraft manufacturers, and operators in helping them to better determine the direction of future investigations in this area. In the following text, brief discussions of some of the noteworthy findings of this preliminary effort are outlined.

The results presented in this report appear to match the expected outcomes. The altitude, airspeed, and distance data revealed flight profiles that were consistent with the purposes of these aircraft. One aircraft was used exclusively for agricultural spraying, whereas the others were flown as single-engine air tankers (SEATs). The fact that the two types of aircraft were flown differently was apparent in the usage data. The former was flown with very large pitch and roll angle excursions, whereas the latter group was subjected to more docile maneuvers. Nonetheless, a comparison of the usage data with their operational limits and other published data revealed that all aircraft were operated well within their limits. Some of the interesting findings that may require further investigation were:

- In general, SEATs are used for shorter missions than those flown for agricultural applications. Therefore, the former airframes are subjected to a larger number of takeoffs and landings per 100 hours. The necessity for slightly shorter inspection intervals of the landing gear components for these aircraft should be studied.
- SEATs experience relatively large load factors during the drop phase. These load factors, mostly driven by the release of nearly half of the aircraft weight, occur once per flight. Conversely, aircraft used for agricultural applications are subjected to more moderate loads but with a significantly higher frequency per flight.
- The load factors alone do not necessarily translate into large wing bending moments because of the change in aircraft weight. Generally, the largest vertical load factors are associated with the drop phase on SEAT, but the largest wing bending moments occur when the aircraft is flown near maximum takeoff weight.
- A comparison of the maneuver vertical load factor spectra with that of other sources revealed much less severity than expected. The differences warrant further scrutiny of the current and past results. This can be accomplished only through the collection of much larger volumes of operational data.
- Traditionally, the severity of structural loads is inferred from measured normal load factors. However, in the case of agricultural and firefighting operations, where up to half of the weight can be in the form of retardant or chemicals, this practice may result in erroneous conclusions concerning airframe fatigue life.

## 8. REFERENCES

1. FAA Report. (1996). Flight Loads Data for a Boeing 737-400 in Commercial Operation (DOT/FAA/AR-95/21).
2. FAA Report. (2005). Statistical Data for the Boeing-747-400 Aircraft in Commercial Operations (DOT/FAA/AR-04/44).
3. FAA Report. (2006). Statistical Loads Data for the Boeing 777-200ER Aircraft in Commercial Operations (DOT/FAA/AR-06/11).
4. FAA Report. (2000). Statistical Loads Data for BE-1900D Aircraft in Commuter Operations (DOT/FAA/AR-00/11).
5. FAA Report. (2007). Statistical Loads Data for the Embraer-145XR Aircraft in Commercial Operations (DOT/FAA/AR-07/61).
6. FAA Report. (1993). General Aviation Aircraft–Normal Acceleration Data, Analysis and Collection Project (DOT/FAA/CT-91/20).
7. FAA Report. (2005). Consolidation and Analysis of Loading Data in Firefighting Operations: Analysis of Existing Data and Definition of Preliminary Air Tanker and Lead Aircraft Spectra (DOT/FAA/AR-05/35).
8. Appareo. GAU 2000. Retrieved from <http://www.appareo.com>.
9. USGS. (2015, July, 2). 3DEP Products and Services. Retrieved from <http://ned.usgs.gov/about.html>.
10. FAA Report. (1999). An Evaluation of Methods to Separate Maneuver and Gust Load Factors from Measured Acceleration Time Histories (DOT/FAA/AR-99/14).
11. FAA Report. (2011). Usage and Maneuver Loads Monitoring of Heavy Air Tankers (DOT/FAA/AR-11/7).

APPENDIX A—USAGE DATA

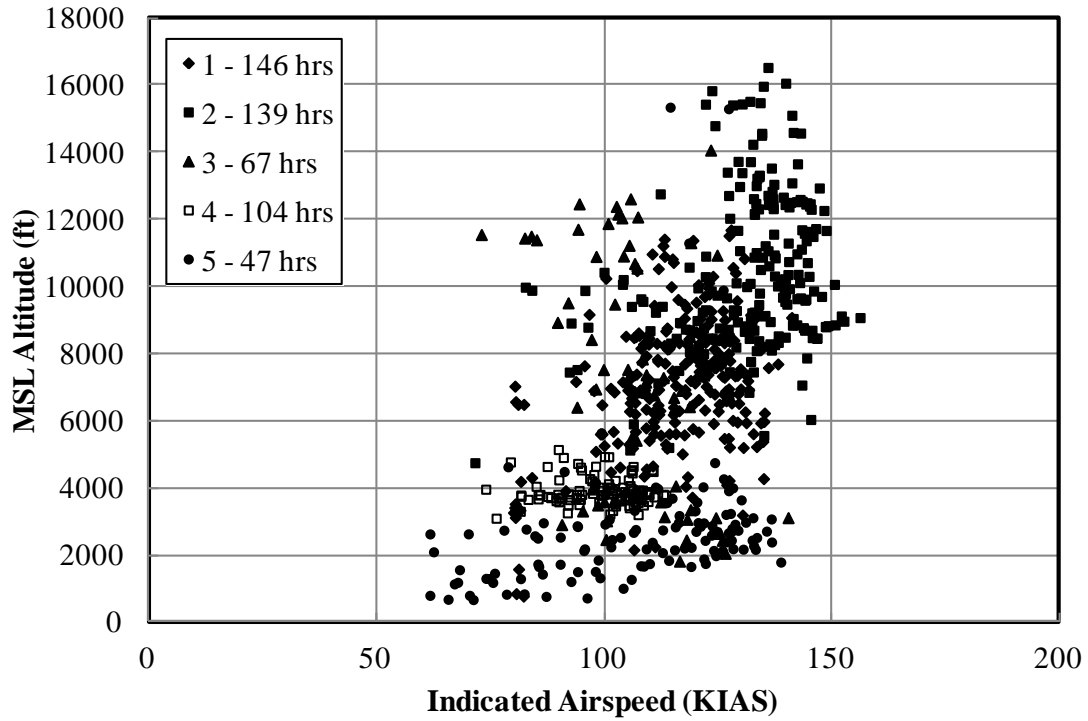


Figure A-1. Maximum altitude and coincident indicated airspeed—all phases

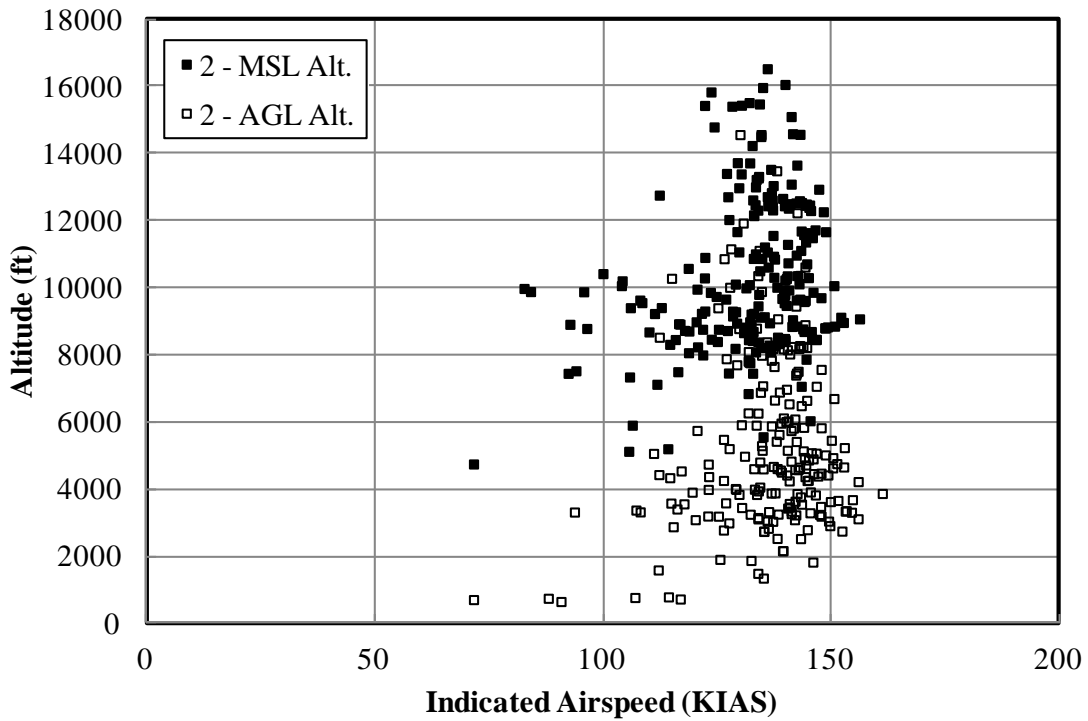


Figure A-2. Comparison of maximum MSL and AGL altitudes—Aircraft 2

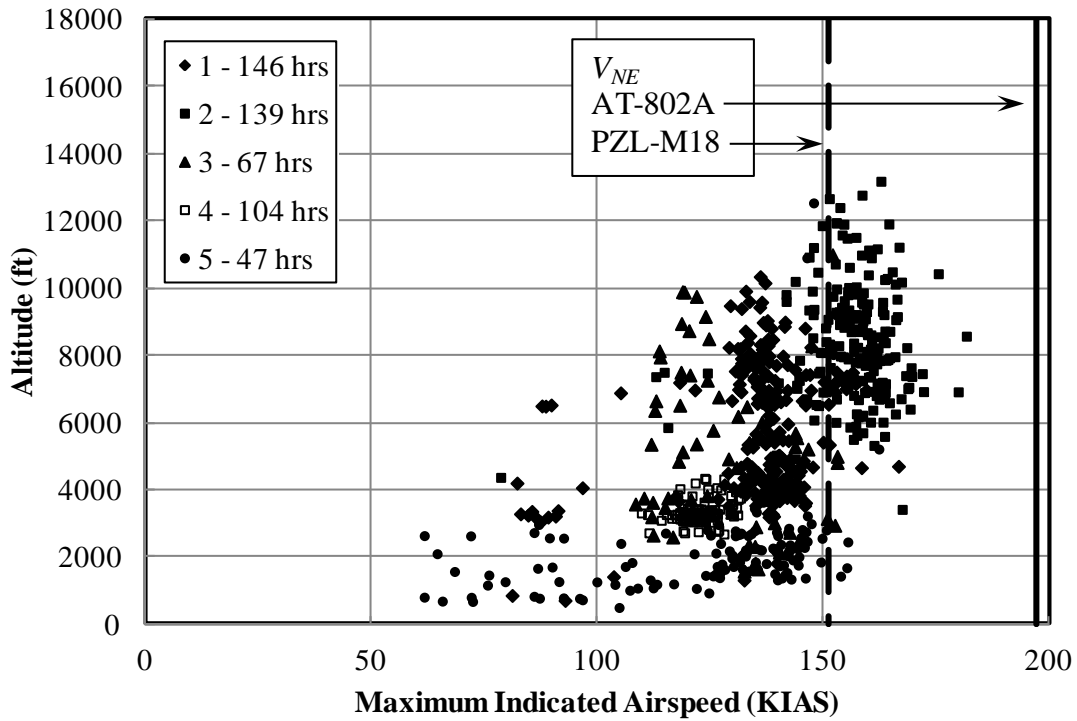


Figure A-3. Maximum indicated airspeed and coincident MSL altitude—all phases

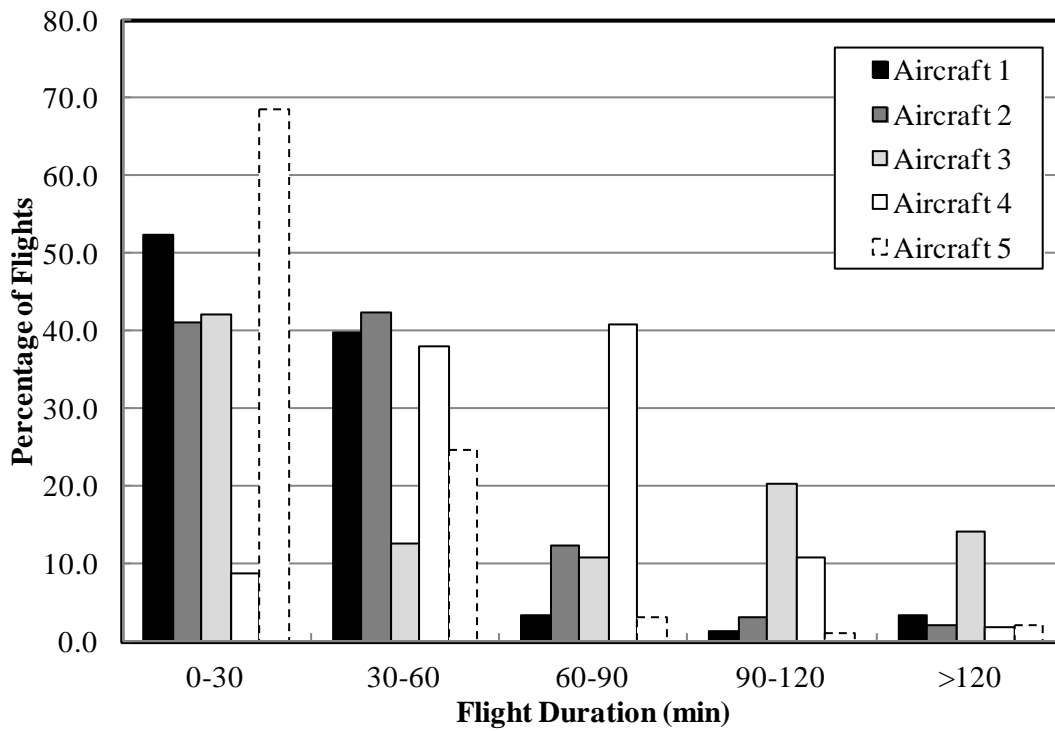
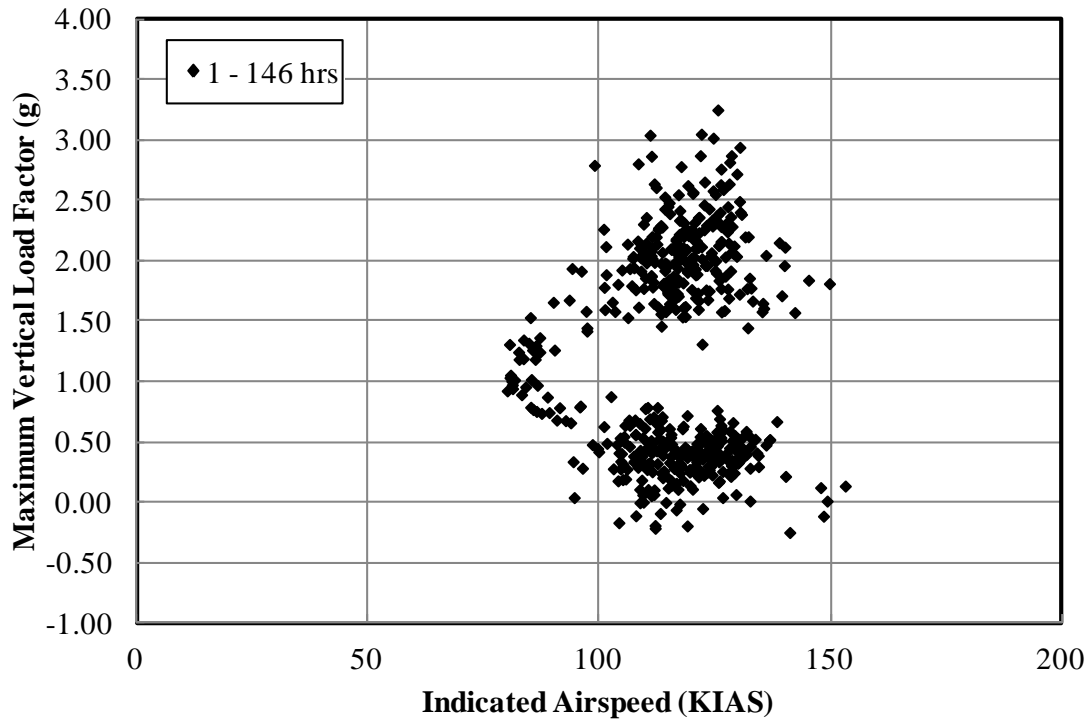
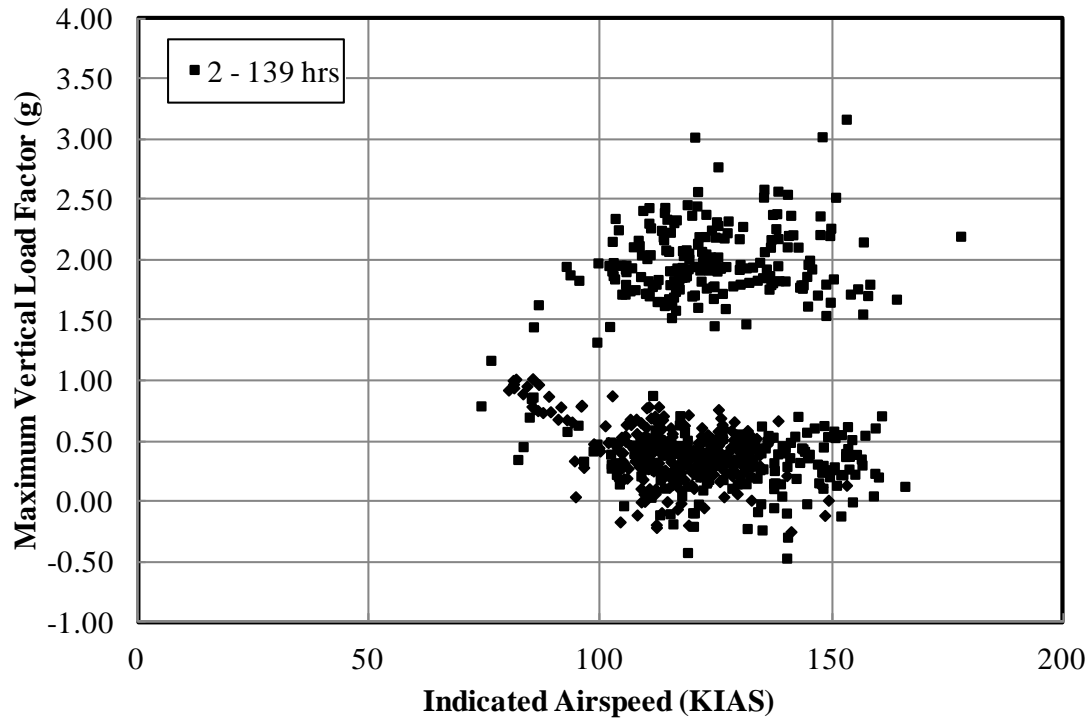


Figure A-4. Percentage of flights based on duration—all phases



(a) Aircraft 1



(b) Aircraft 2

**Figure A-5. Vertical load factor and coincident indicated airspeed—all phases**

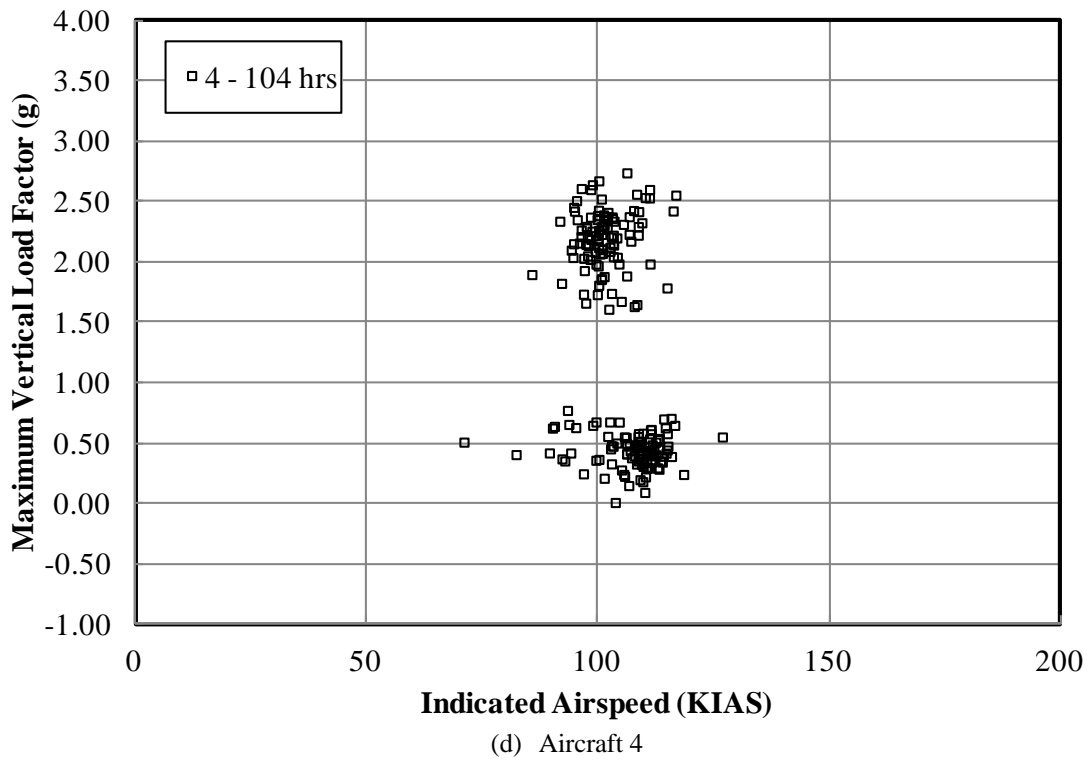
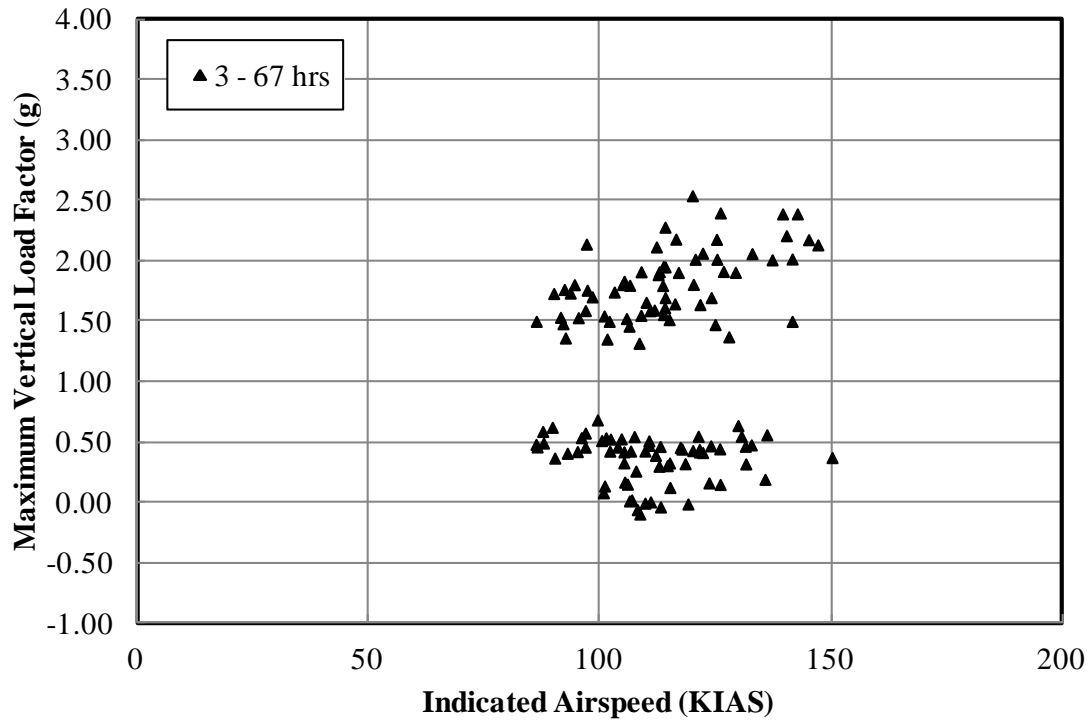
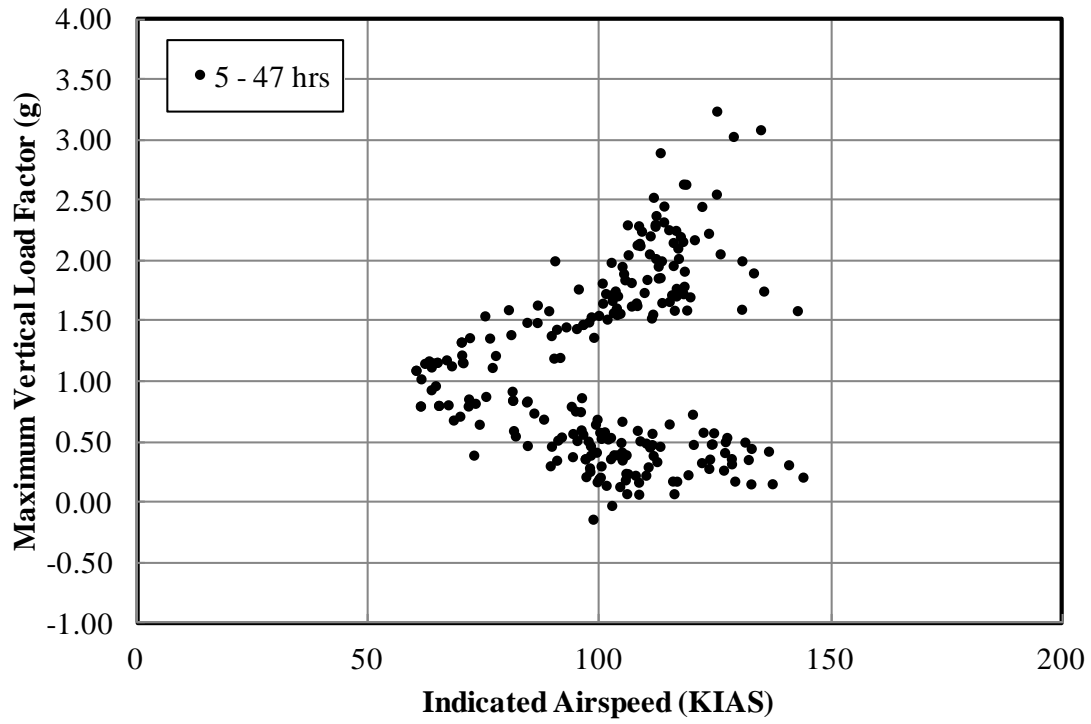
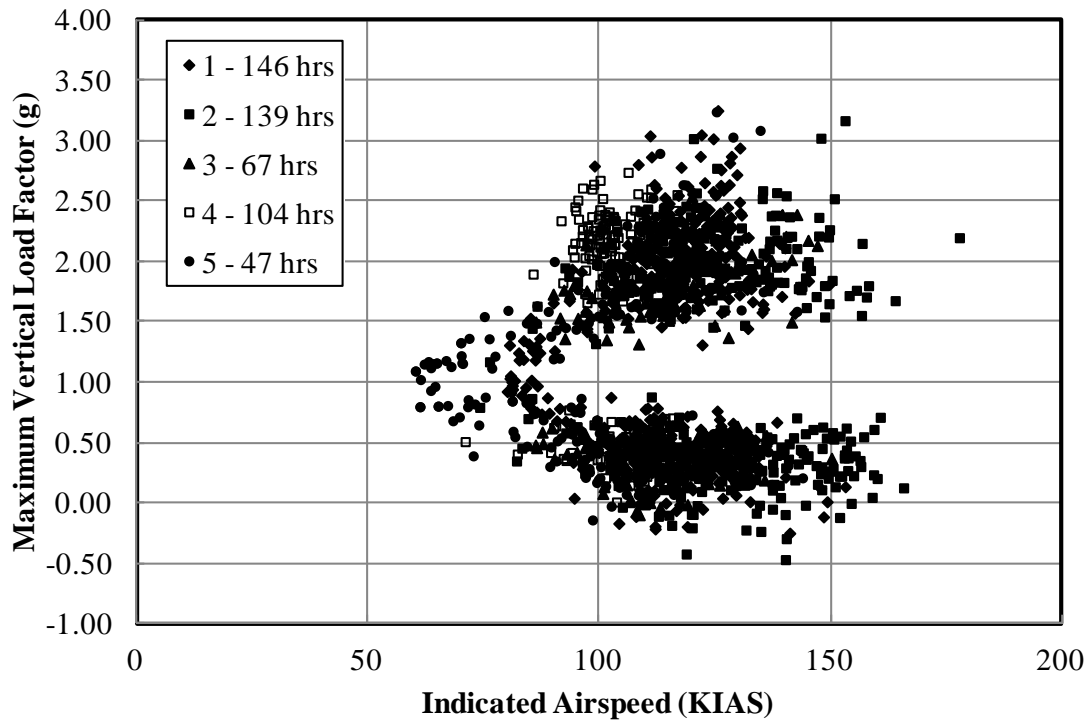


**Figure A-5. Vertical load factor and coincident indicated airspeed—all phases (continued)**



(e) Aircraft 5



(f) All aircraft

**Figure A-5. Vertical load factor and coincident indicated airspeed—all phases (continued)**

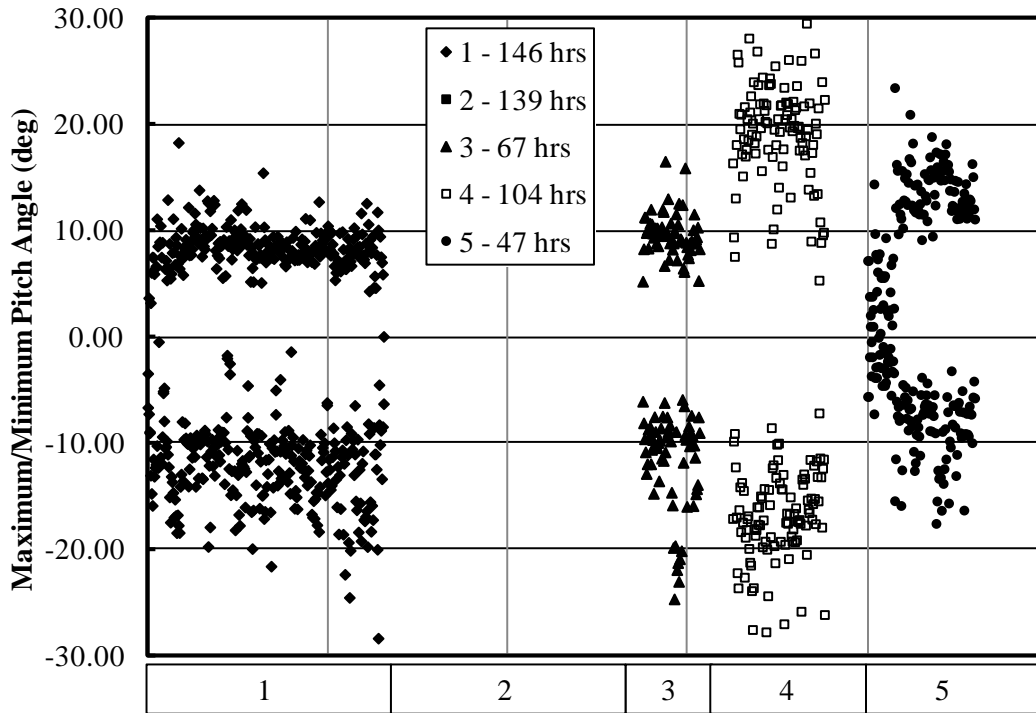


Figure A-6. Maximum and minimum pitch angle—all phases

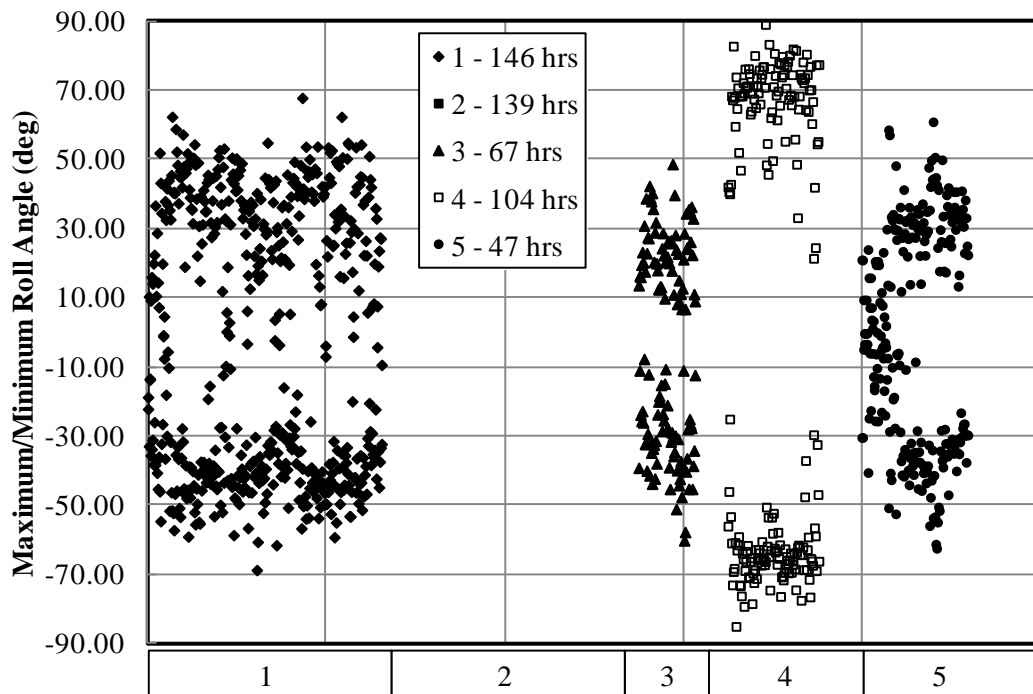
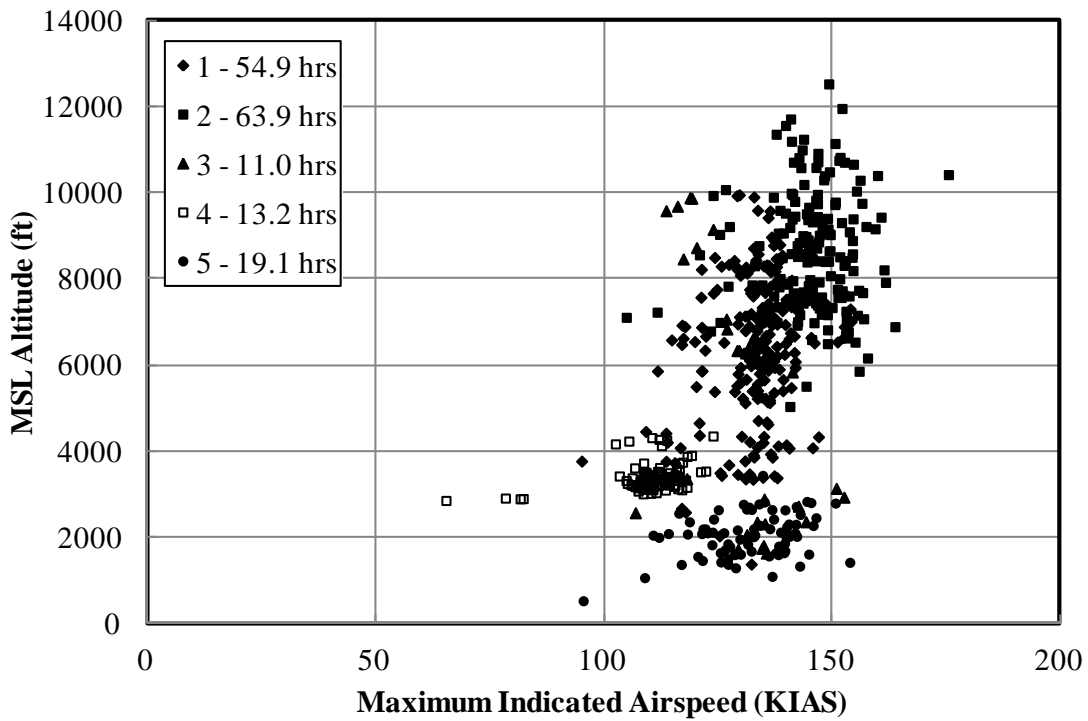


Figure A-7. Maximum and minimum roll angle—all phases

Duration			
Aircraft	Average (minutes)		
	Cruise 1	Cruise 2	Ferry
1	15.10	10.23	66.65
2	21.78	13.62	54.12
3	17.79	14.28	101.64
4*	7.90	7.79	—
5	14.86	10.17	13.44
Distance			
Aircraft	Average (nm)		
	Cruise 1	Cruise 2	Ferry
1	33.35	23.26	153.50
2	52.01	36.33	147.59
3	35.86	29.04	193.73
4*	13.90	14.85	—
5	28.92	21.08	31.14

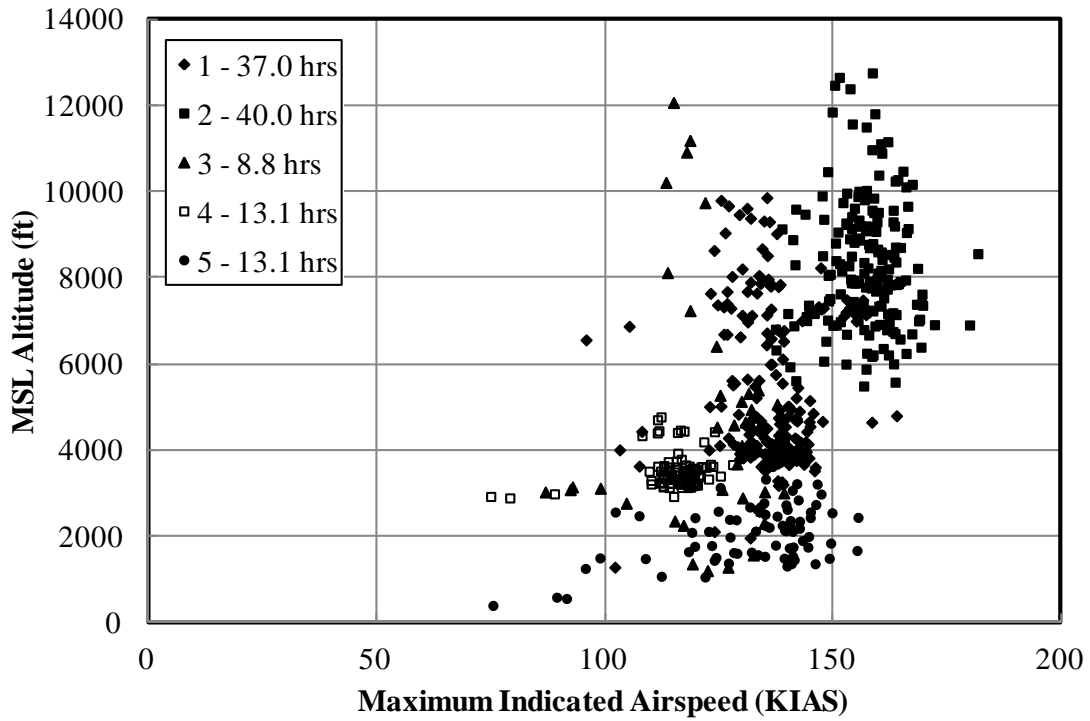
\* Only one ferry flight was detected

**Figure A-8. Average duration and distance for cruise and ferry flights**

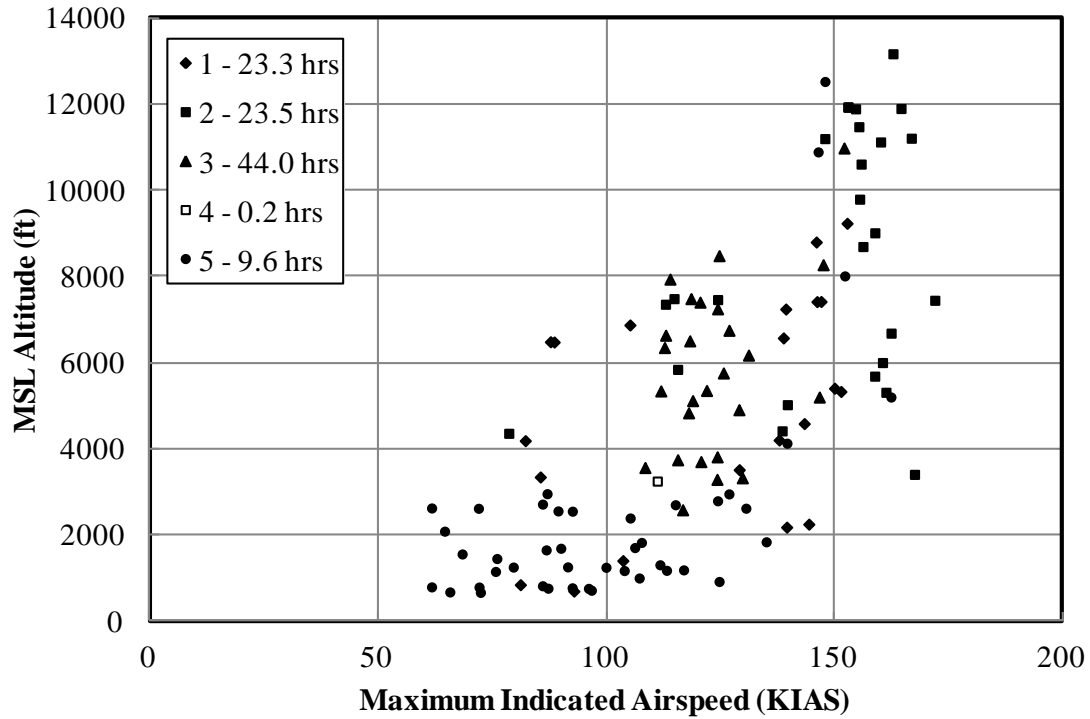


(a) Cruise 1

**Figure A-9. Maximum indicated airspeed and coincident MSL altitude**

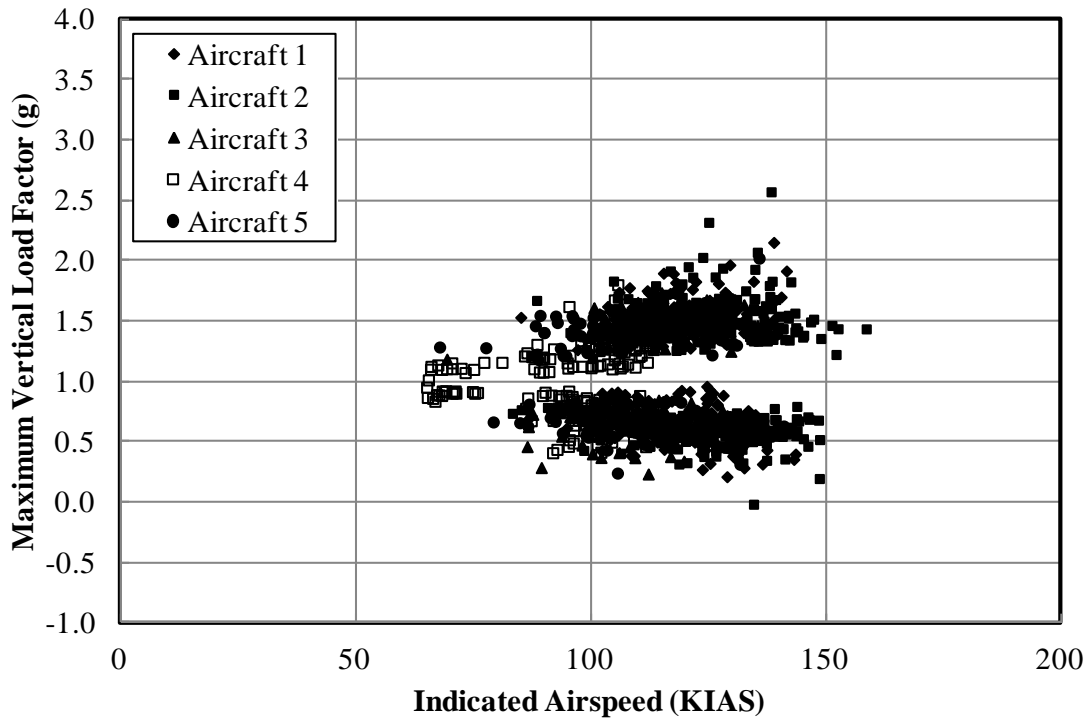


(b) Cruise 2

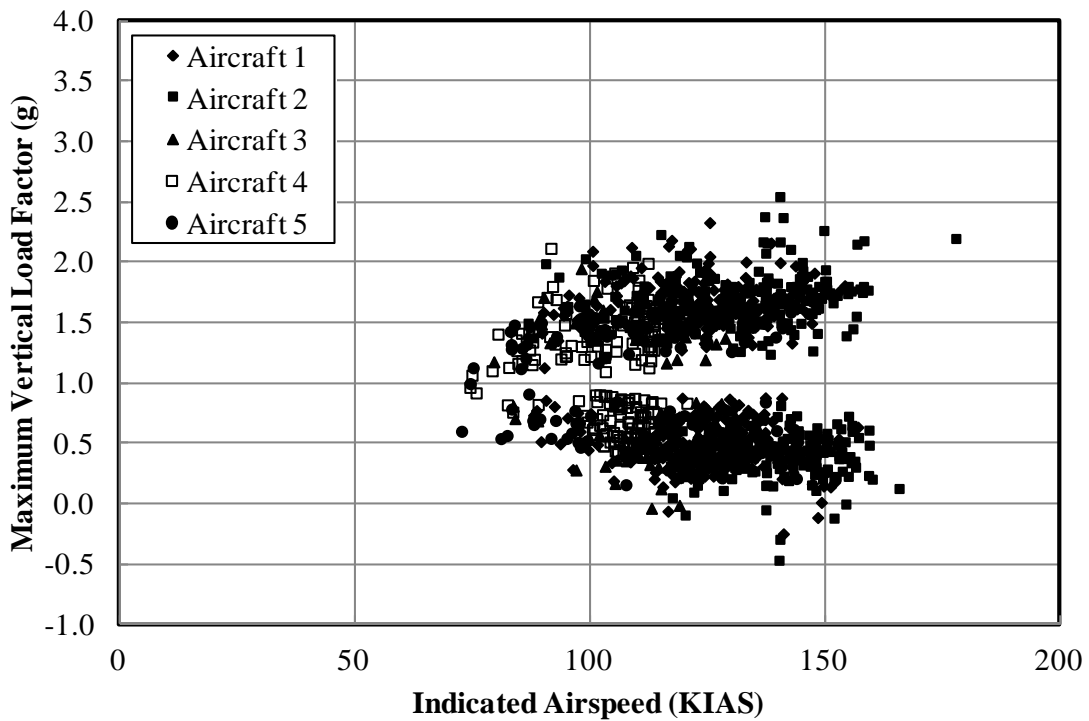


(c) Ferry

**Figure A-9. Maximum indicated airspeed and coincident MSL altitude (continued)**



(a) Cruise 1



(b) Cruise 2

**Figure A-10. Maximum vertical load factor and coincident indicated airspeed**

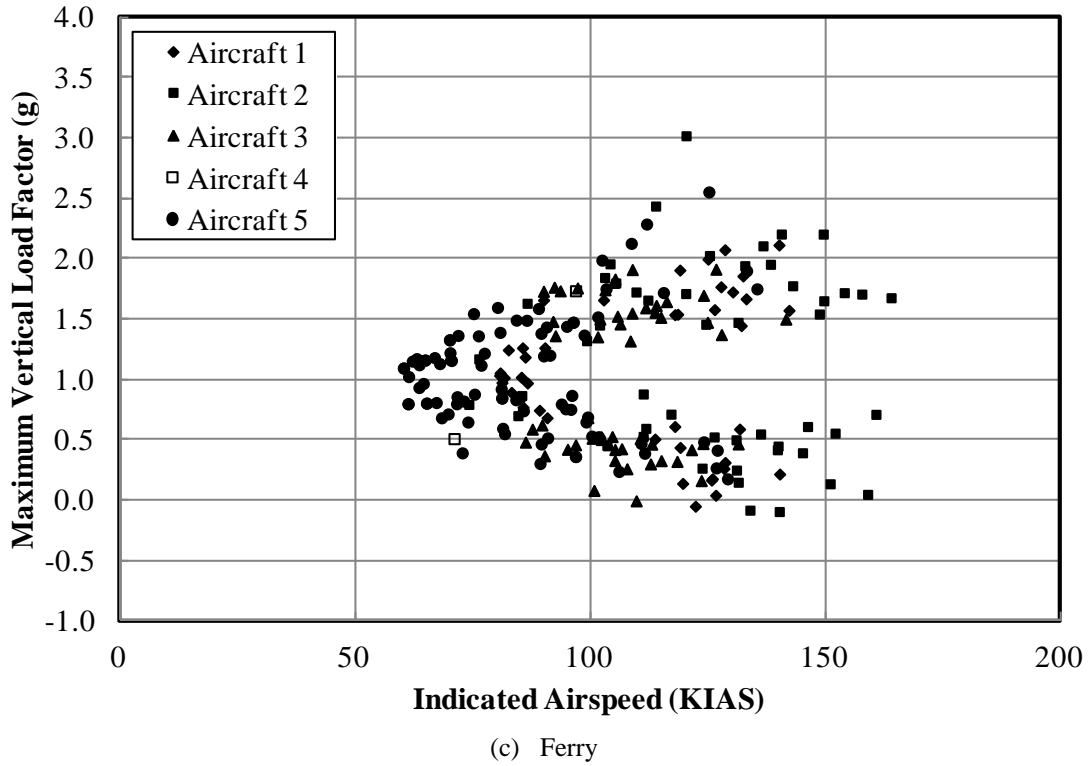
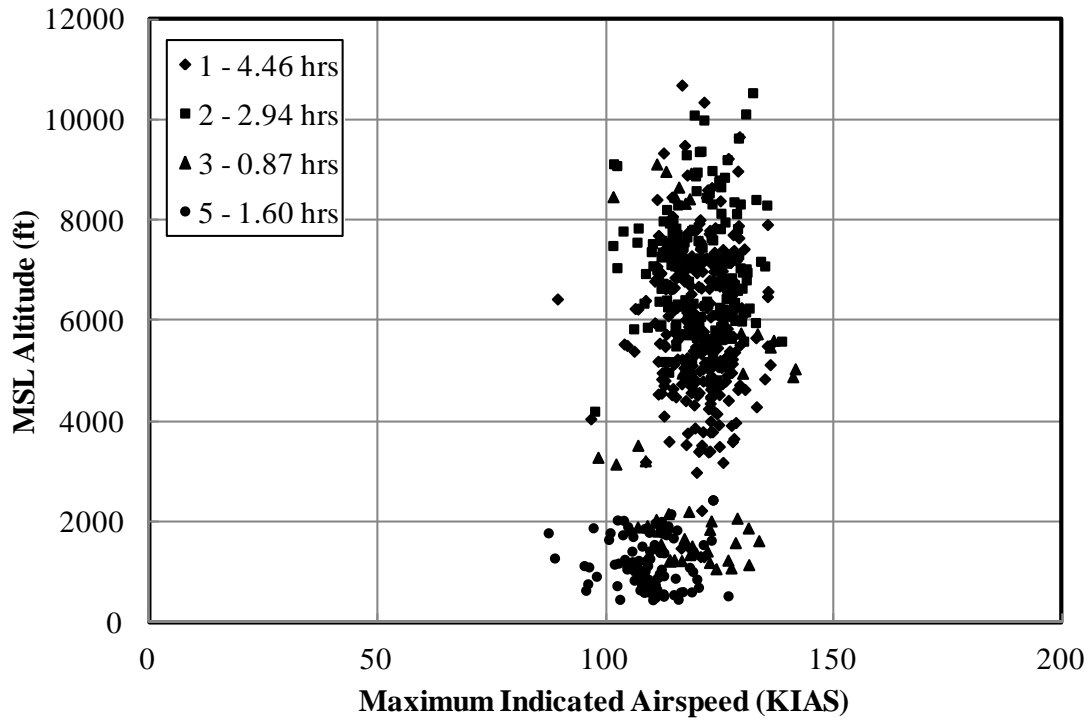


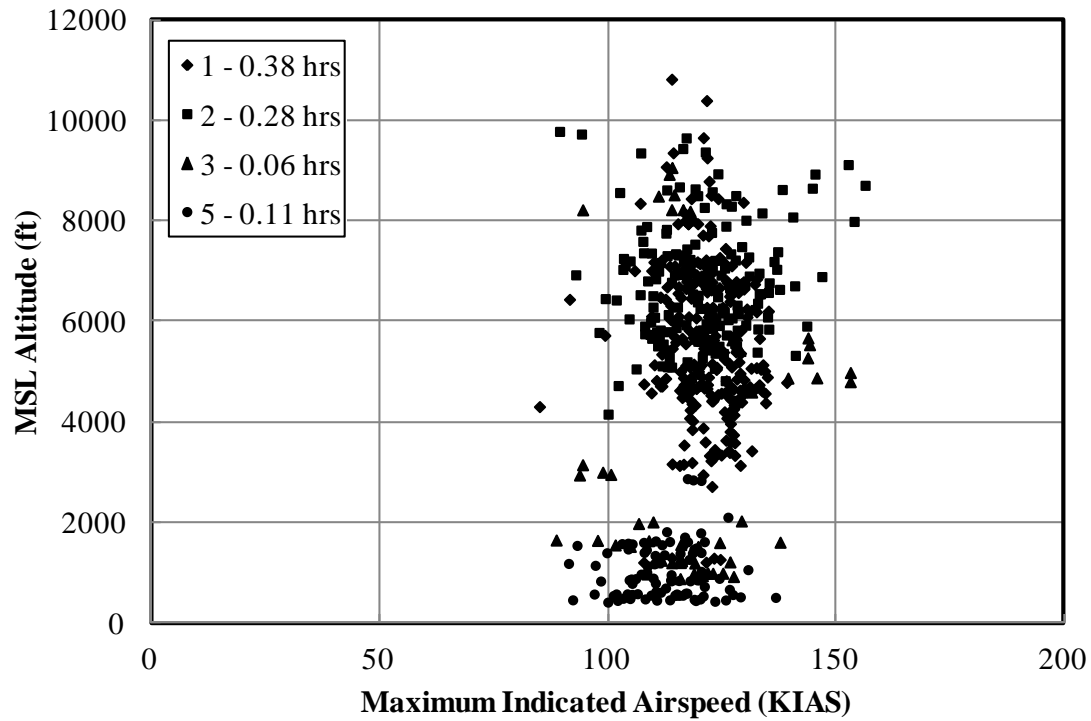
**Figure A-10. Maximum vertical load factor and coincident indicated airspeed (continued)**

Duration (sec)		
Aircraft	Average	
	Drop	Turn
1	5.15	—
2	5.00	—
3	4.12	—
4	16.24	40.31
5	4.24	—
Distance (nm)		
Aircraft	Average	
	Drop	Turn
1	0.19	—
2	0.20	—
3	0.14	—
4	0.52	1.21
5	0.13	—

**Figure A-11. Average duration and distance for drops and turns**

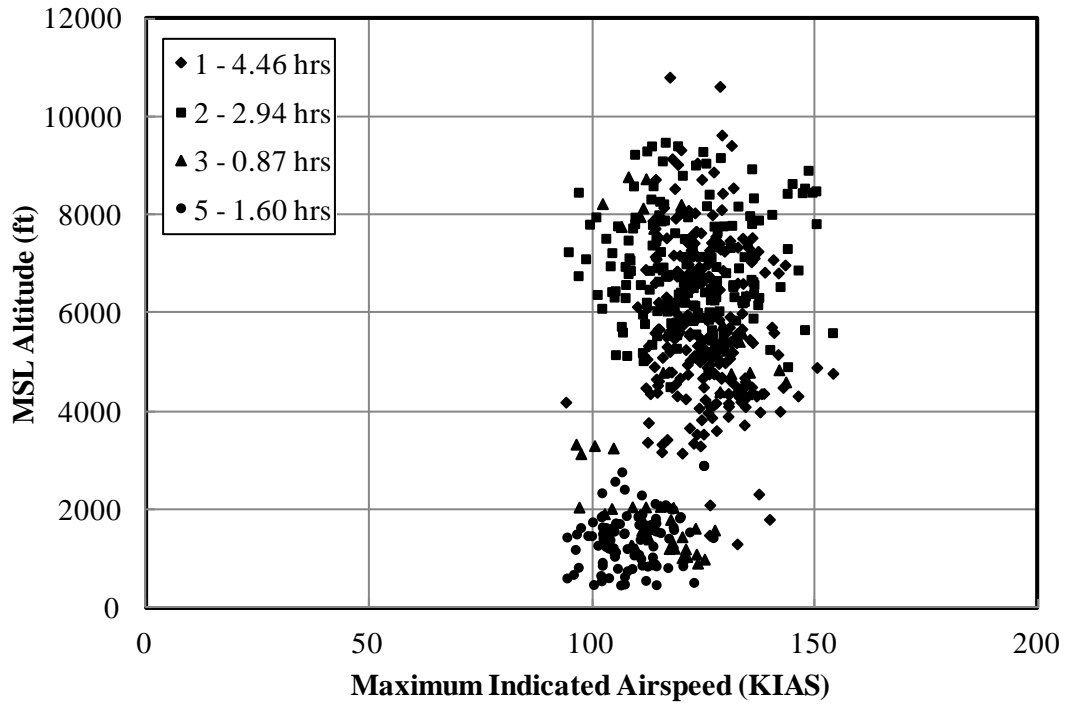


(a) Entry



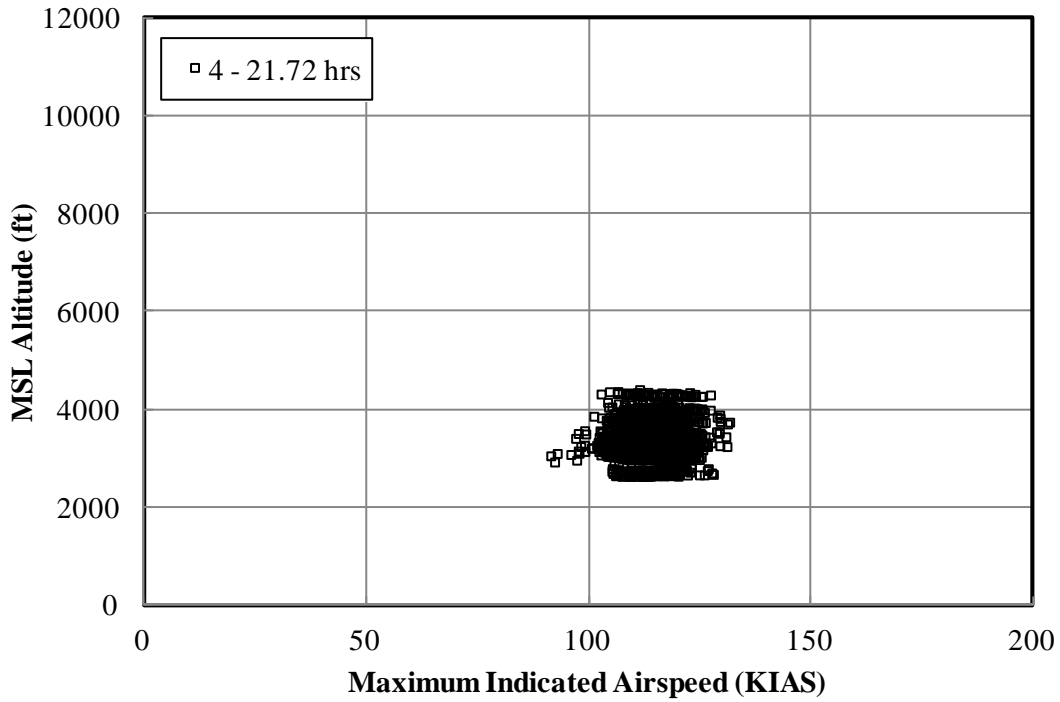
(b) Drop

**Figure A-12. Max indicated airspeed and coincident MSL altitude–SEAT**



(c) Exit

**Figure A-12. Max indicated airspeed and coincident MSL altitude–SEAT (continued)**



(a) Drop

**Figure A-13. Maximum indicated airspeed and coincident MSL altitude–agricultural application**

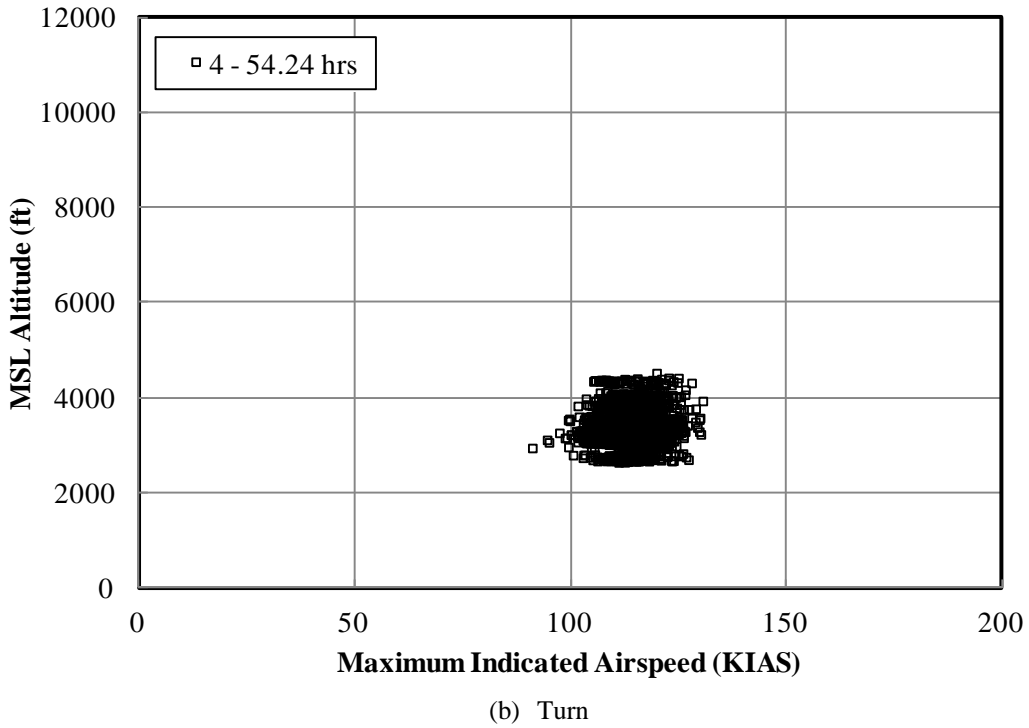


**Figure A-13. Maximum indicated airspeed and coincident MSL altitude—agricultural application (continued)**

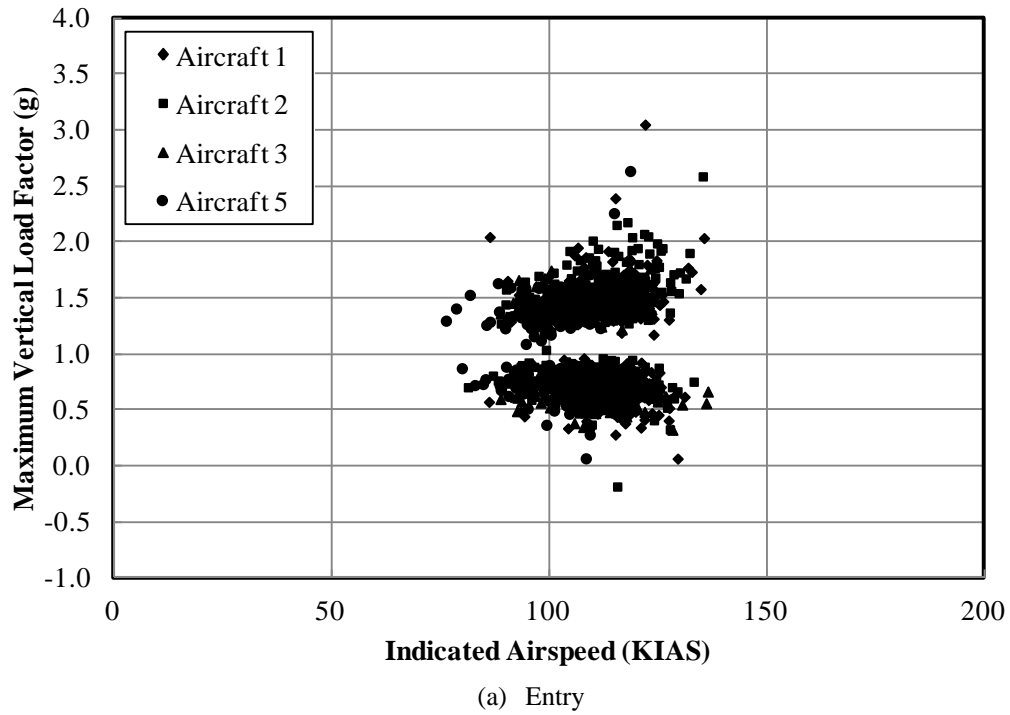
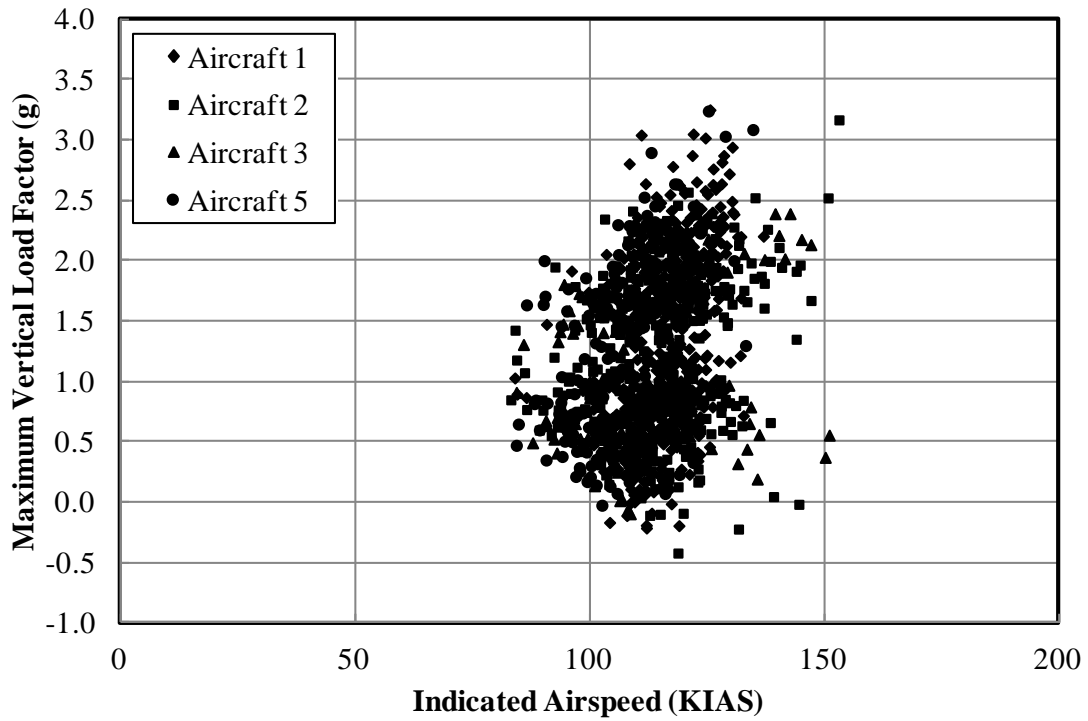
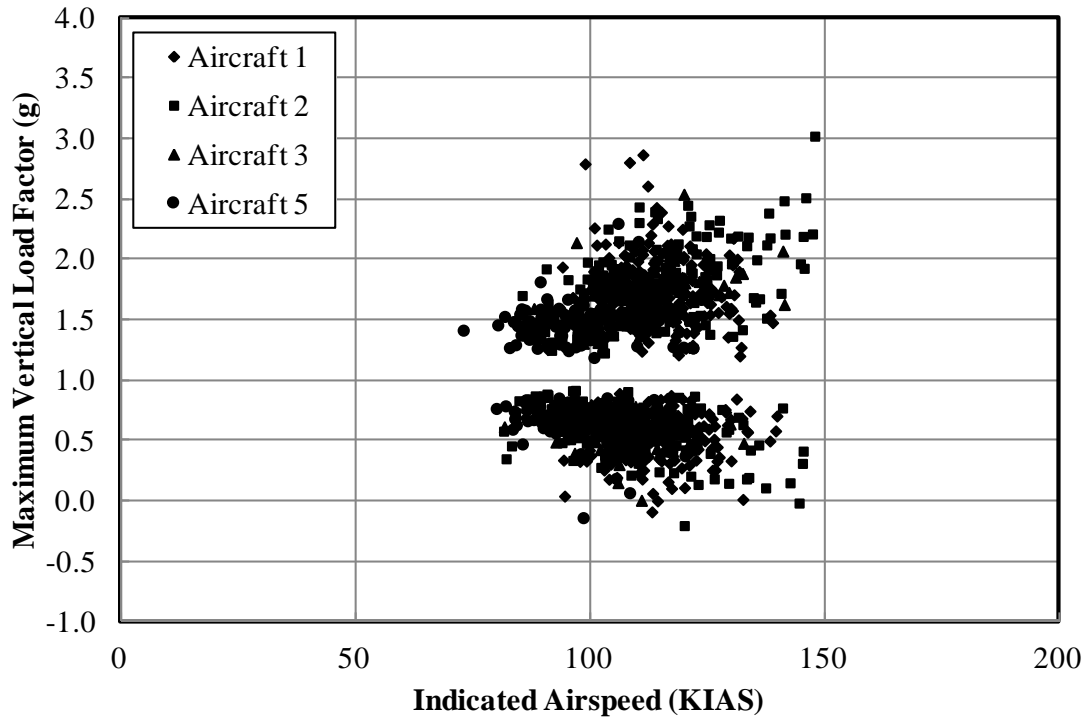


**Figure A-14. Maximum vertical load factor and coincident indicated airspeed—SEAT**

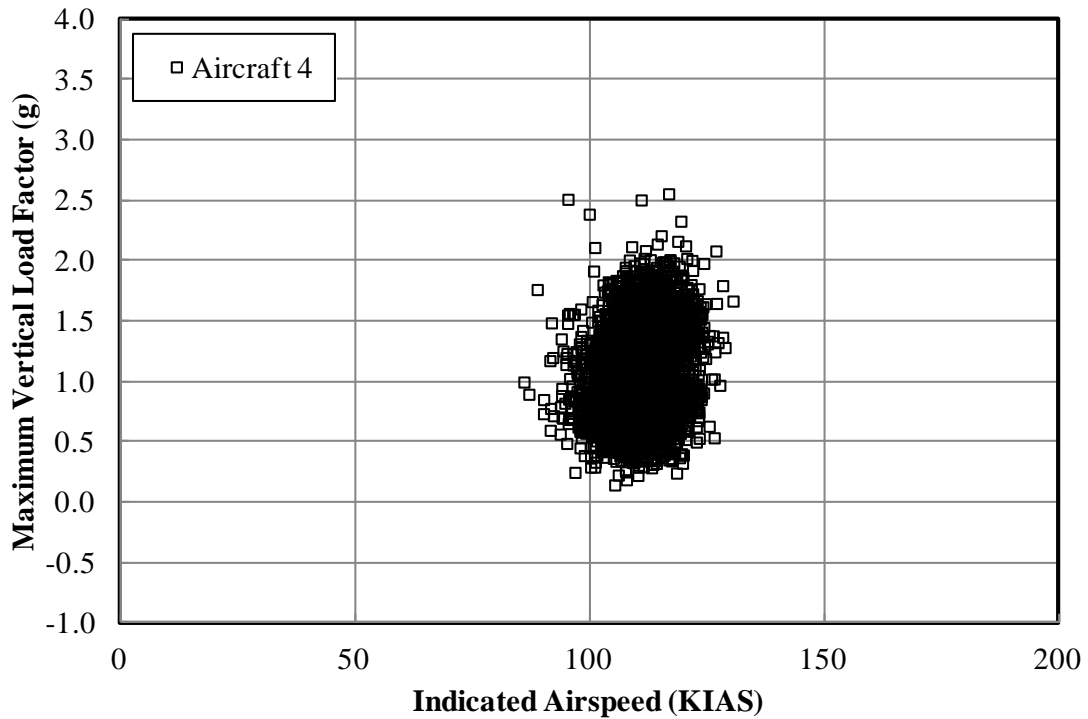


(b) Drop

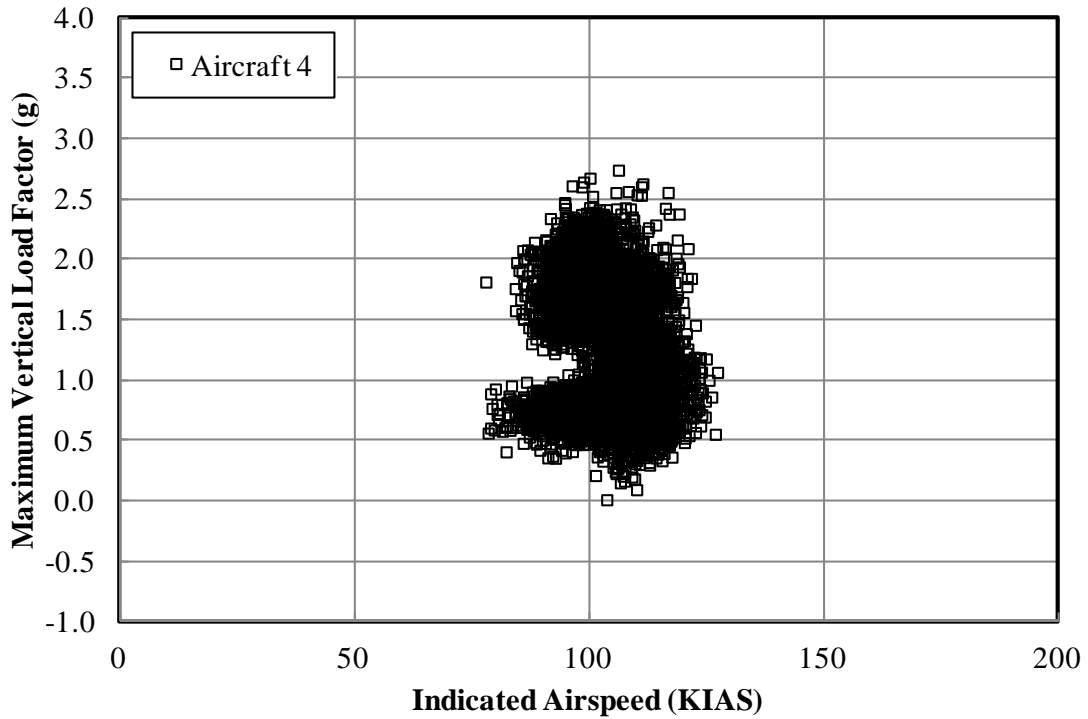


(c) Exit

**Figure A-14. Maximum vertical load factor and coincident indicated airspeed–SEAT (continued)**



(a) Drop



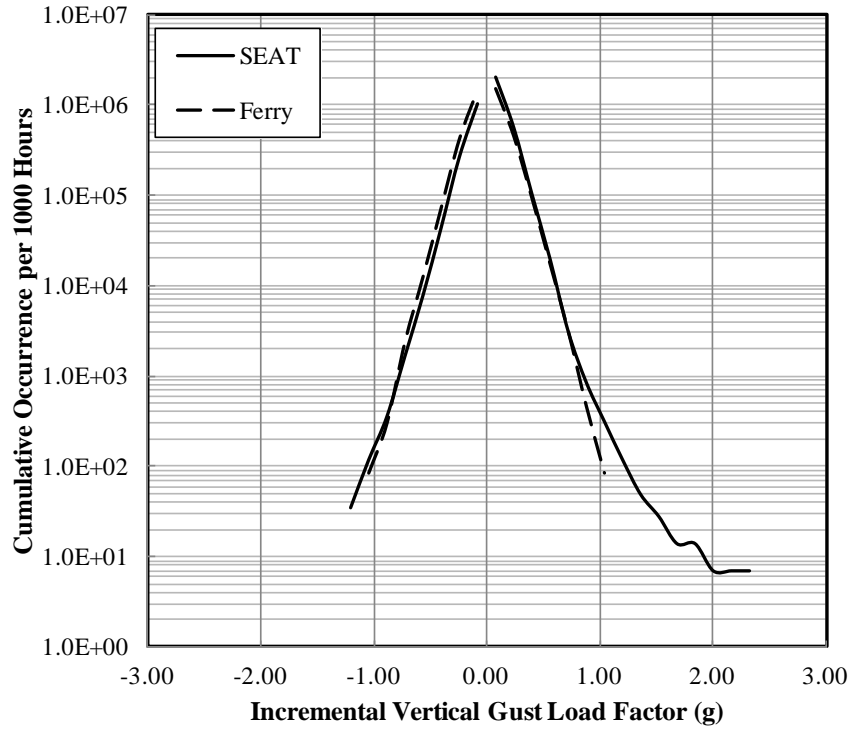
(b) Turn

**Figure A-15. Maximum vertical load factor and coincident indicated airspeed—agricultural applications**

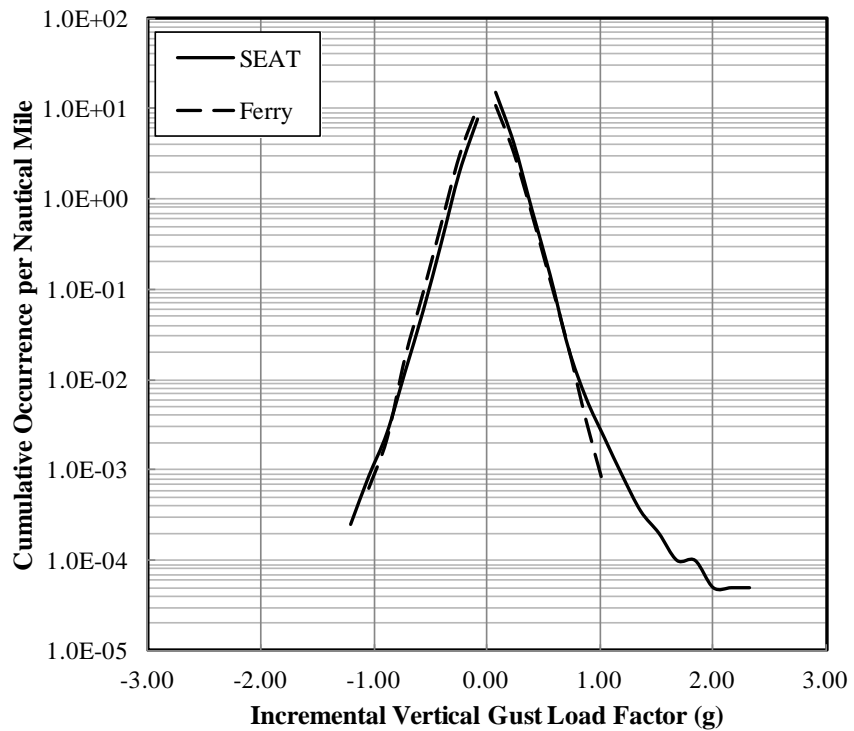
APPENDIX B—LOADS DATA

Aircraft	Duration (hr)	Distance (nm)
1	146.46	19,838
2	115.83	17,085
3	44.04	5,037
4	103.98	11,463
5	47.47	5,792

**Figure B-1. Summary of overall duration and distance**

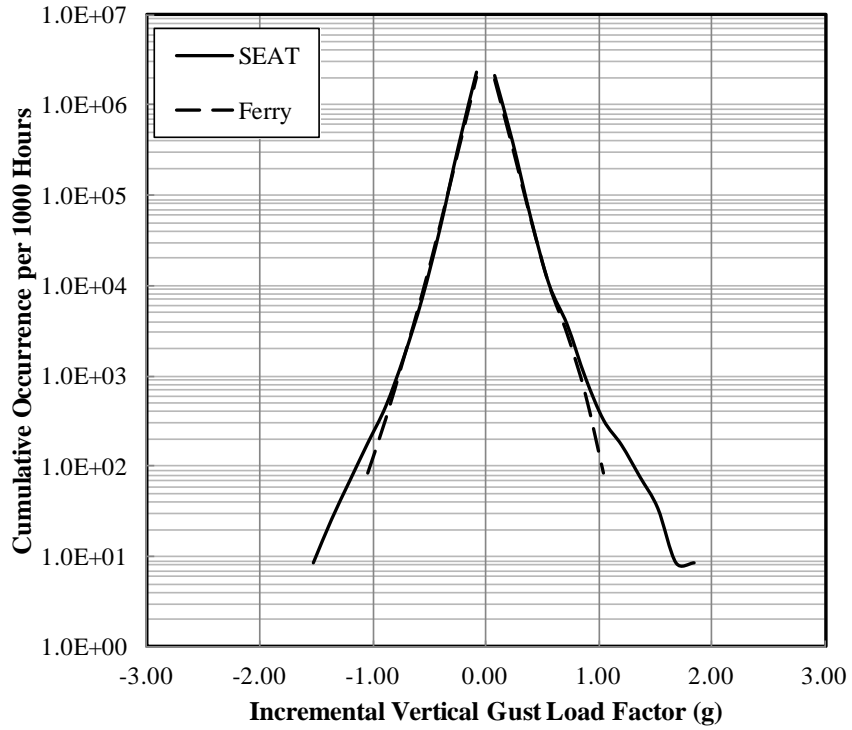


(a) Per 1000 hours

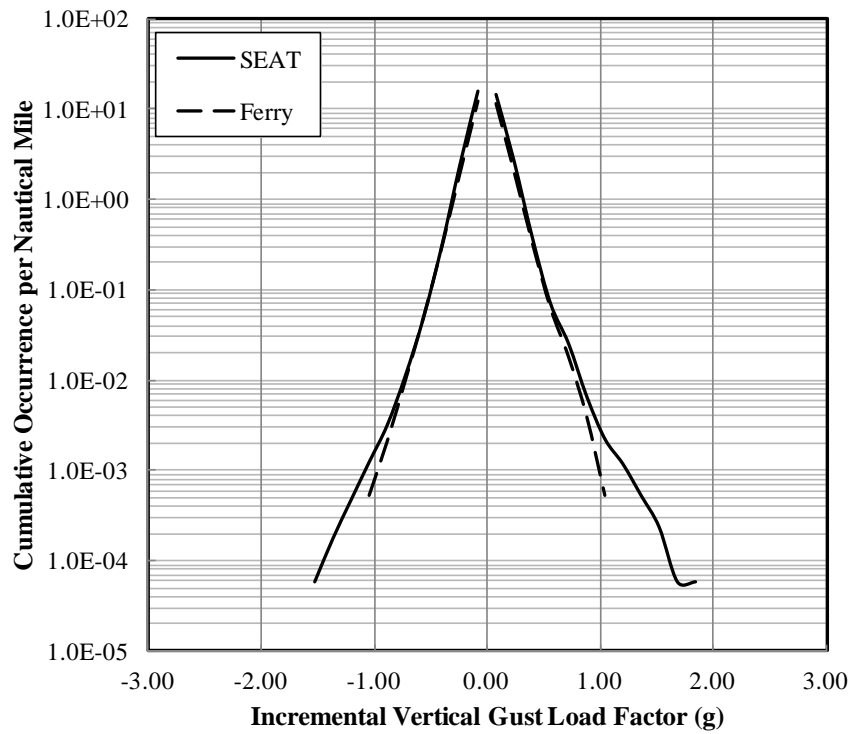


(b) Per nautical mile

**Figure B-2. Cumulative occurrence of incremental gust vertical load factor–Aircraft 1**

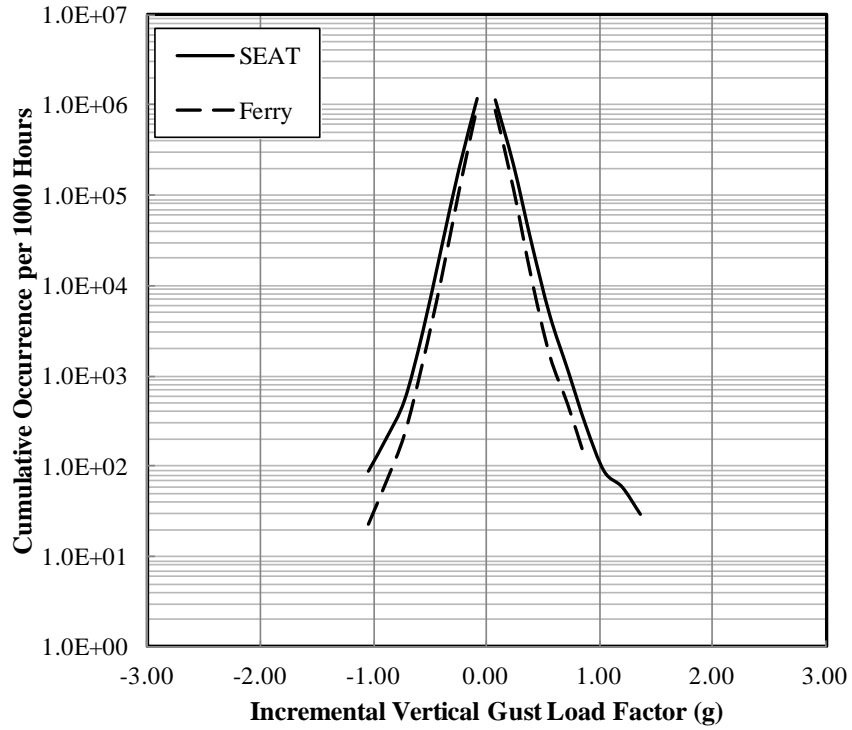


(a) Per 1000 hours

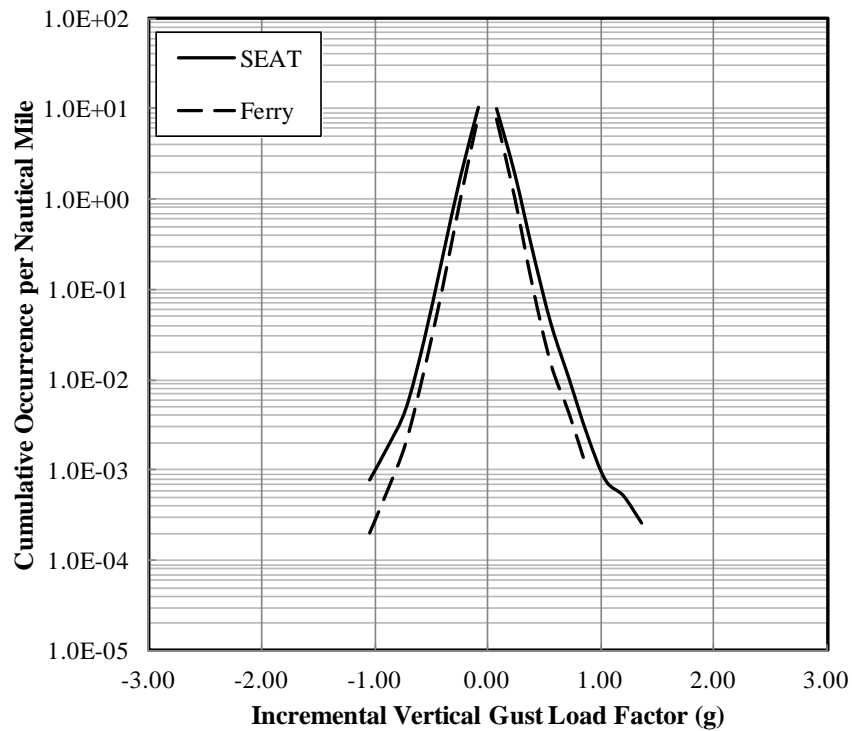


(b) Per nautical mile

Figure B-3. Cumulative occurrence of incremental gust vertical load factor–Aircraft 2

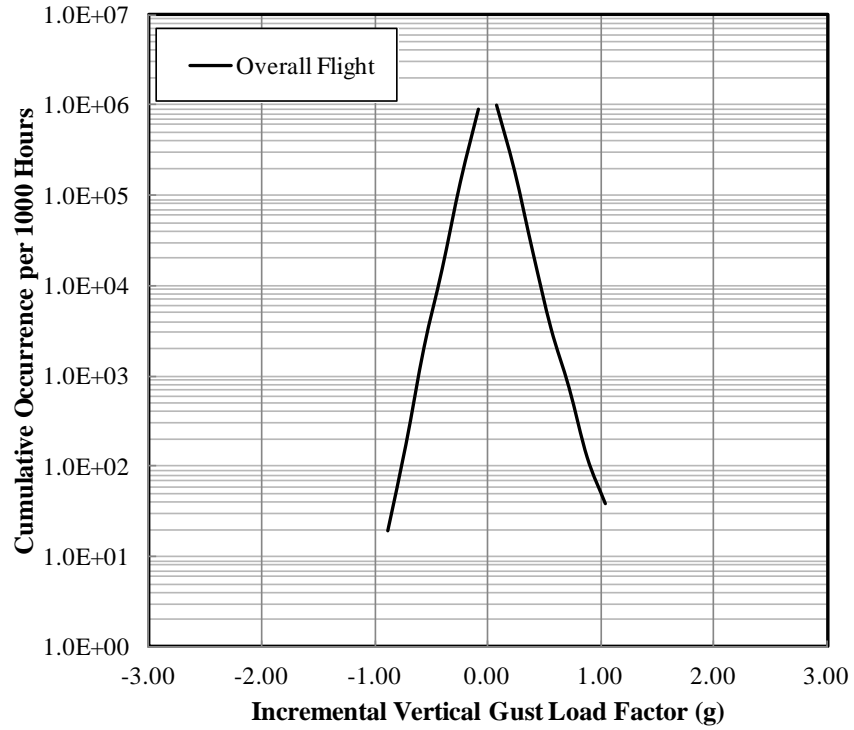


(a) Per 1000 hours

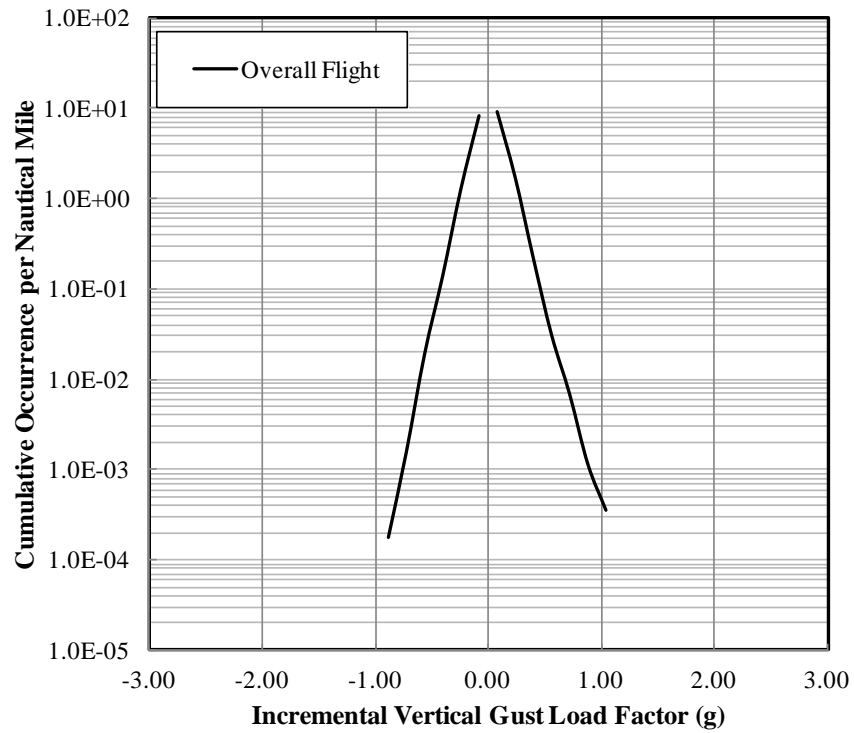


(b) Per nautical mile

**Figure B-4. Cumulative occurrence of incremental gust vertical load factor–Aircraft 3**

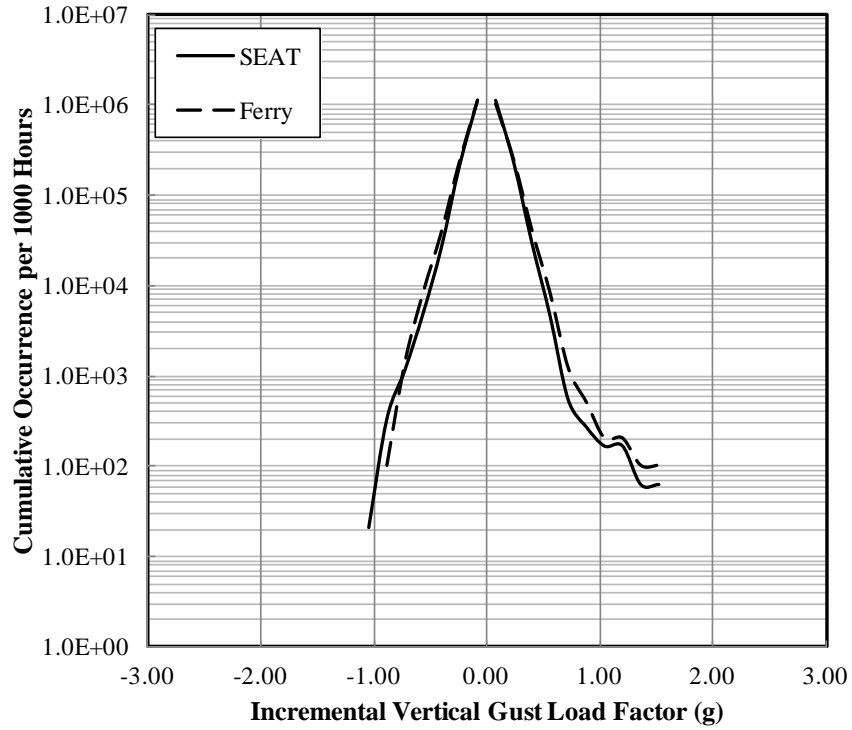


(a) Per 1000 hours

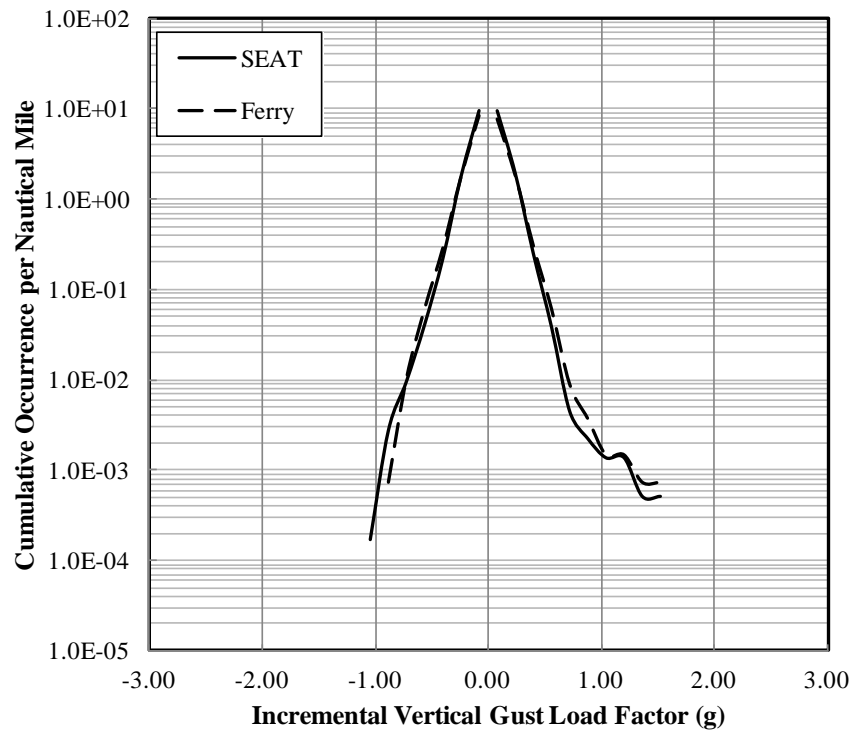


(b) Per nautical mile

**Figure B-5. Cumulative occurrence of incremental gust vertical load factor—Aircraft 4**

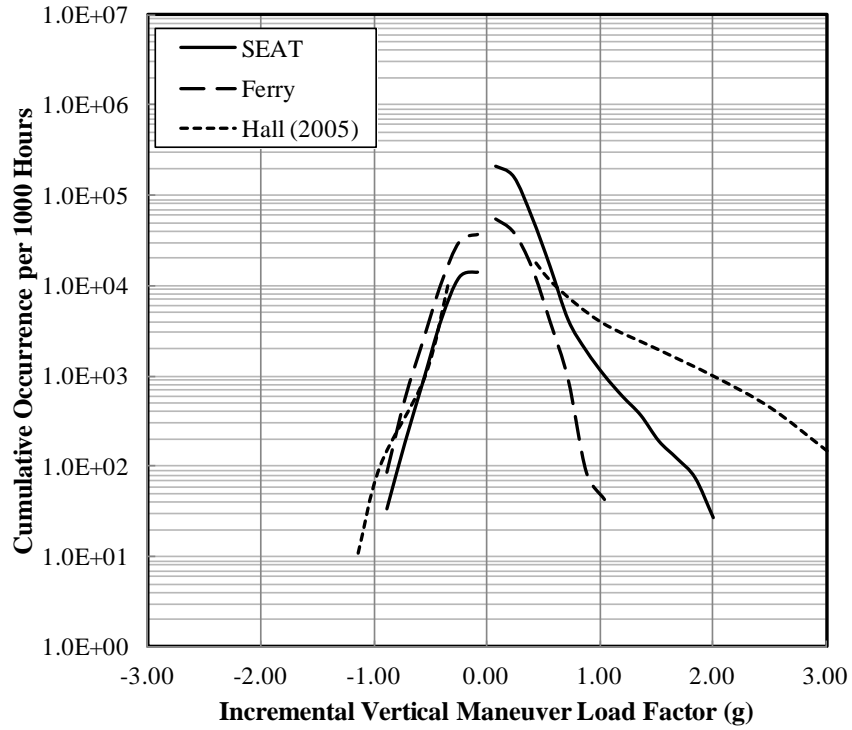


(a) Per 1000 hours

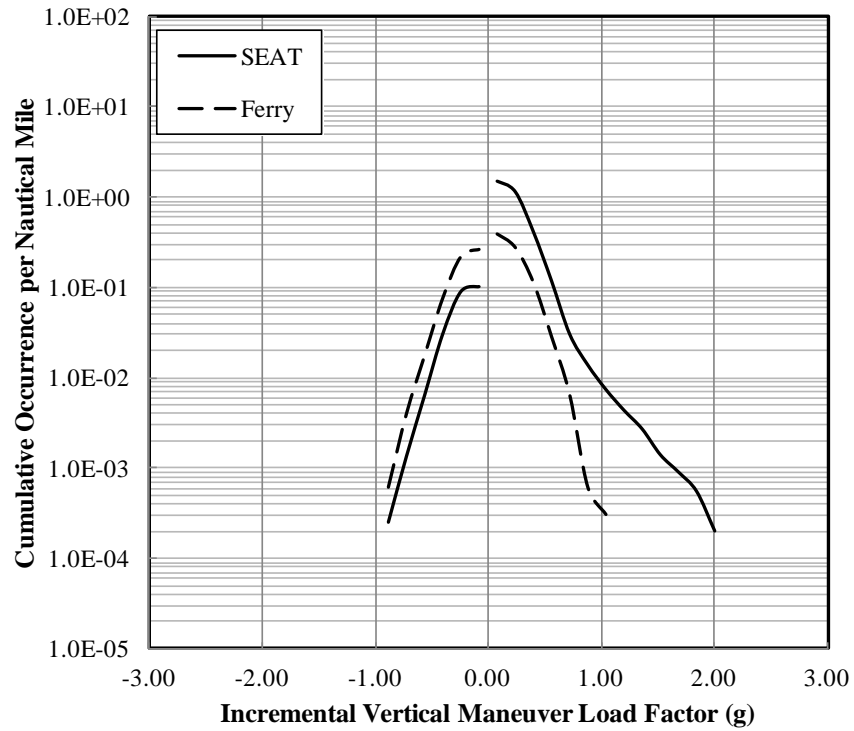


(b) Per nautical mile

Figure B-6. Cumulative occurrence of incremental gust vertical load factor—Aircraft 5

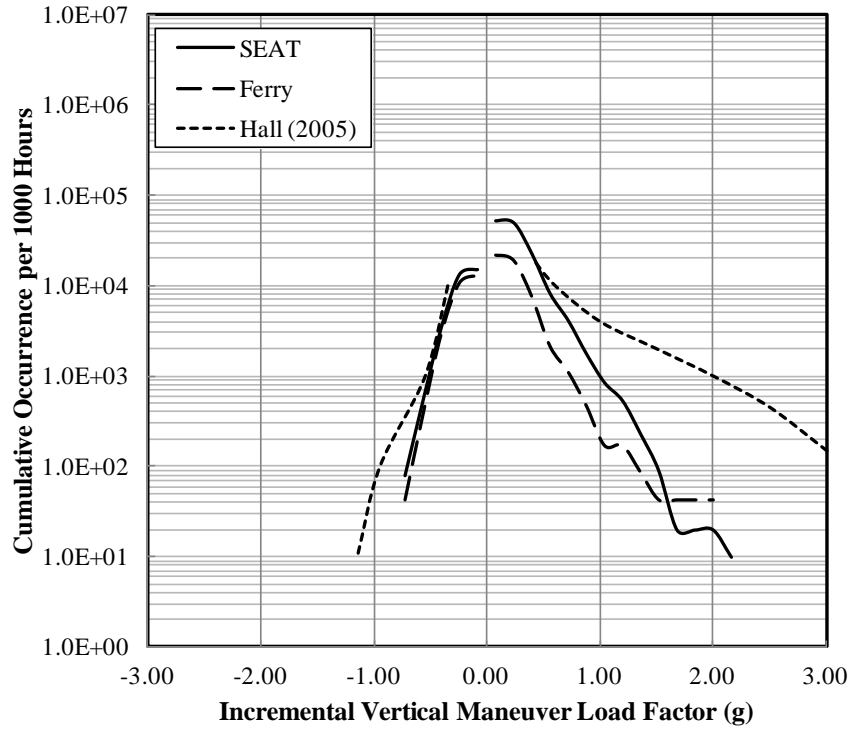


(a) Per 1000 hours

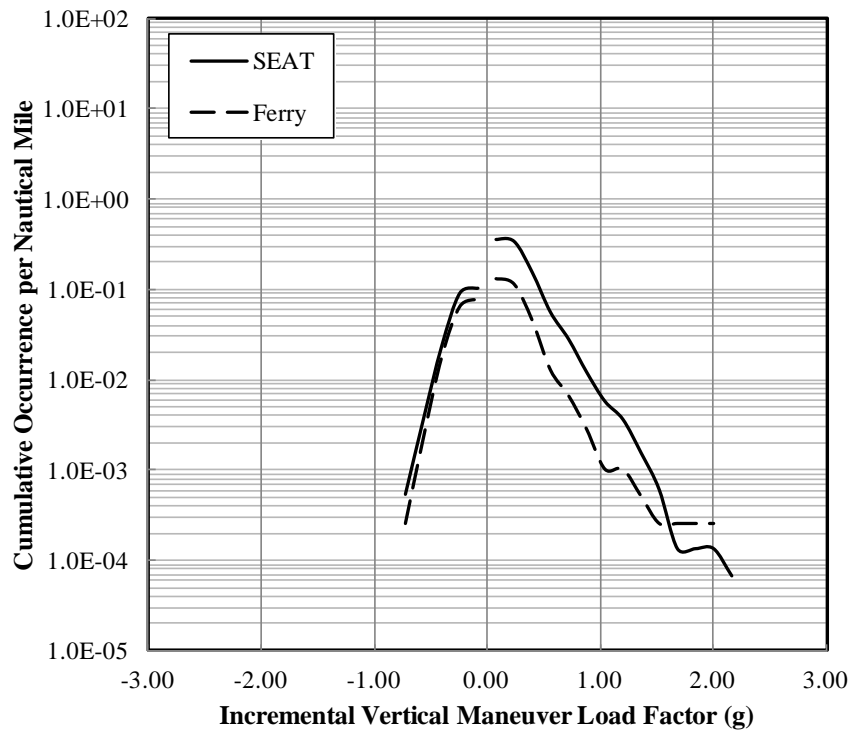


(b) Per nautical mile

**Figure B-7. Cumulative occurrence of incremental maneuver vertical load factor—Aircraft 1**

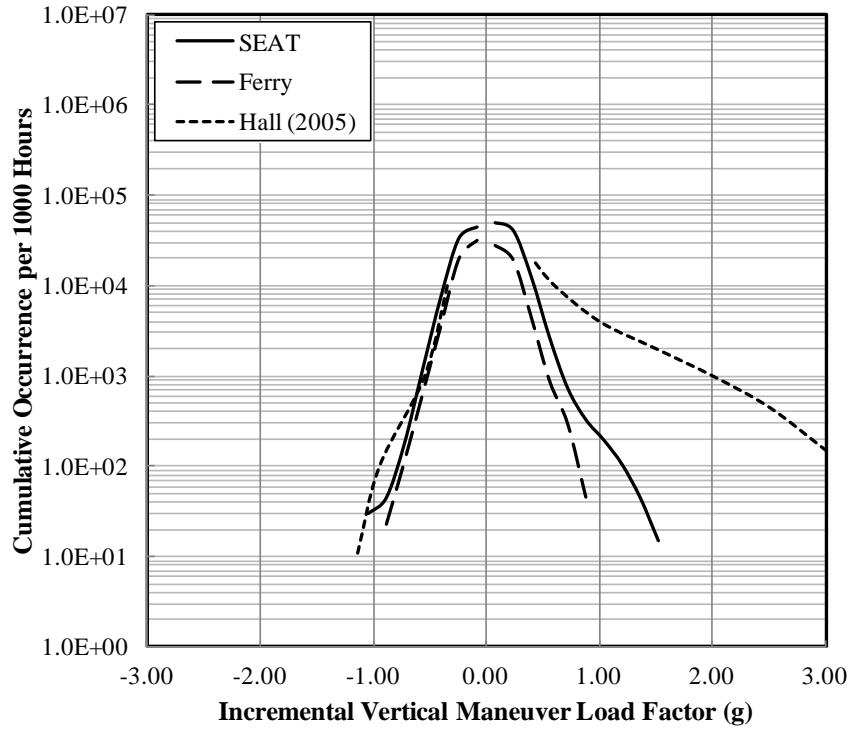


(a) Per 1000 hours

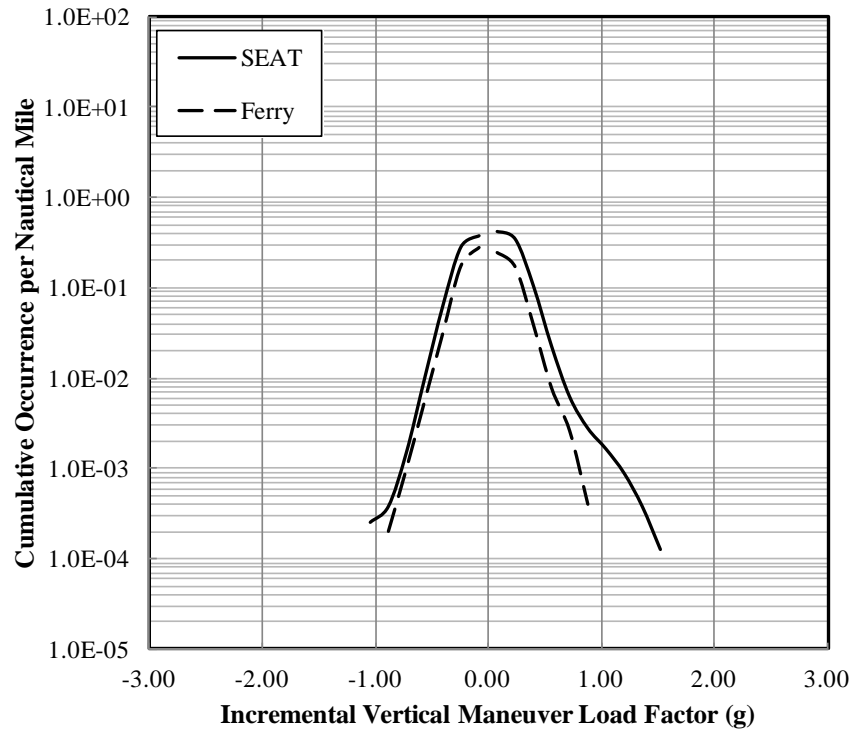


(b) Per nautical mile

**Figure B-8. Cumulative occurrence of incremental maneuver vertical load factor— Aircraft 2**

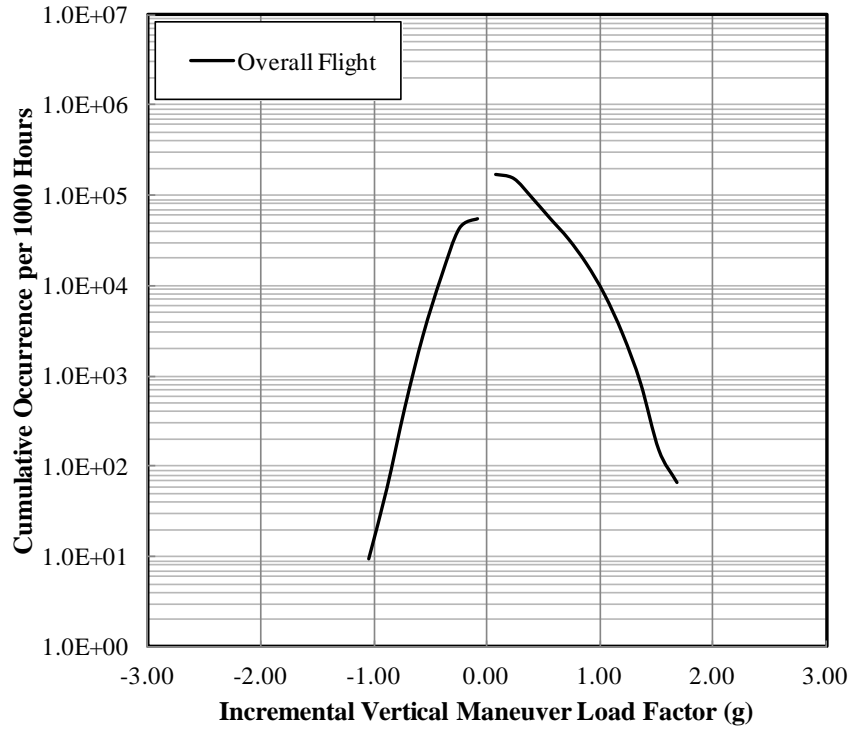


(a) Per 1000 hours

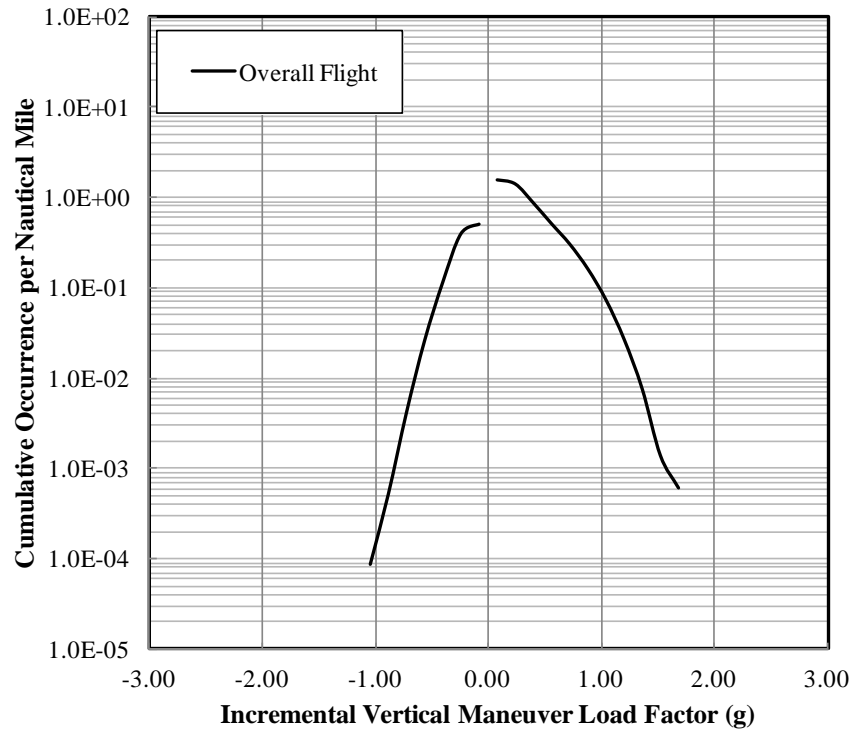


(b) Per nautical mile

**Figure B-9. Cumulative occurrence of incremental maneuver vertical load factor—  
Aircraft 3**

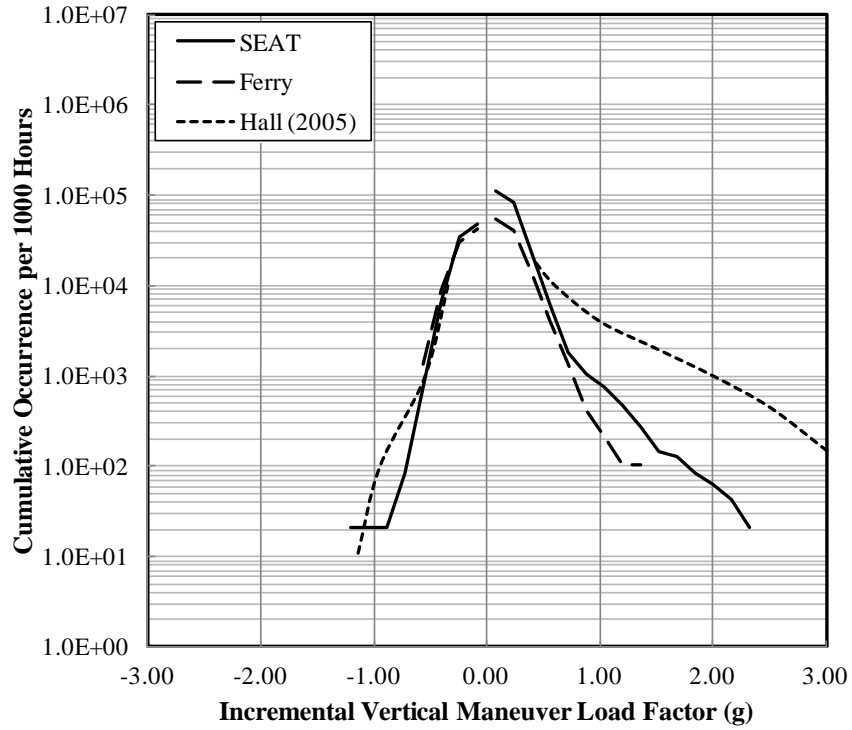


(a) Per 1000 hours

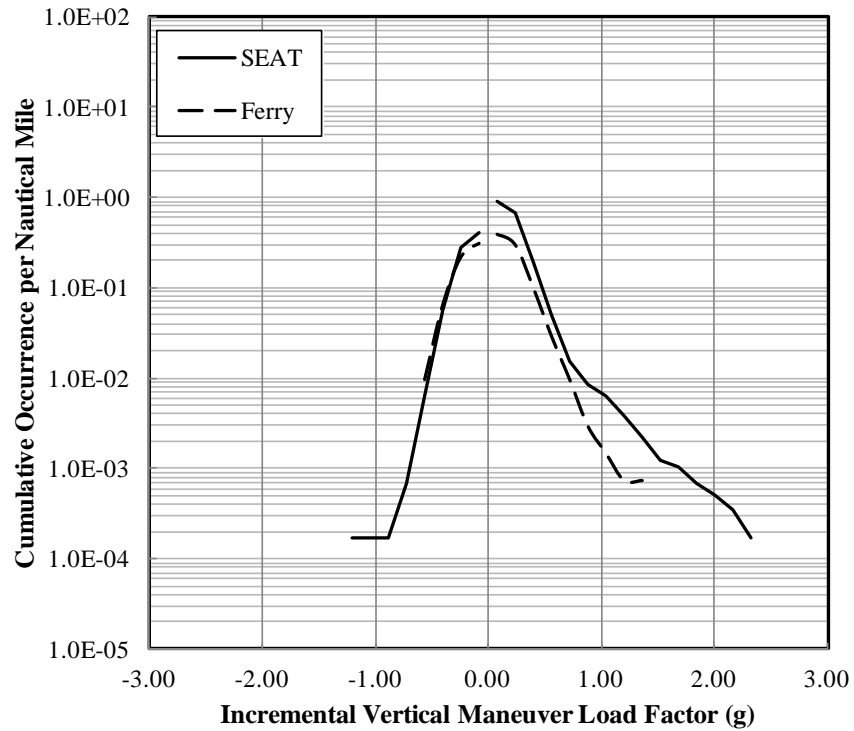


(b) Per nautical mile

**Figure B-10. Cumulative occurrence of incremental maneuver vertical load factor—  
Aircraft 4**

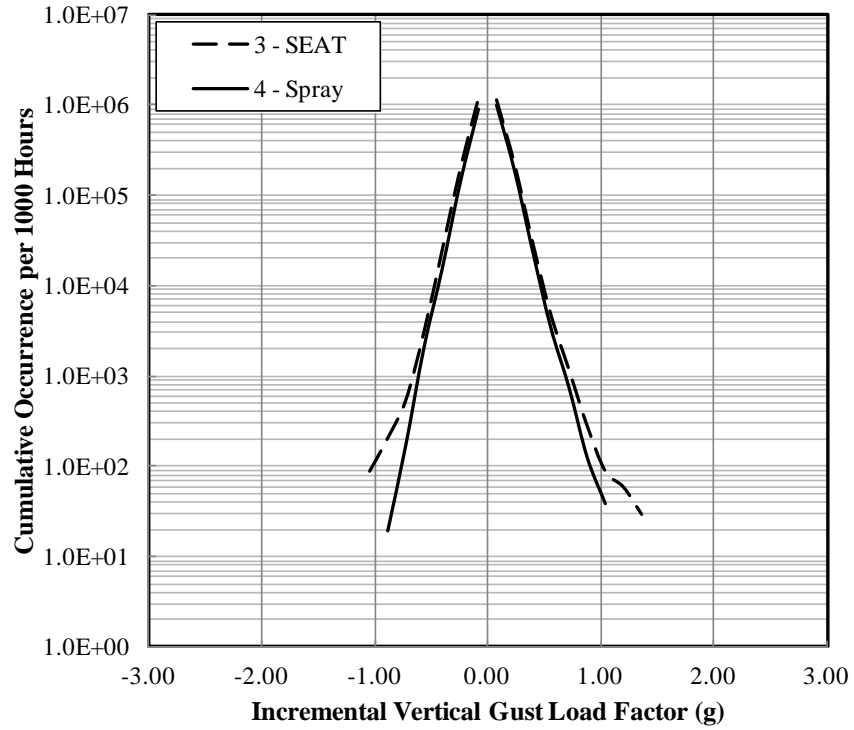


(a) Per 1000 hours

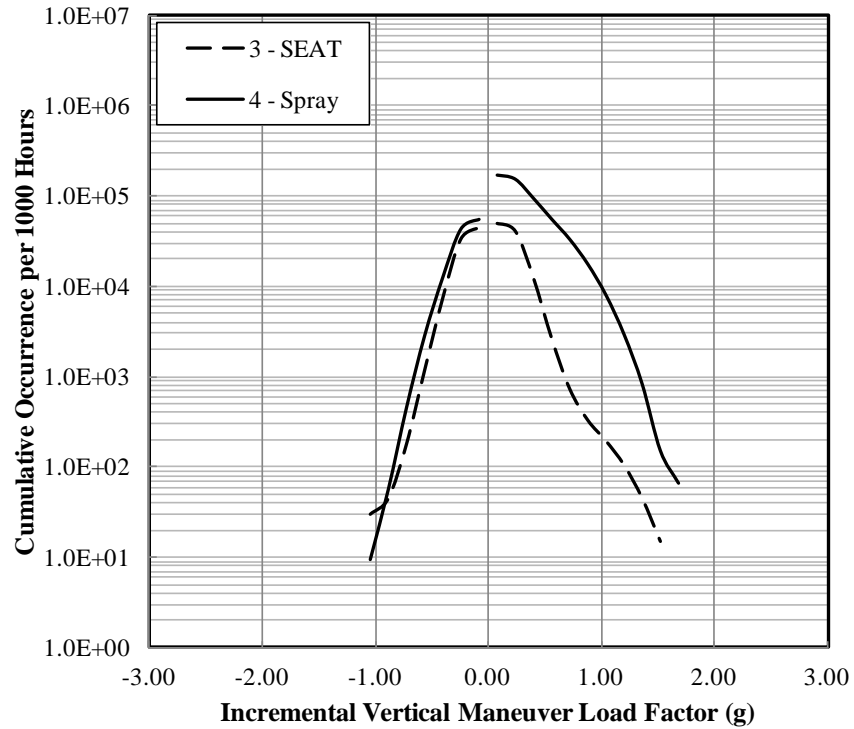


(b) Per nautical mile

**Figure B-11. Cumulative occurrence of incremental maneuver vertical load factor– Aircraft 5**



(a) Cumulative occurrence of gust load factor



(b) Cumulative occurrence of maneuver load factor

**Figure B-12. Comparison of the cumulative occurrences of incremental vertical load factor–Aircraft 3 and 4**

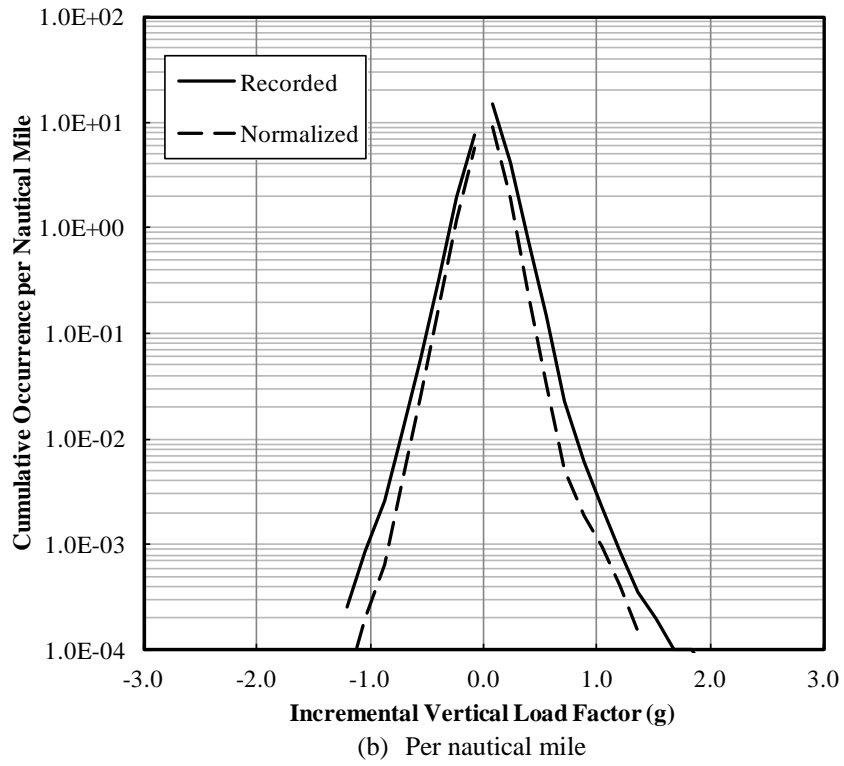
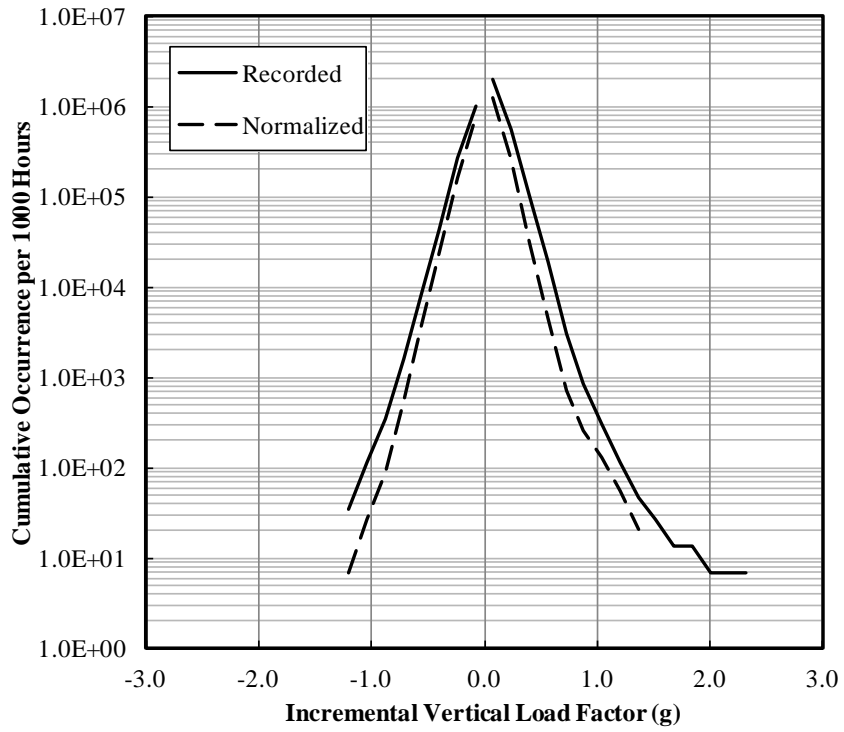


**Figure B-13. Impact of weight on overall cumulative occurrence of incremental gust vertical load factor–Aircraft 1**

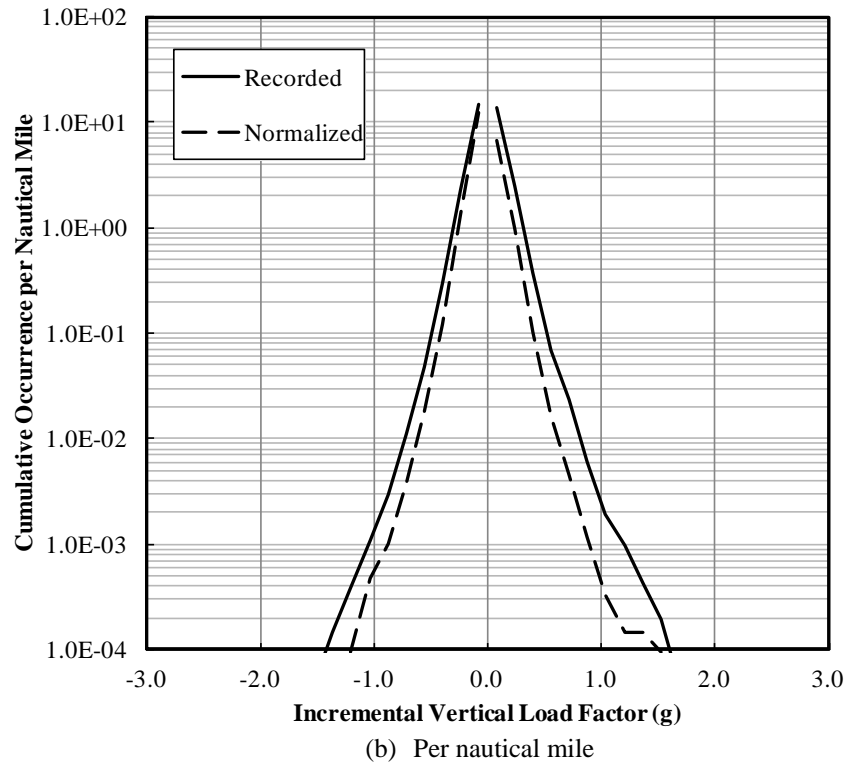
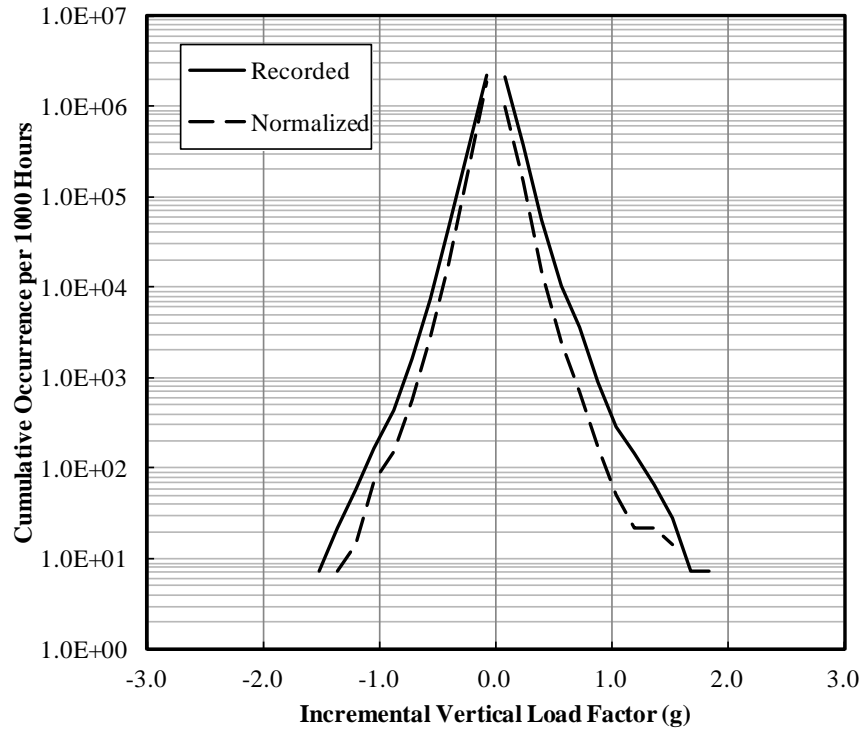
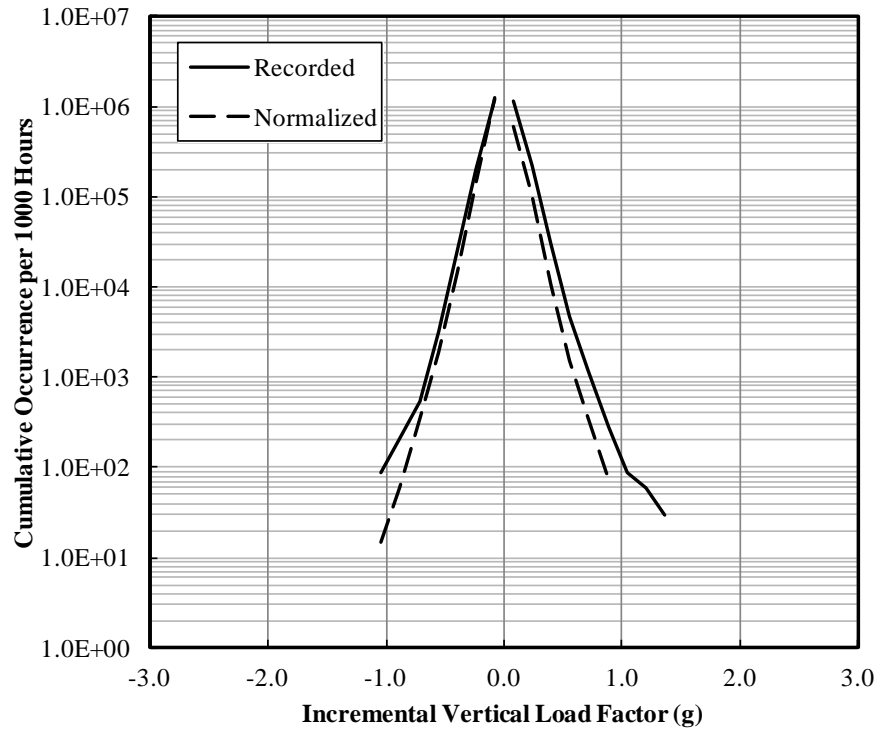
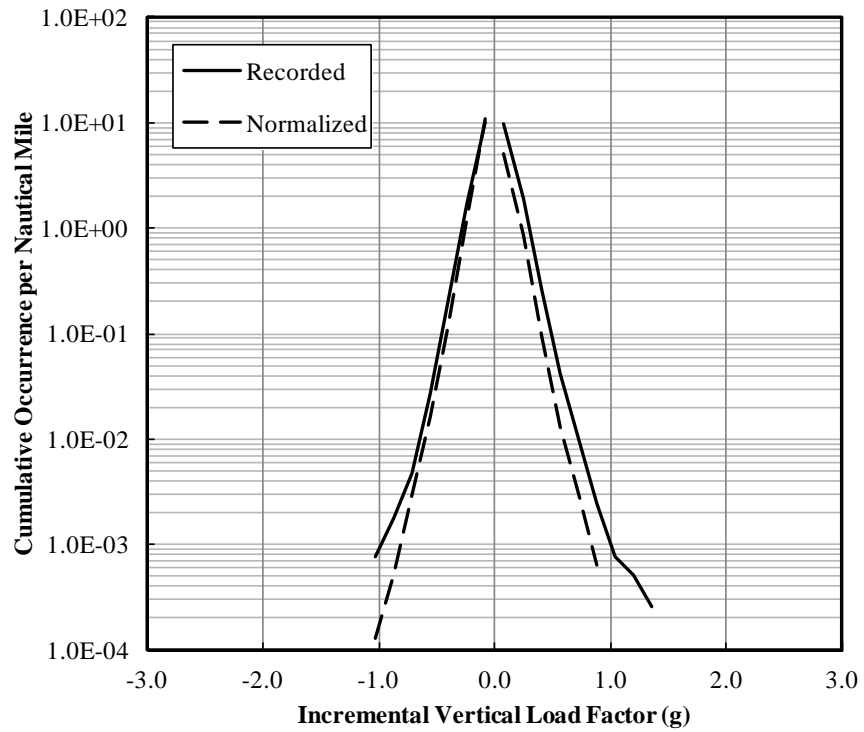


**Figure B-14. Impact of weight on overall cumulative occurrence of incremental gust vertical load factor—Aircraft 2**

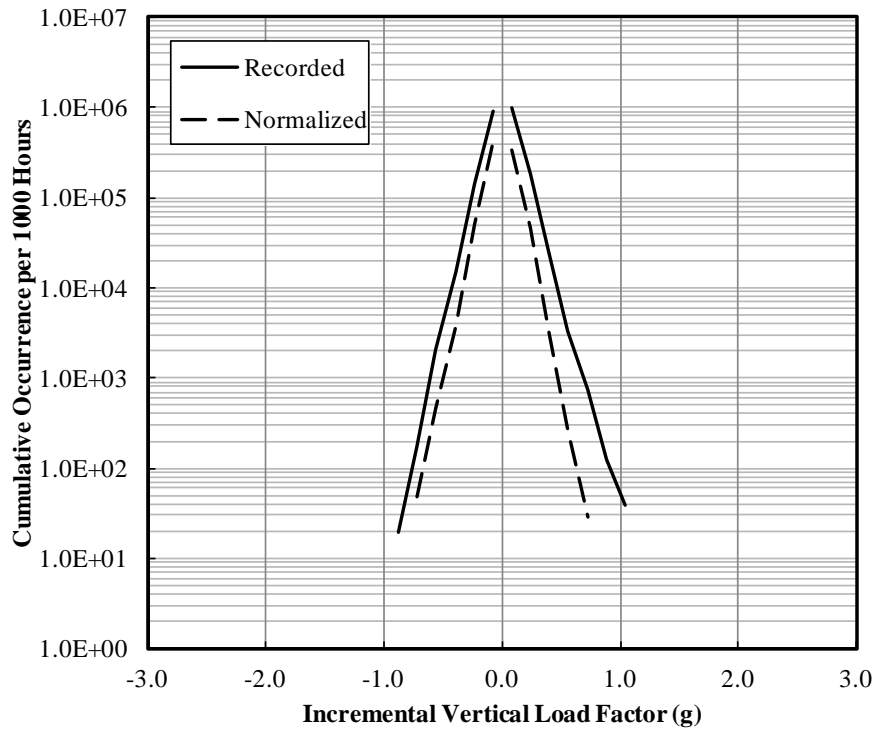


(a) Per 1000 hours

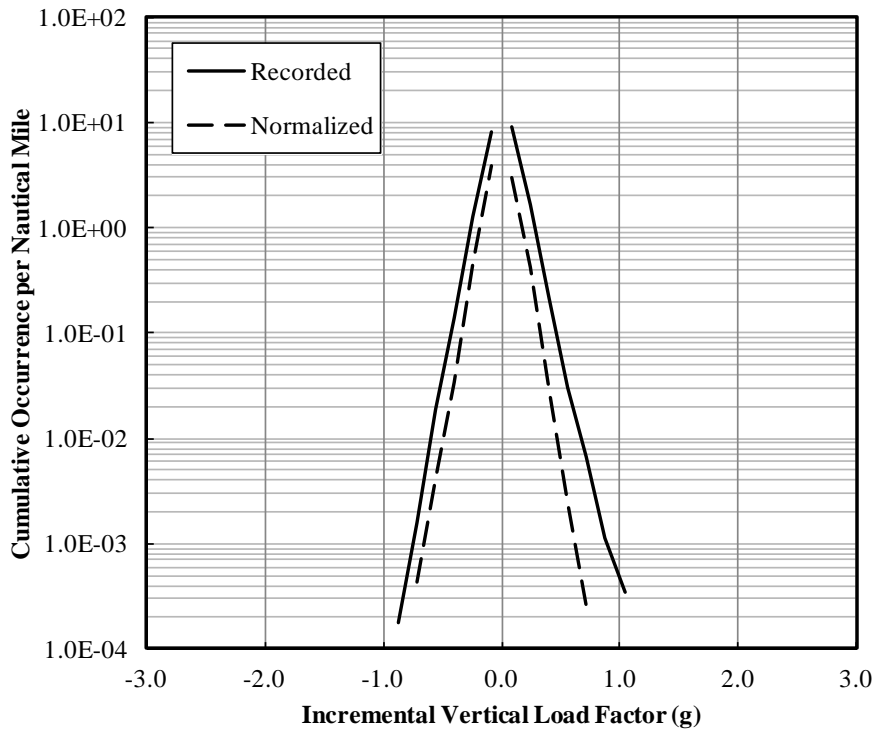


(b) Per nautical mile

**Figure B-15. Impact of weight on overall cumulative occurrence of incremental gust vertical load factor—Aircraft 3**

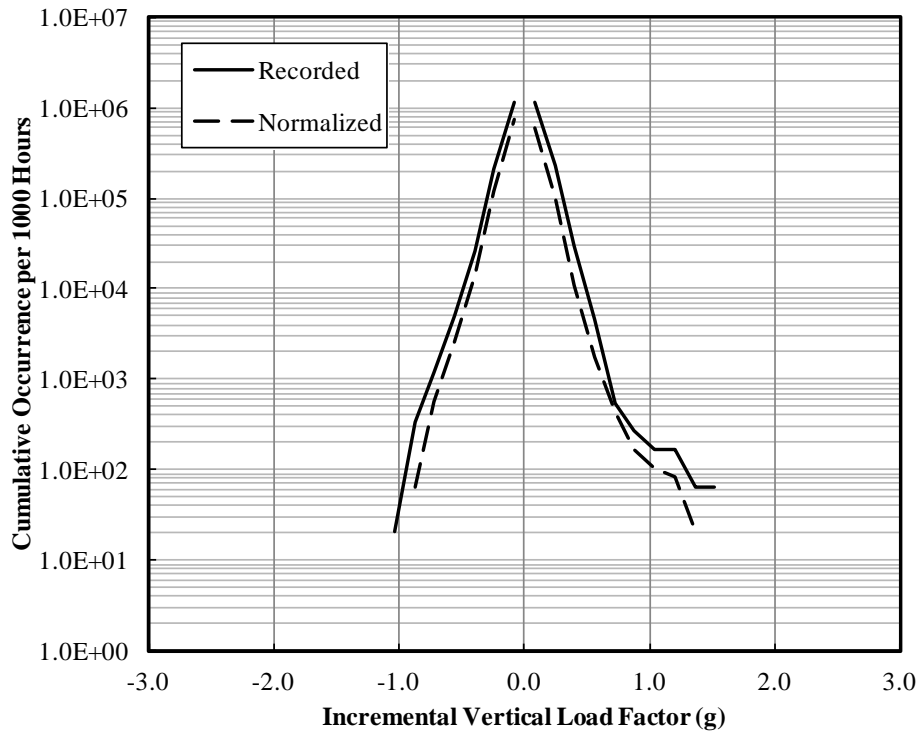


(a) Per 1000 hours

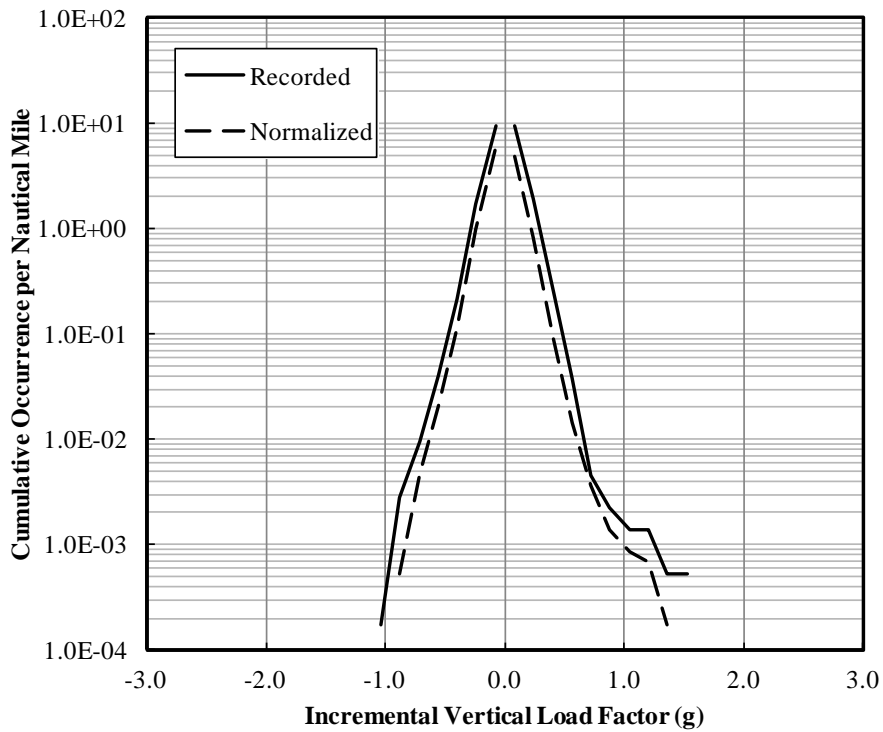


(b) Per nautical mile

**Figure B-16. Impact of weight on overall cumulative occurrence of incremental gust vertical load factor—Aircraft 4**

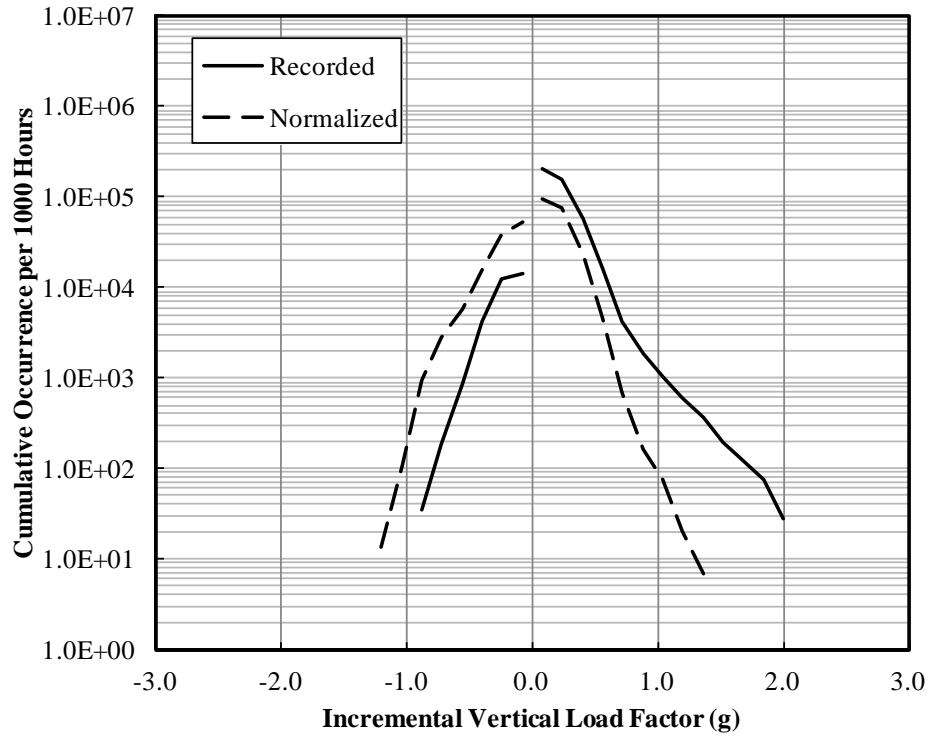


(a) Per 1000 hours

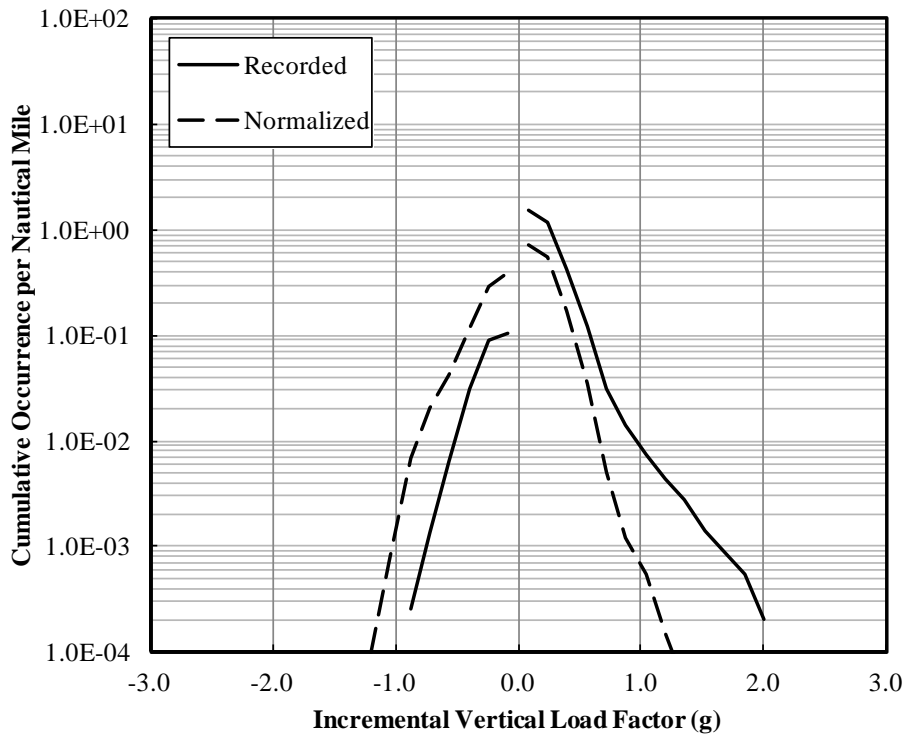


(b) Per nautical mile

**Figure B-17. Impact of weight on overall cumulative occurrence of incremental gust vertical load factor—Aircraft 5**

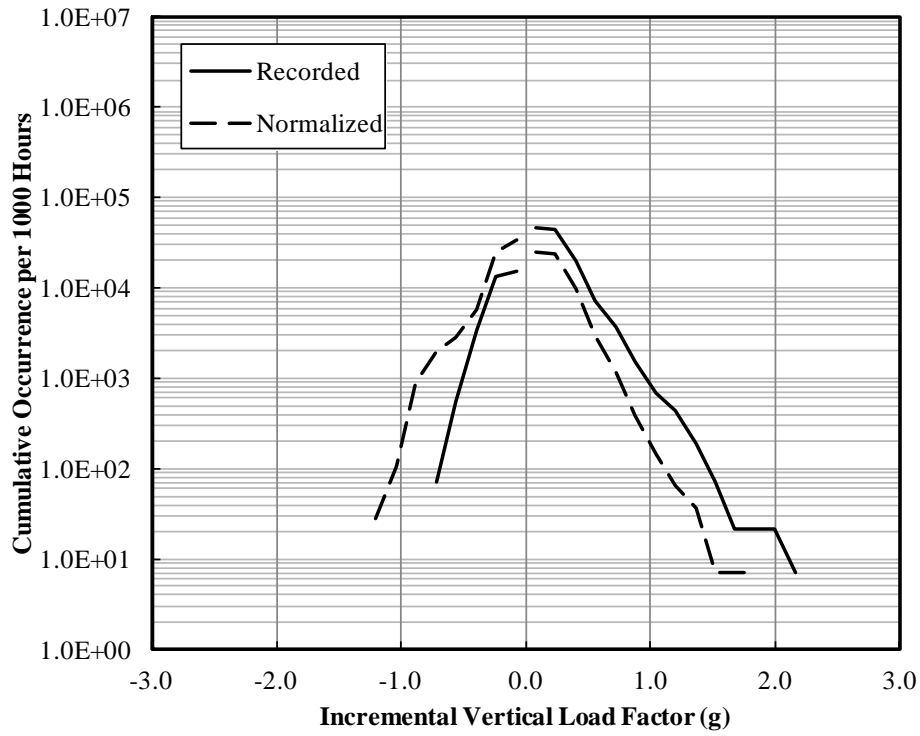


(a) Per 1000 hours

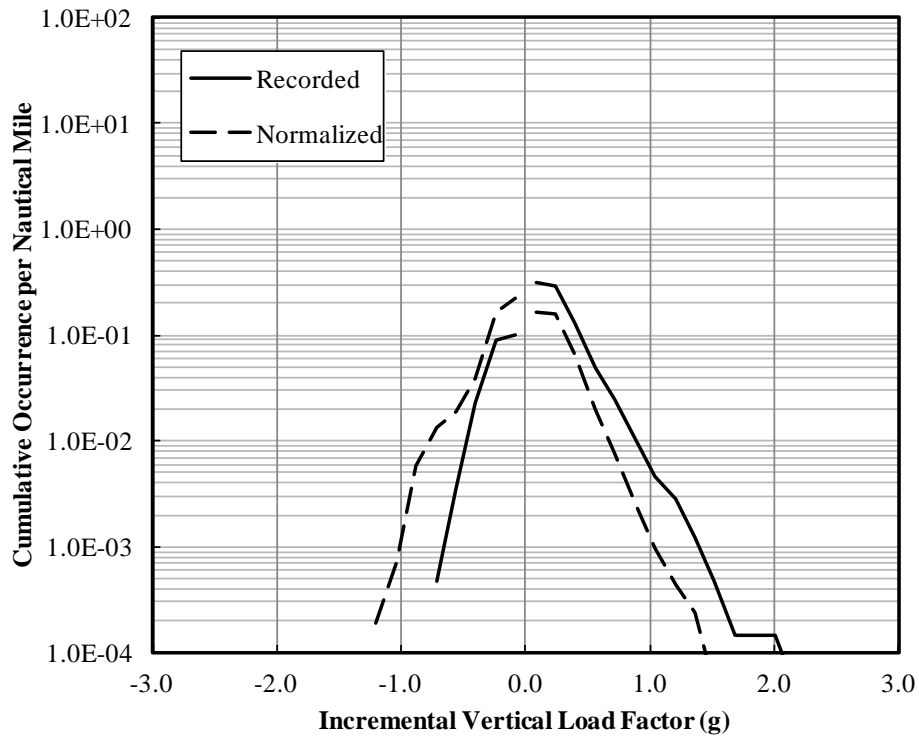


(b) Per nautical mile

**Figure B-18. Impact of weight on overall cumulative occurrence of incremental maneuver vertical load factor–Aircraft 1**

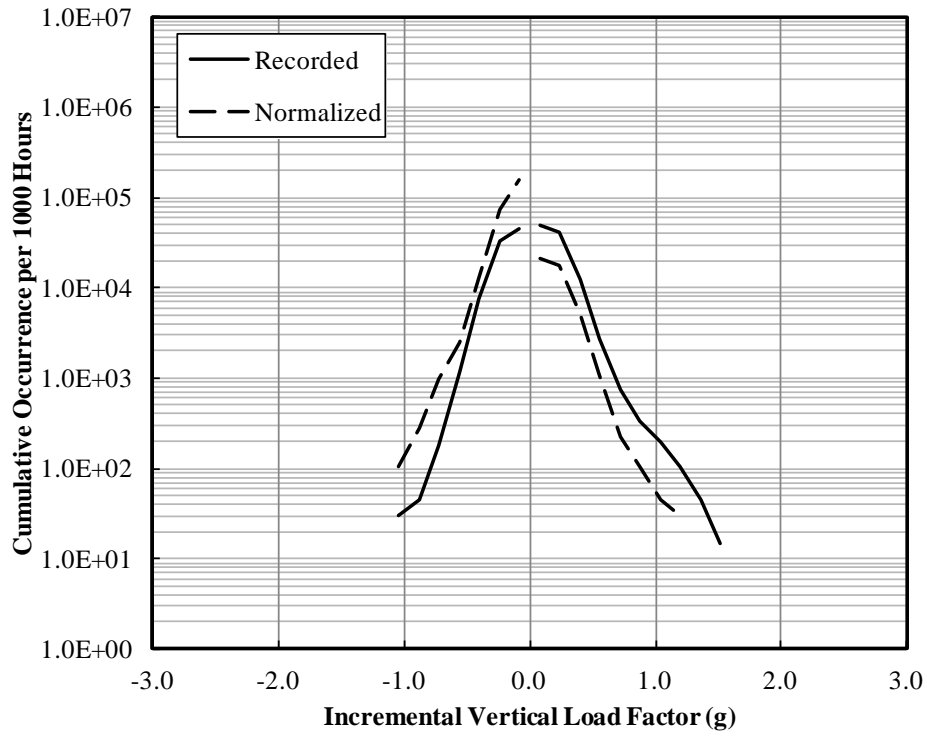


(a) Per 1000 hours

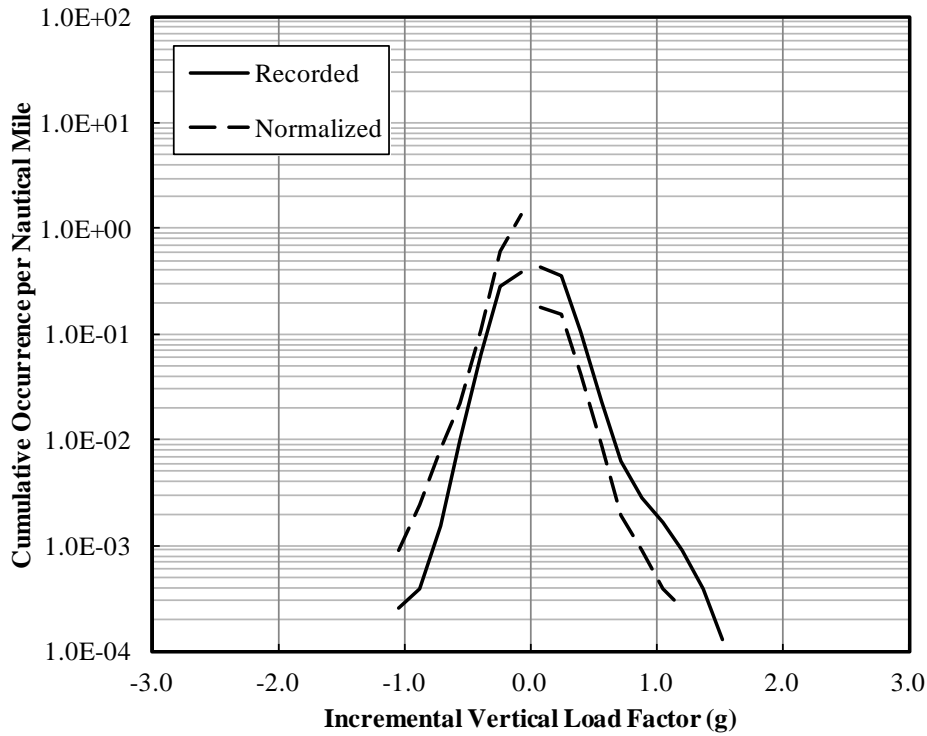


(b) Per nautical mile

**Figure B-19. Impact of weight on overall cumulative occurrence of incremental maneuver vertical load factor–Aircraft 2**

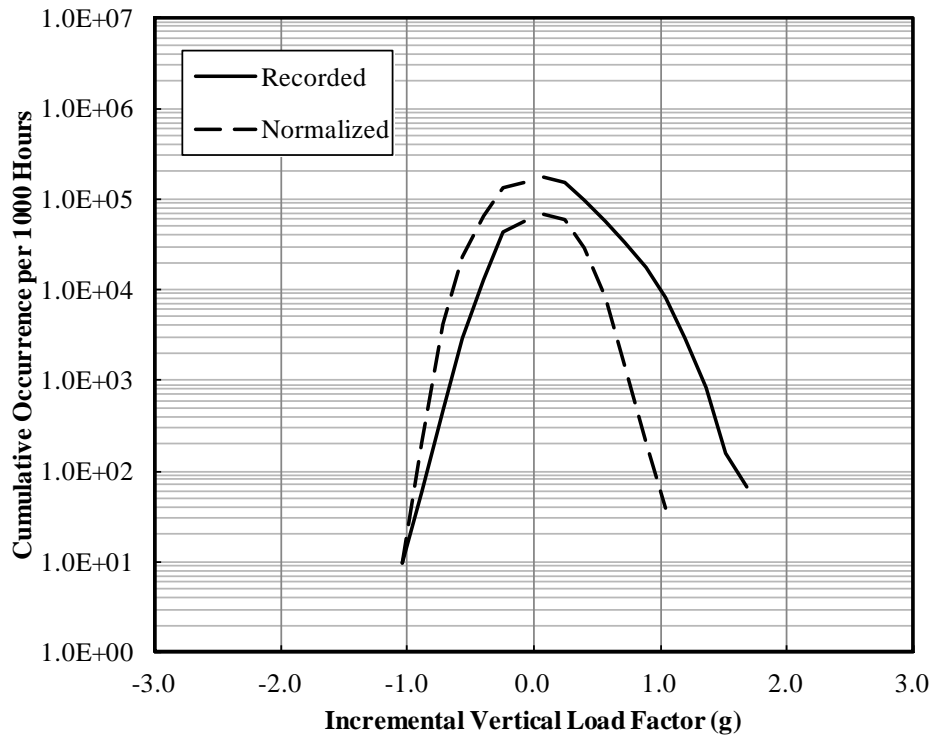


(a) Per 1000 hours

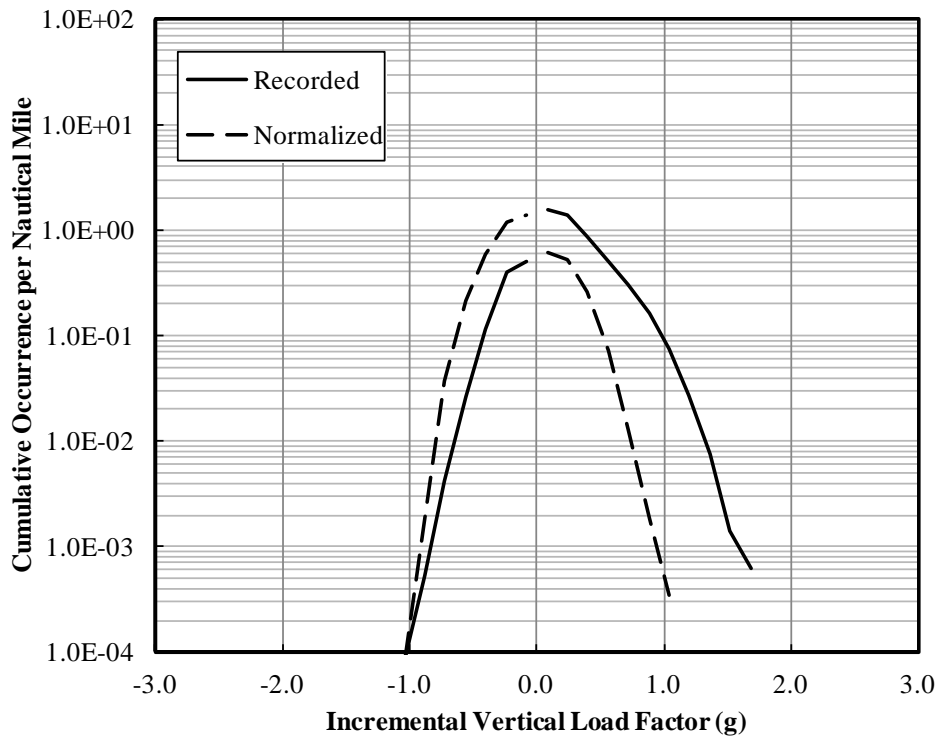


(b) Per nautical mile

**Figure B-20. Impact of weight on overall cumulative occurrence of incremental maneuver vertical load factor—Aircraft 3**

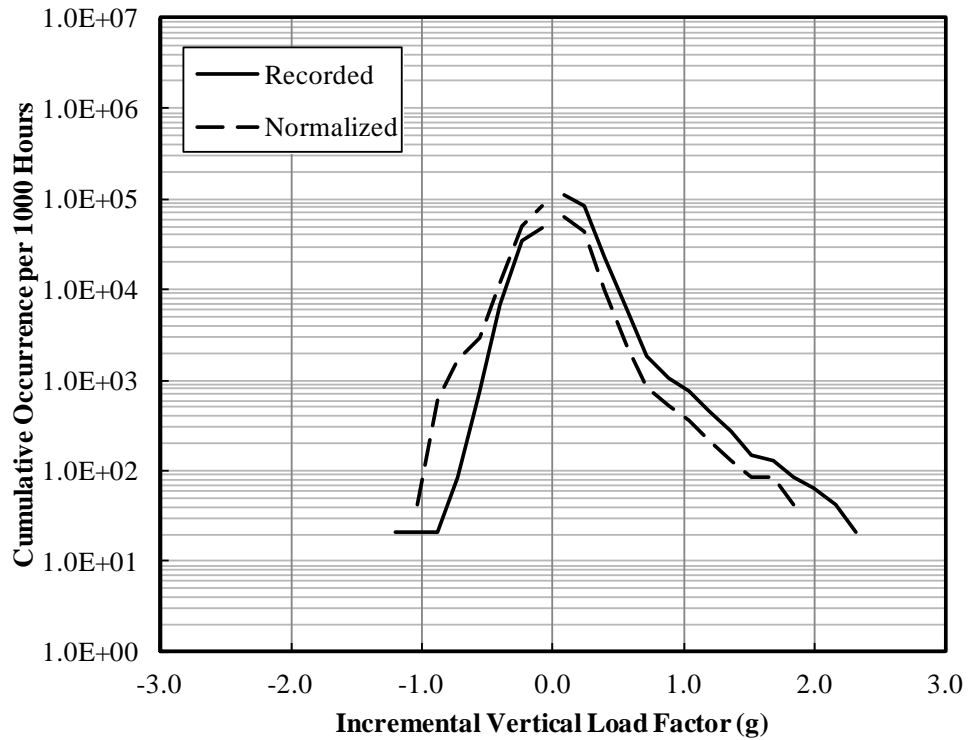


(a) Per 1000 hours

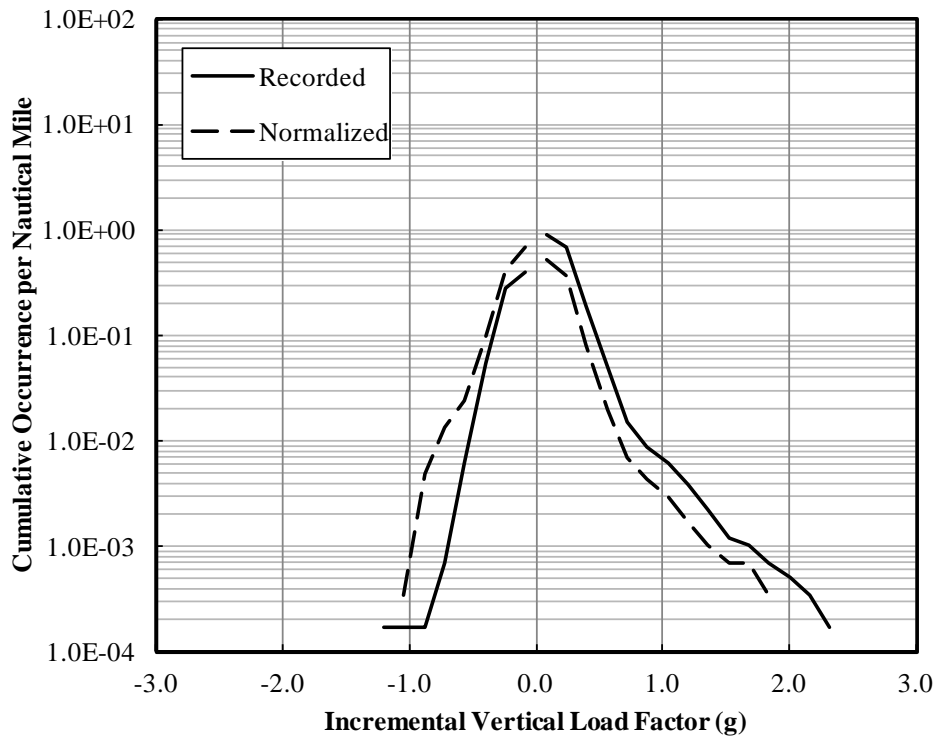


(b) Per nautical mile

**Figure B-21. Impact of weight on overall cumulative occurrence of incremental maneuver vertical load factor–Aircraft 4**

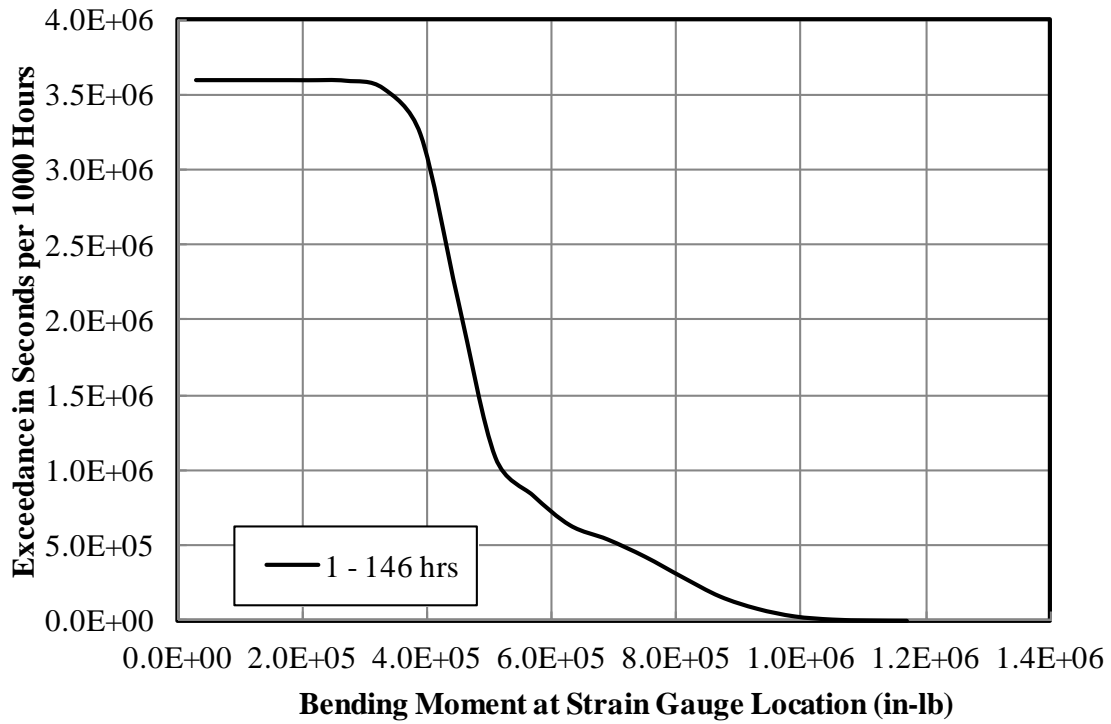


(a) Per 1000 hours

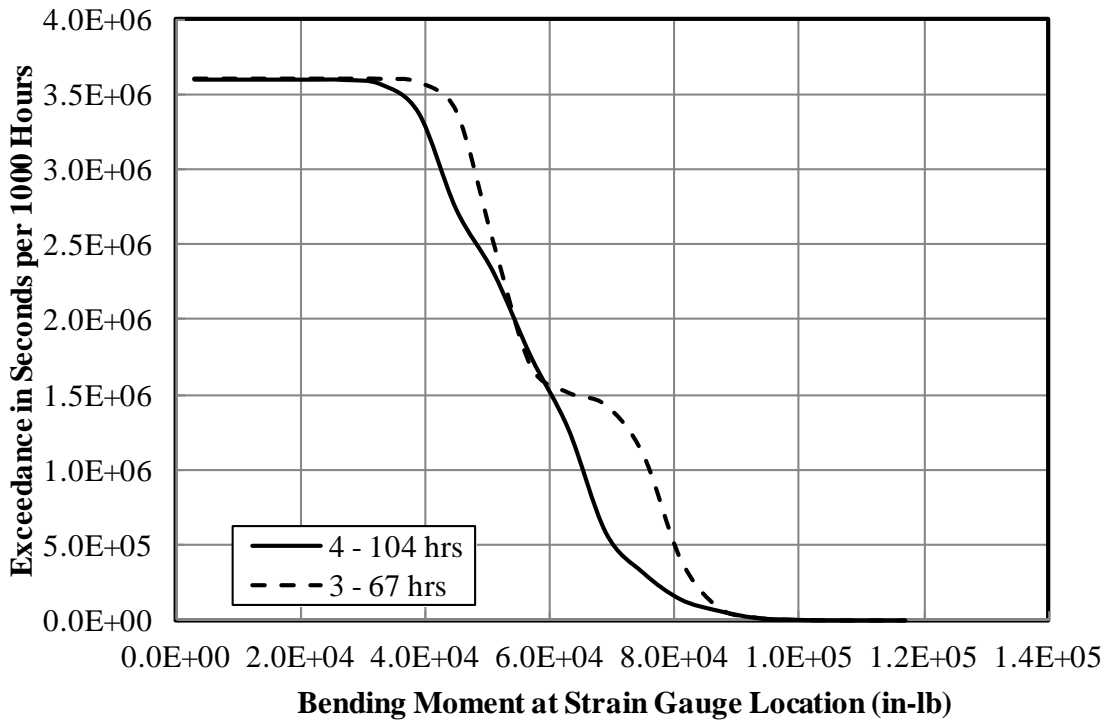


(b) Per nautical mile

**Figure B-22. Impact of weight on overall cumulative occurrence of incremental maneuver vertical load factor–Aircraft 5**

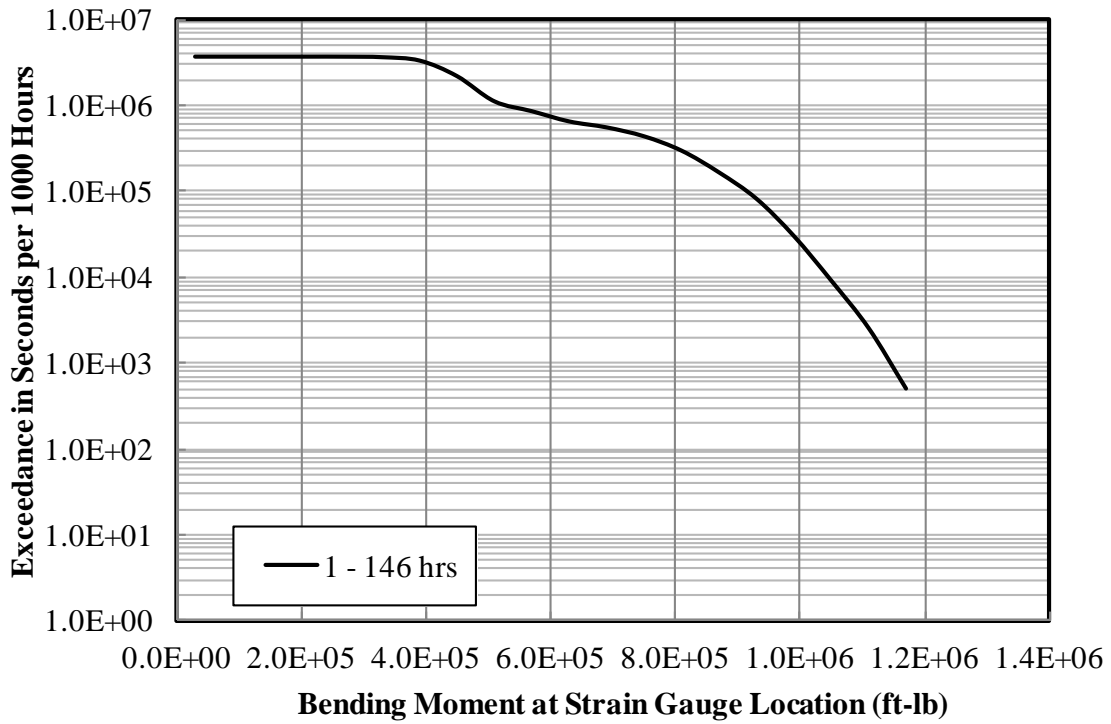


(a) Aircraft 1

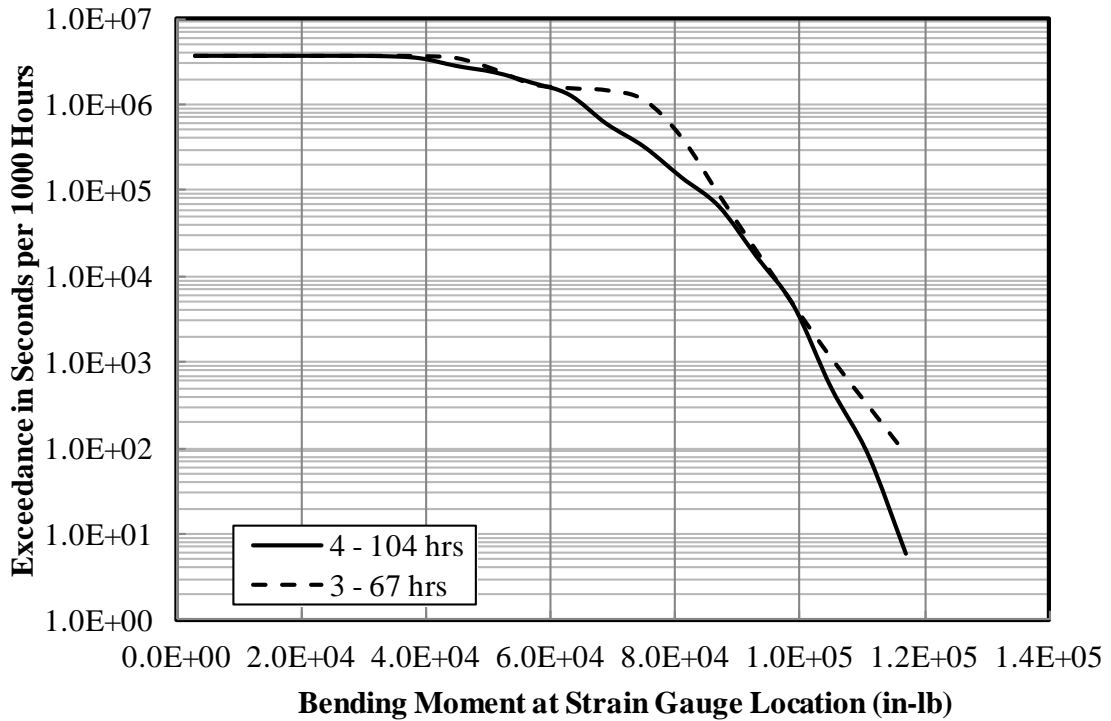


(b) Aircraft 3 and 4

**Figure B-23. Exceedance in seconds of maximum bending moment per 1000 hours—linear scale**

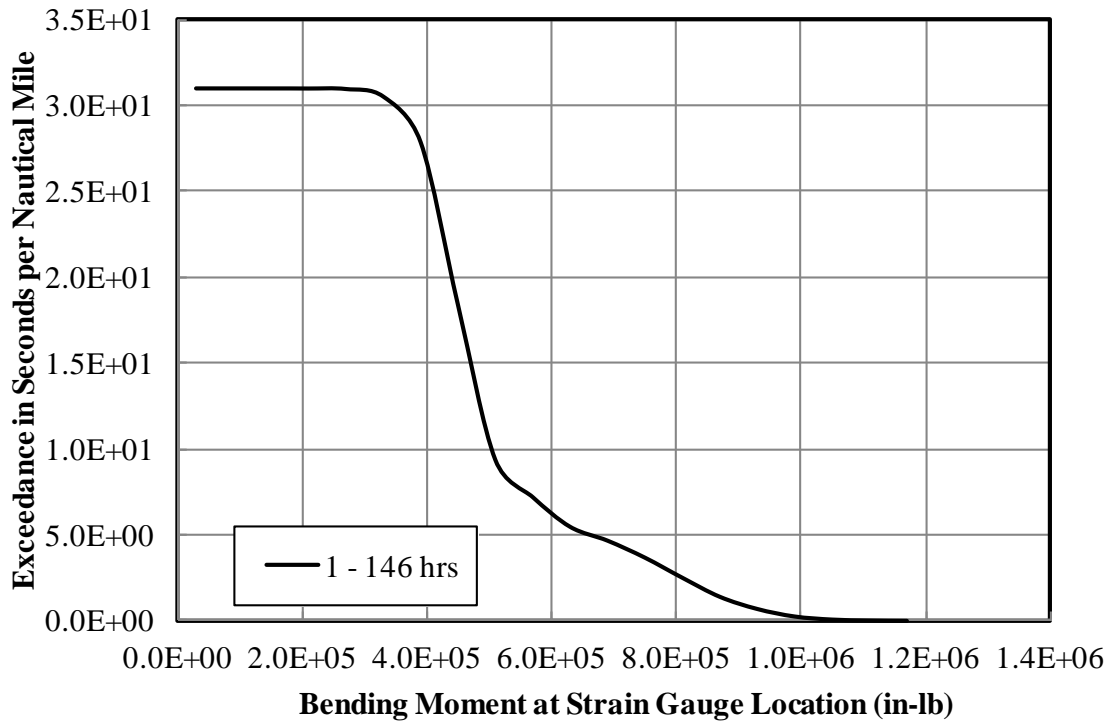


(a) Aircraft 1

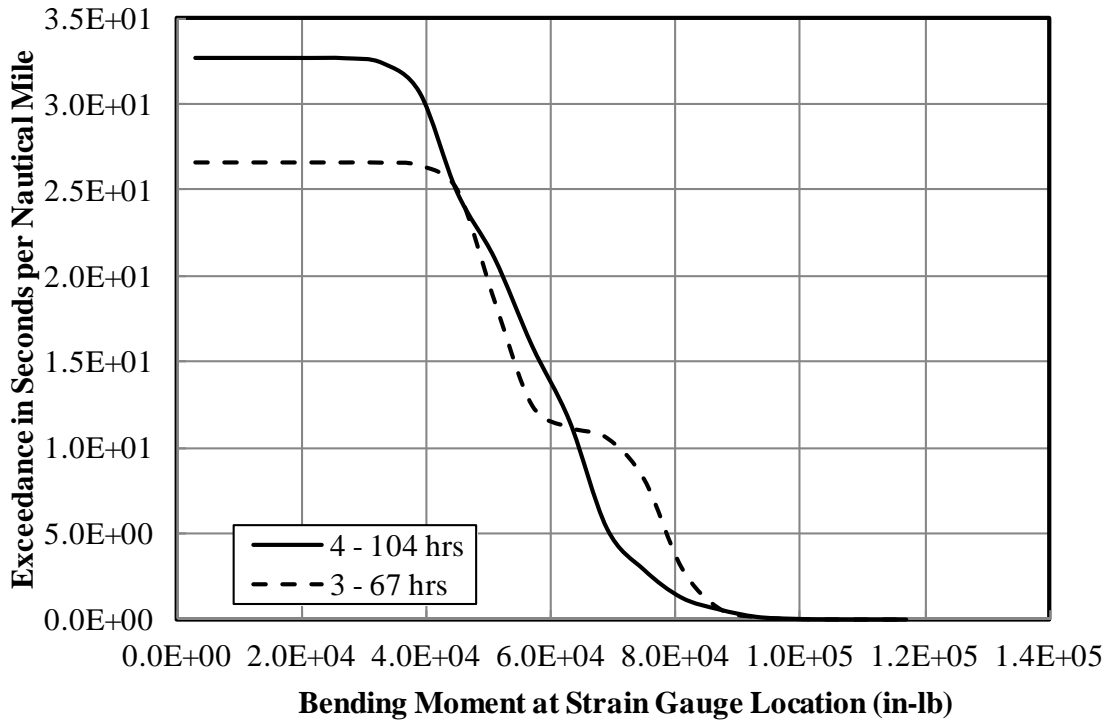


(b) Aircraft 3 and 4

**Figure B-24. Exceedance in seconds of maximum bending moment per 1000 hours—semi-log scale**

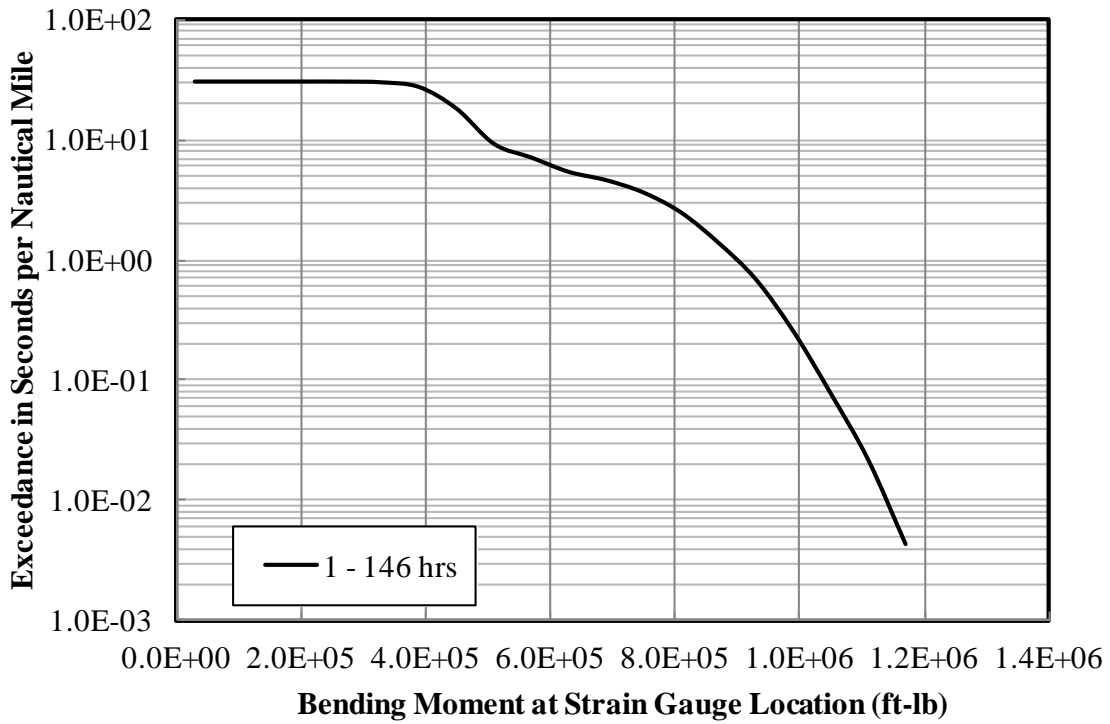


(a) Aircraft 1

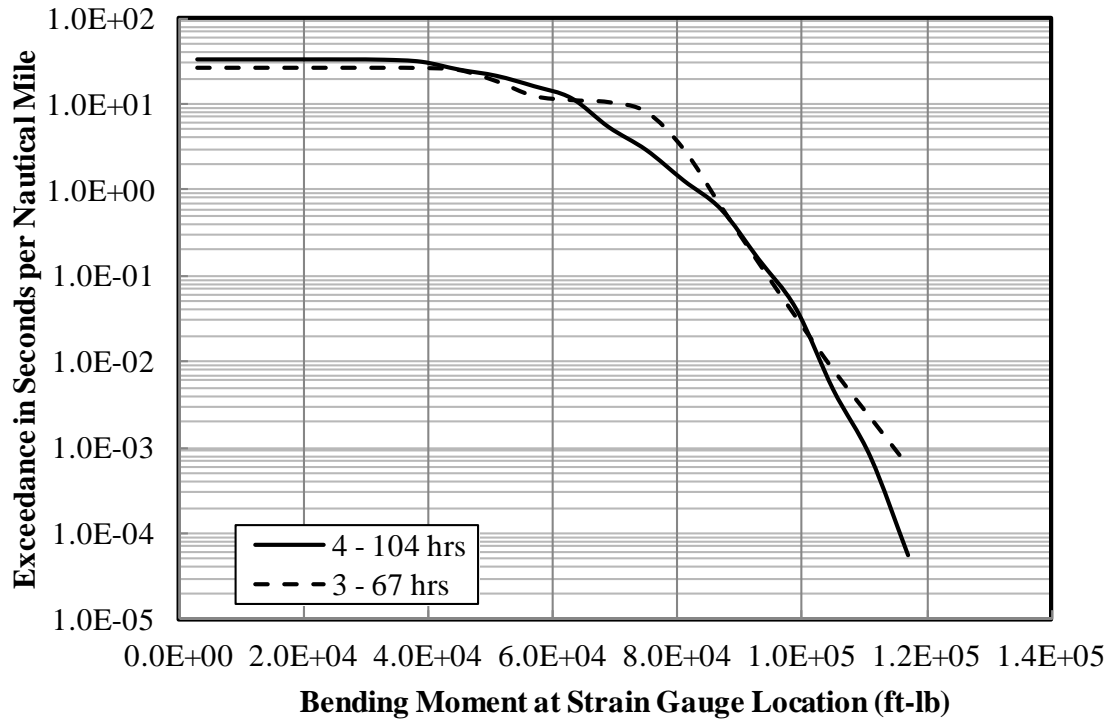


(b) Aircraft 3 and 4

**Figure B-25. Exceedance in seconds of maximum bending moment per nautical mile-linear scale**



(a) Aircraft 1



(b) Aircraft 3 and 4

**Figure B-26. Exceedance in seconds of maximum bending moment per nautical mile—semi-log scale**

Flight Phase	Aircraft 1	
	Duration (hr)	Distance (nm)
Cruise 1	54.88	7,270
Entry	4.46	558
Drop	0.38	50
Exit	4.46	578
Cruise 2	36.99	5,047
Ferry	23.33	3,224
Overall	146.46	19,838

(a) Aircraft 1

Flight Phase	Aircraft 2	
	Duration (hr)	Distance (nm)
Cruise 1	63.88	9,154
Entry	2.94	362
Drop	0.28	36
Exit	2.94	359
Cruise 2	39.96	6,394
Ferry	23.45	3,837
Overall	115.83	17,085

(b) Aircraft 2

Flight Phase	Aircraft 3	
	Duration (hr)	Distance (nm)
Cruise 1	10.97	1,327
Entry	0.87	99
Drop	0.06	7
Exit	0.87	95
Cruise 2	8.81	1,074
Ferry	67.28	7,829
Overall	44.04	5,037

(c) Aircraft 3

**Figure B-27. Duration and distance flown in each phase**

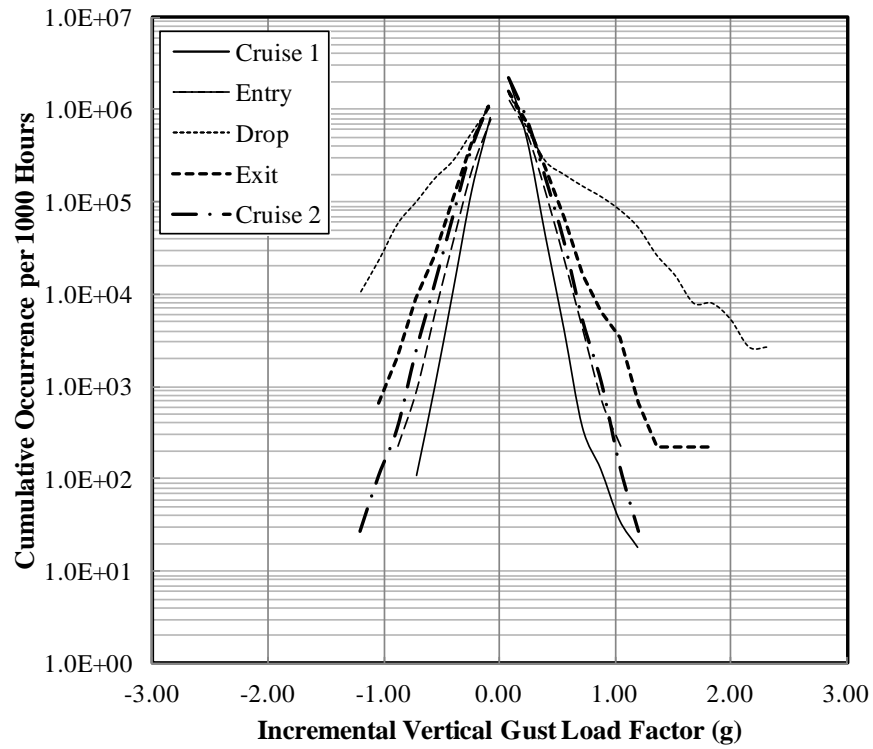
Flight Phase	Aircraft 4	
	Duration (hr)	Distance (nm)
Cruise 1	13.16	1,390
Drop	21.98	2,548
Turn	54.24	5,867
Cruise 2	12.13	1,499
Ferry	0.16	16
Overall	103.98	11,463

(d) Aircraft 4

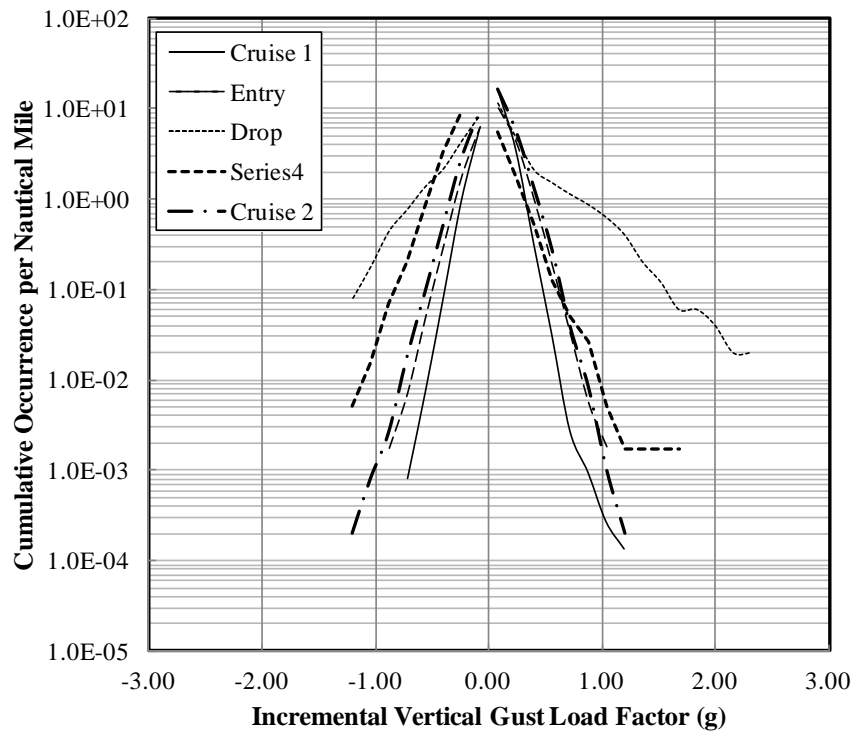
Flight Phases	Aircraft 5	
	Duration (hr)	Distance (nm)
Cruise 1	19.07	2,227
Entry	1.60	166
Drop	0.11	12
Exit	1.60	161
Cruise 2	13.05	1,623
Ferry	9.63	1,339
Overall	47.47	5,792

(e) Aircraft 5

**Figure B-27. Duration and distance flown in each phase (continued)**

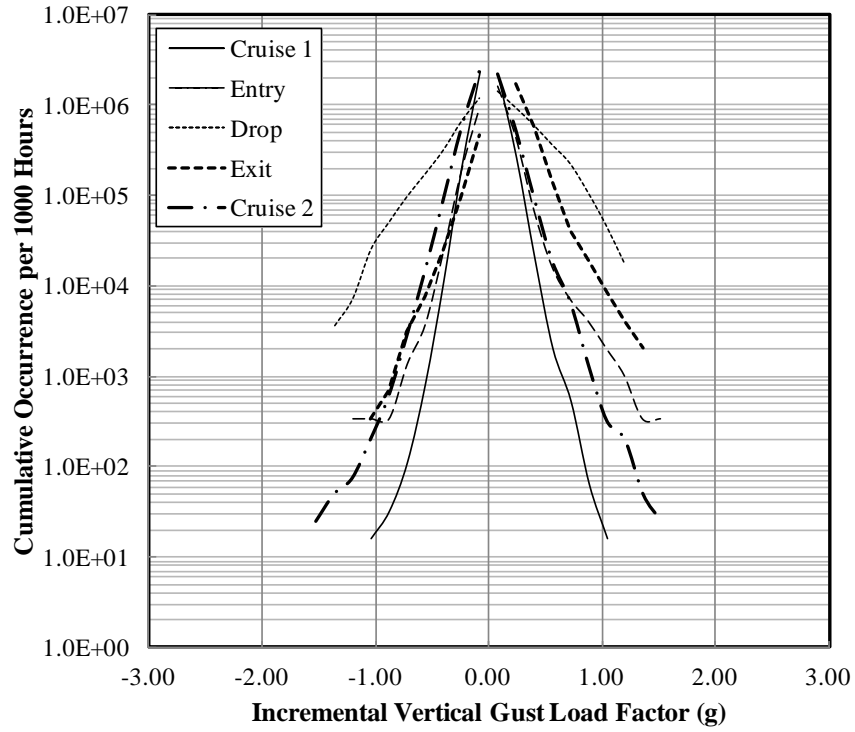


(a) Per 1000 hours

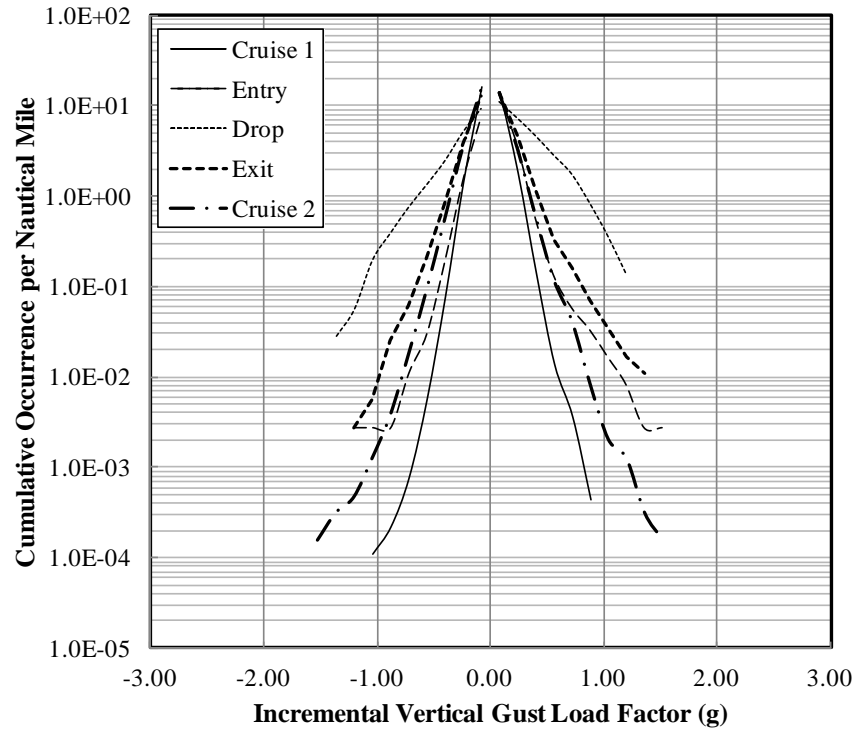


(b) Per nautical mile

**Figure B-28. Cumulative occurrence of incremental gust vertical load factor—  
Aircraft 1**

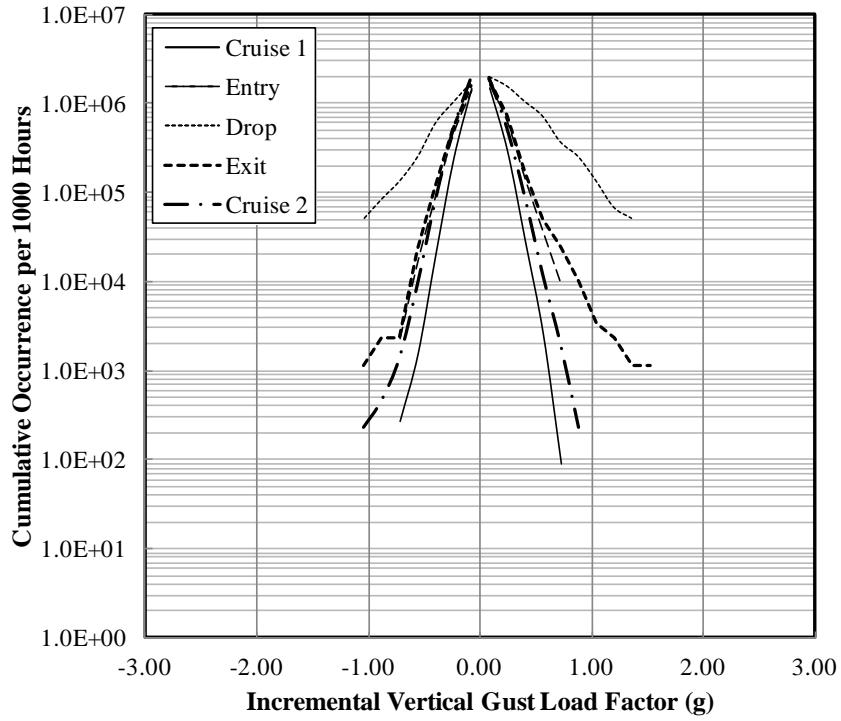


(a) Per 1000 hours

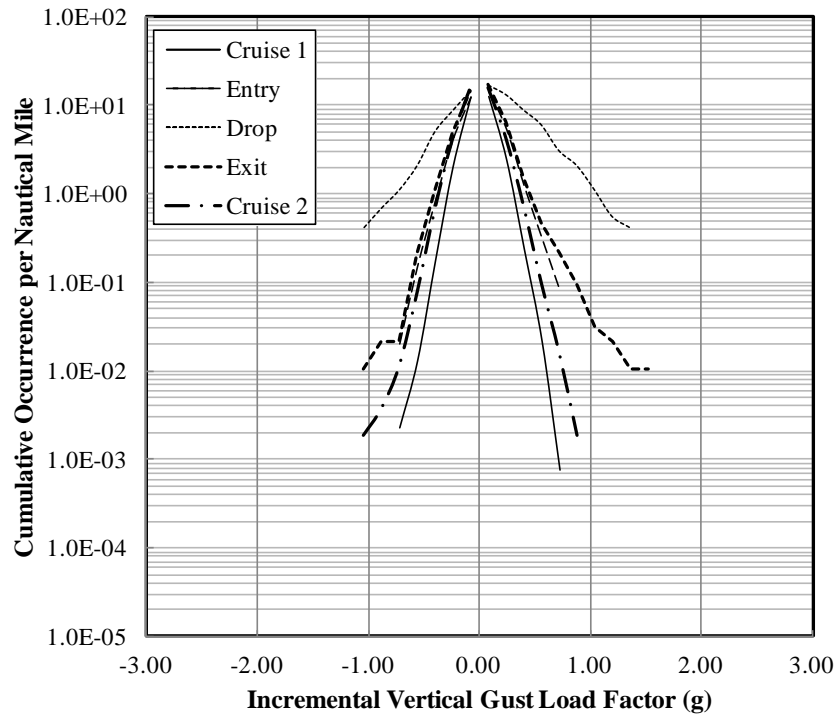


(b) Per nautical mile

**Figure B-29. Cumulative occurrence of incremental gust vertical load factor—  
Aircraft 2**

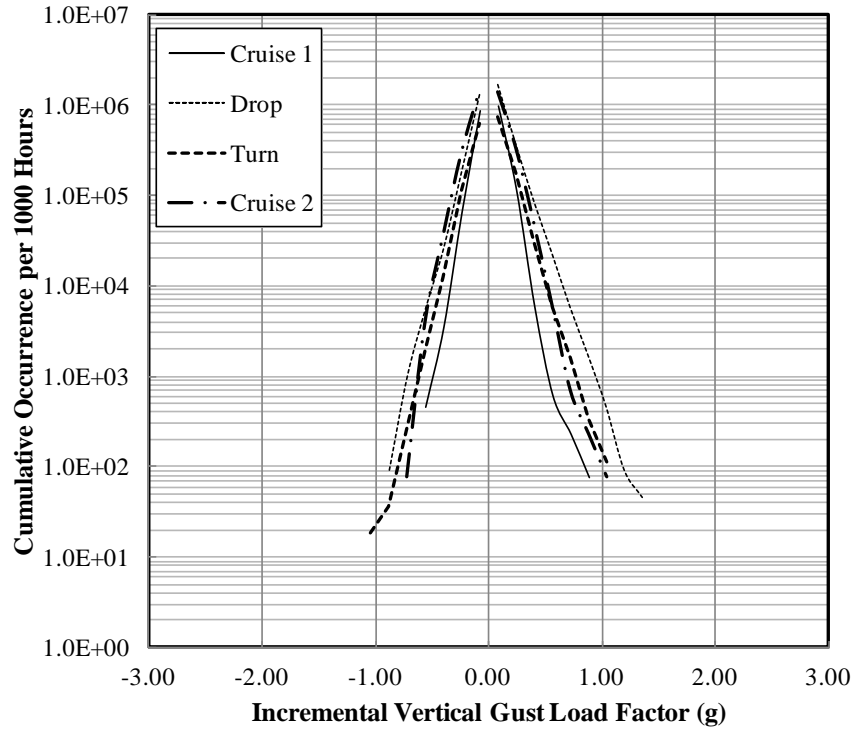


(a) Per 1000 hours

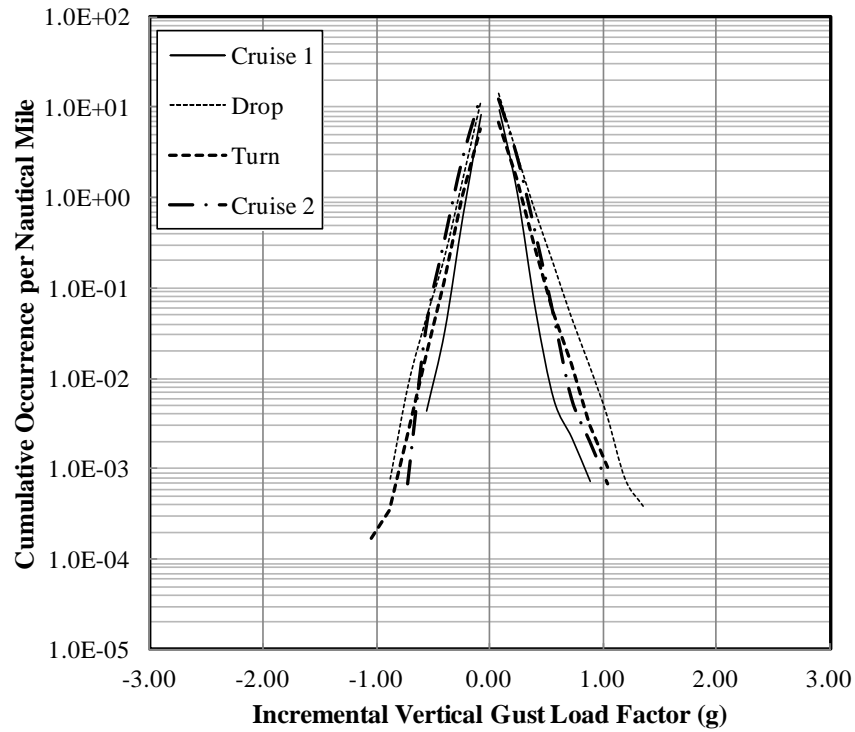


(b) Per nautical mile

**Figure B-30. Cumulative occurrence of incremental gust vertical load factor—  
Aircraft 3**

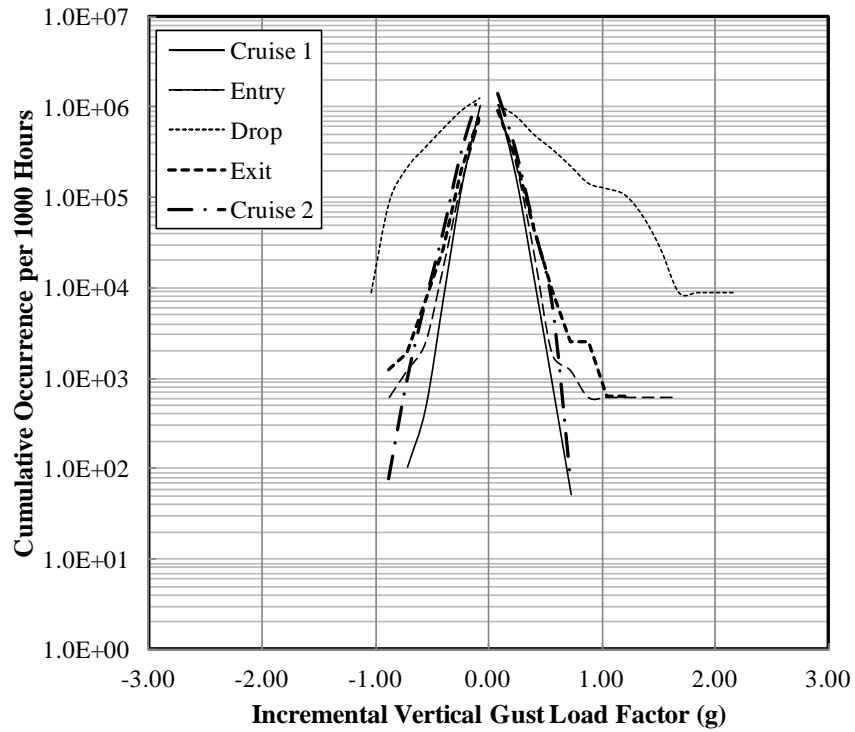


(a) Per 1000 hours

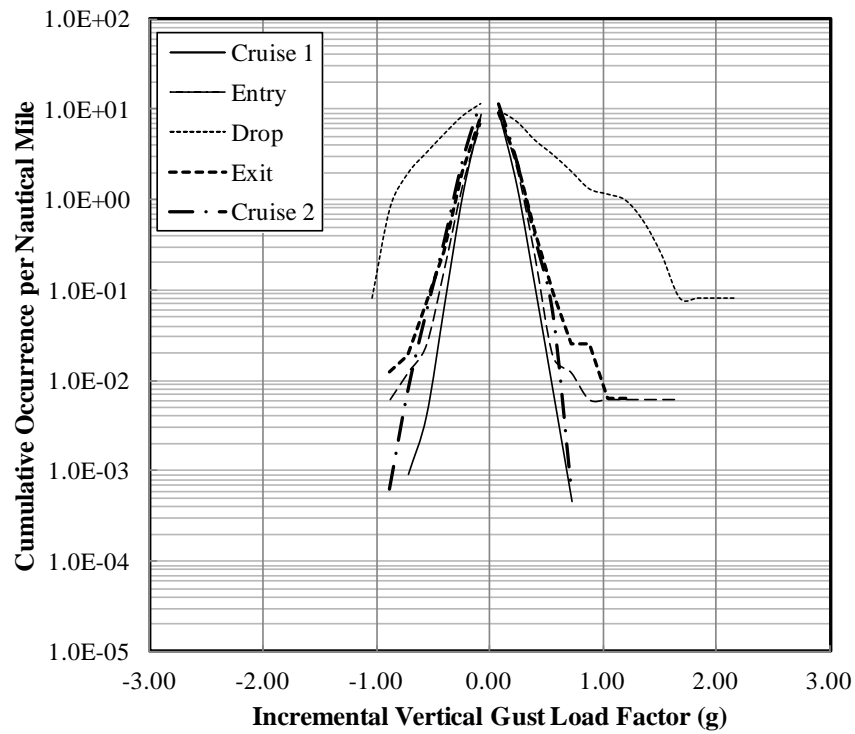


(b) Per nautical mile

**Figure B-31. Cumulative occurrence of incremental gust vertical load factor—  
Aircraft 4**



(a) Per 1000 hours



(b) Per nautical mile

**Figure B-32. Cumulative occurrence of incremental gust vertical load factor— Aircraft 5**

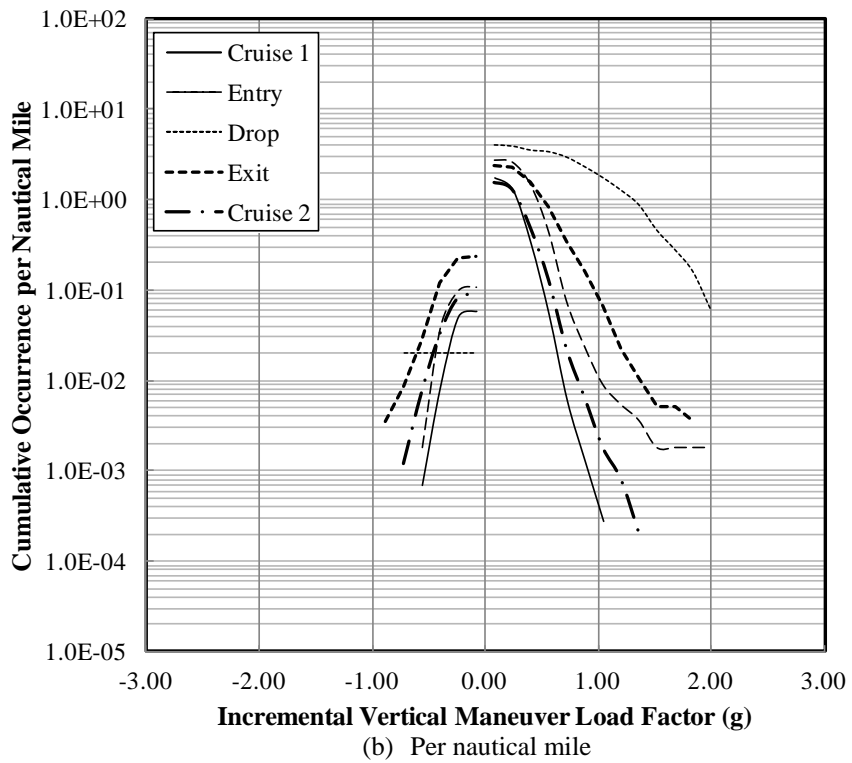
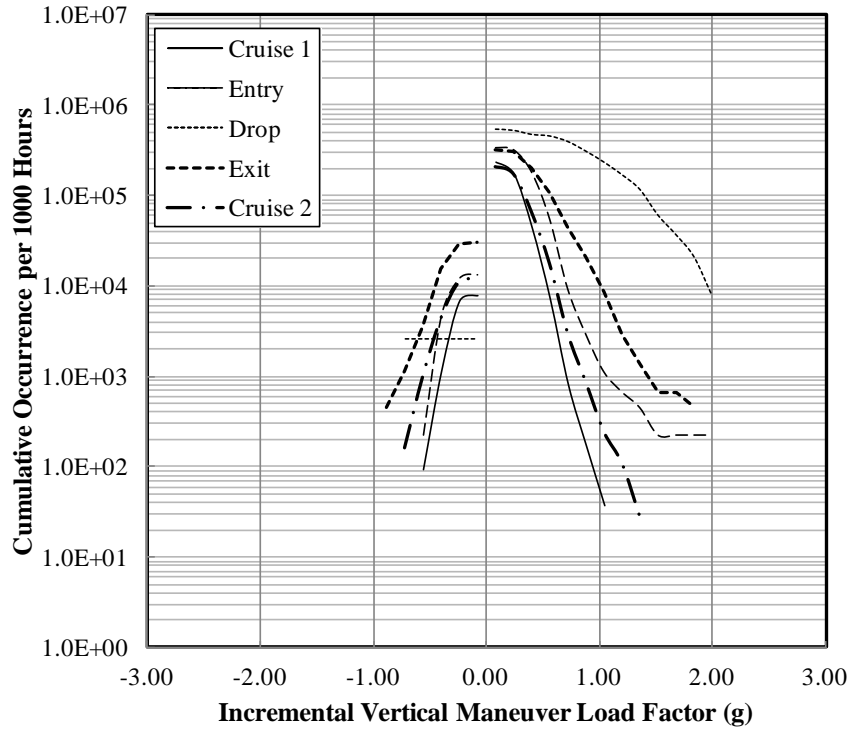


**Figure B-33. Cumulative occurrence of incremental maneuver vertical load factor— Aircraft 1**

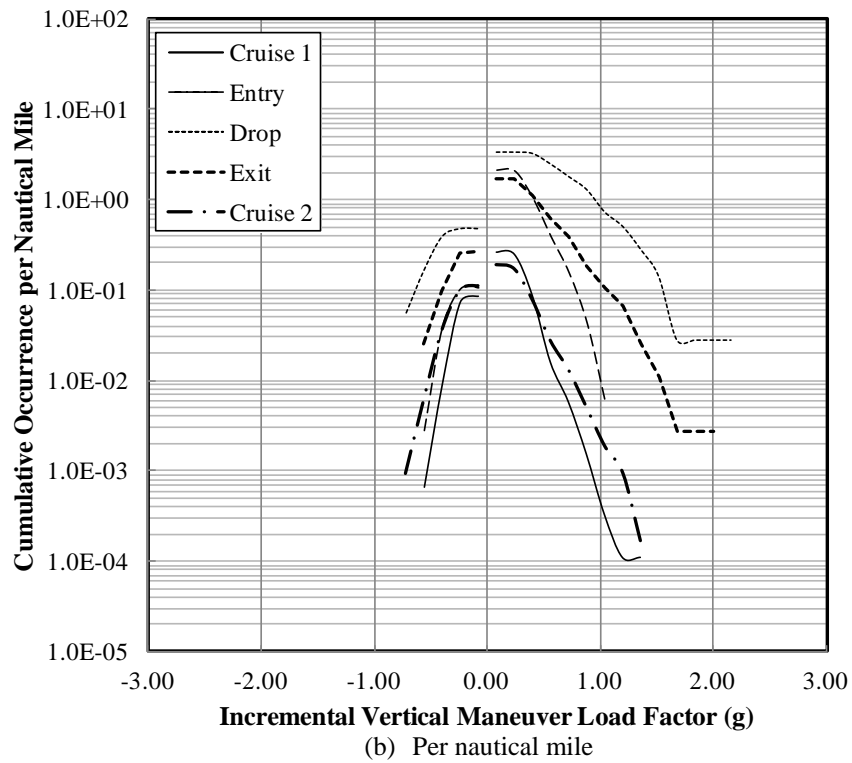
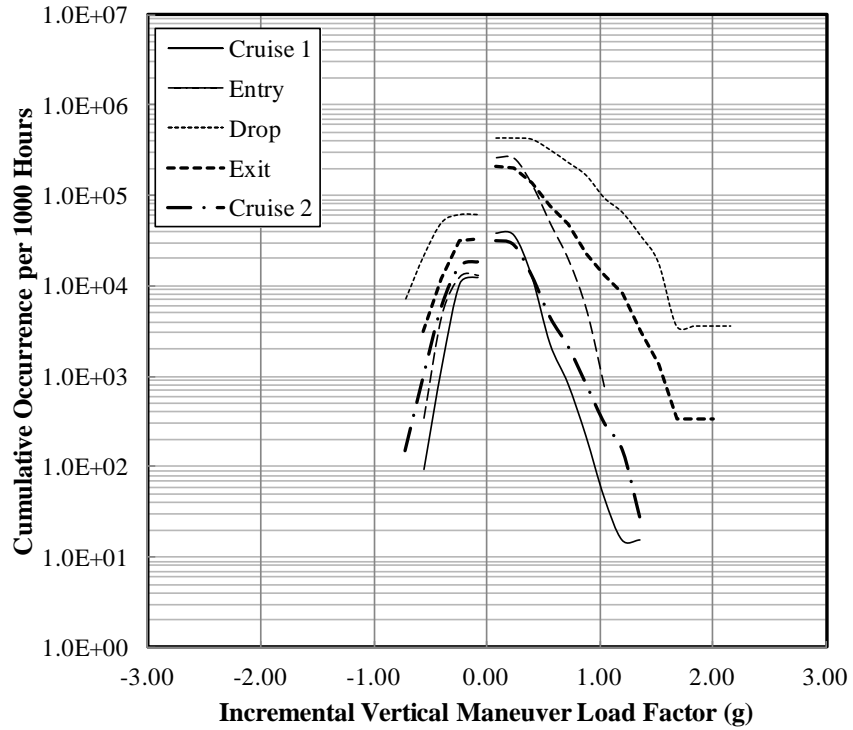


**Figure B-34. Cumulative occurrence of incremental maneuver vertical load factor— Aircraft 2**

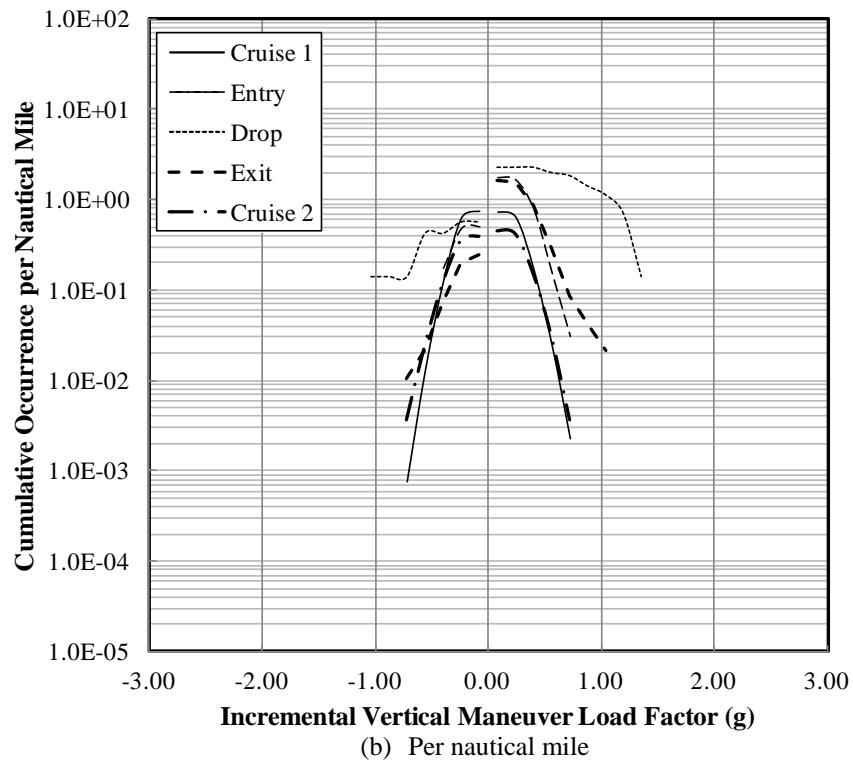
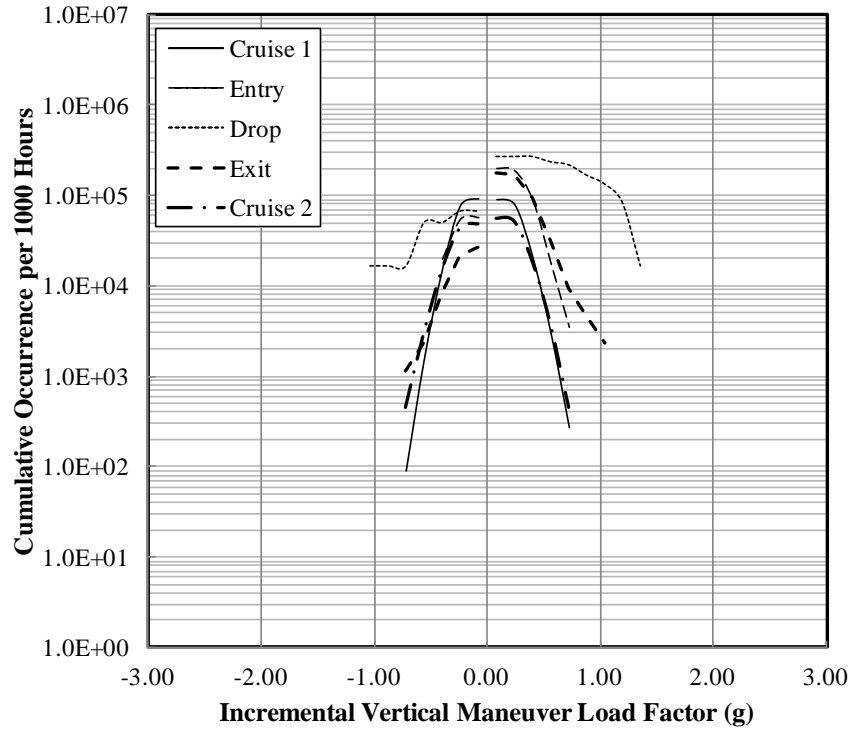


**Figure B-35. Cumulative occurrence of incremental maneuver vertical load factor— Aircraft 3**

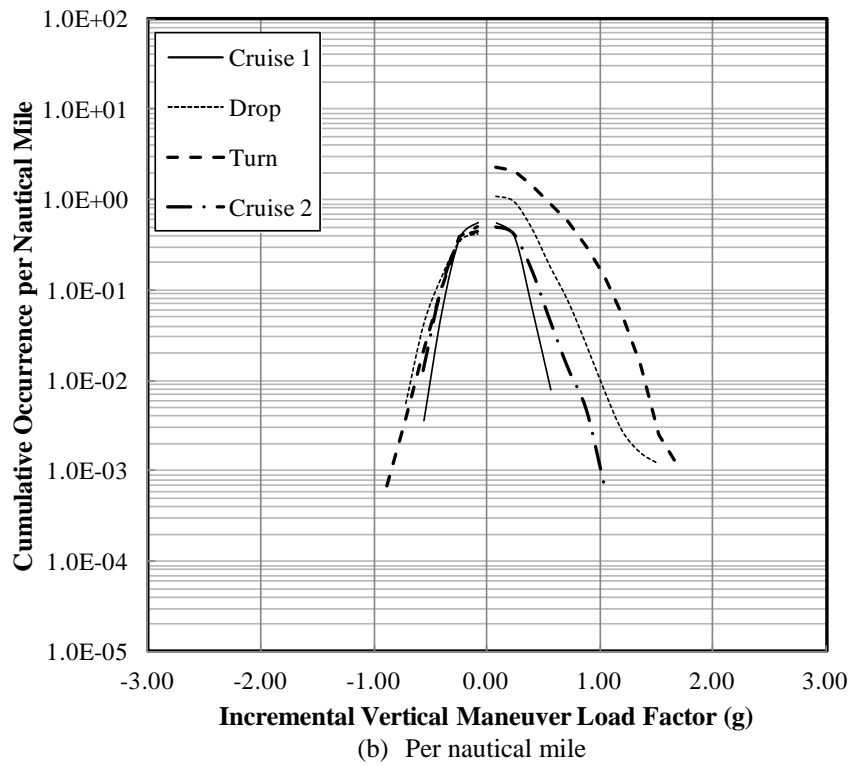
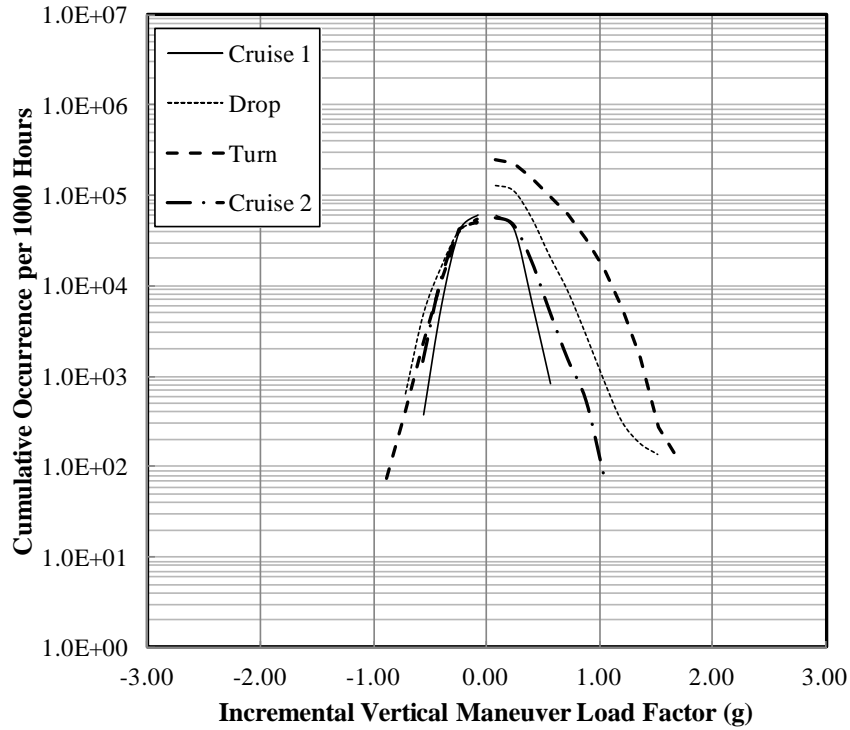
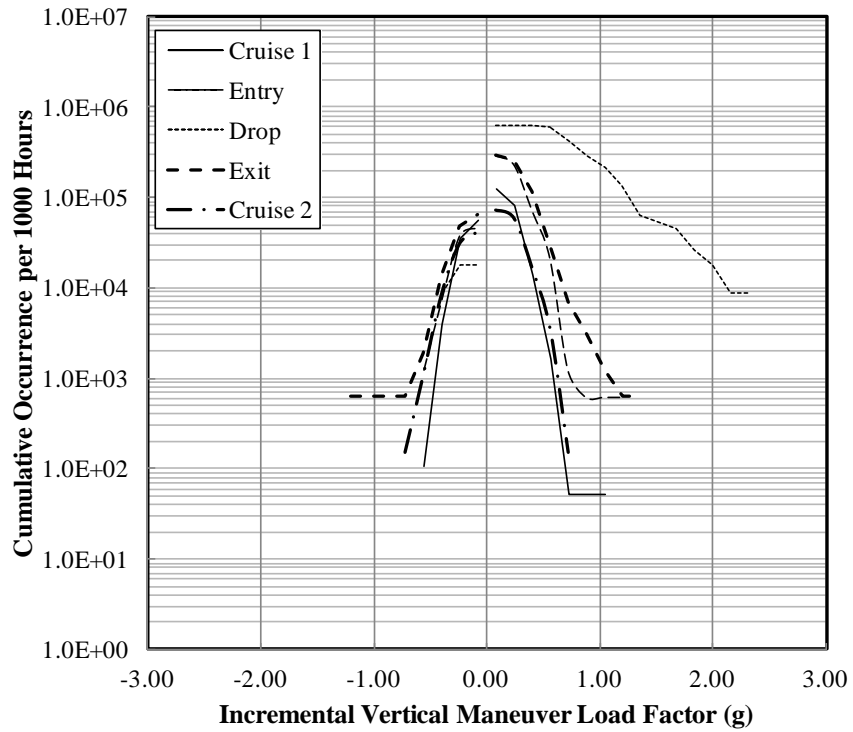
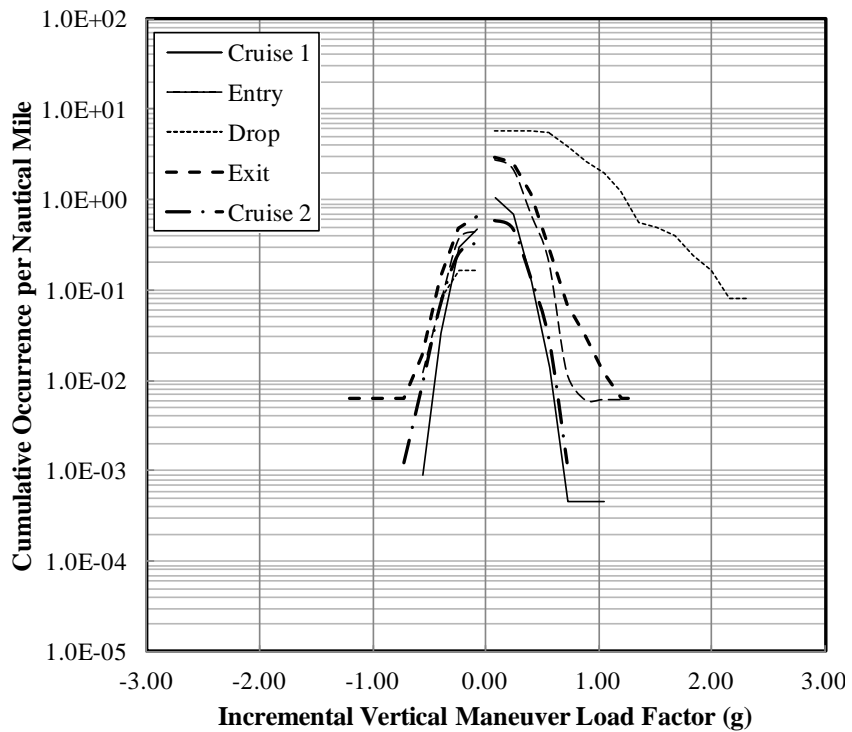


**Figure B-36. Cumulative occurrence of incremental maneuver vertical load factor—Aircraft 4**



(a) Per 1000 hours



(b) Per nautical mile

**Figure B-37. Cumulative occurrence of incremental maneuver vertical load factor—Aircraft 5**

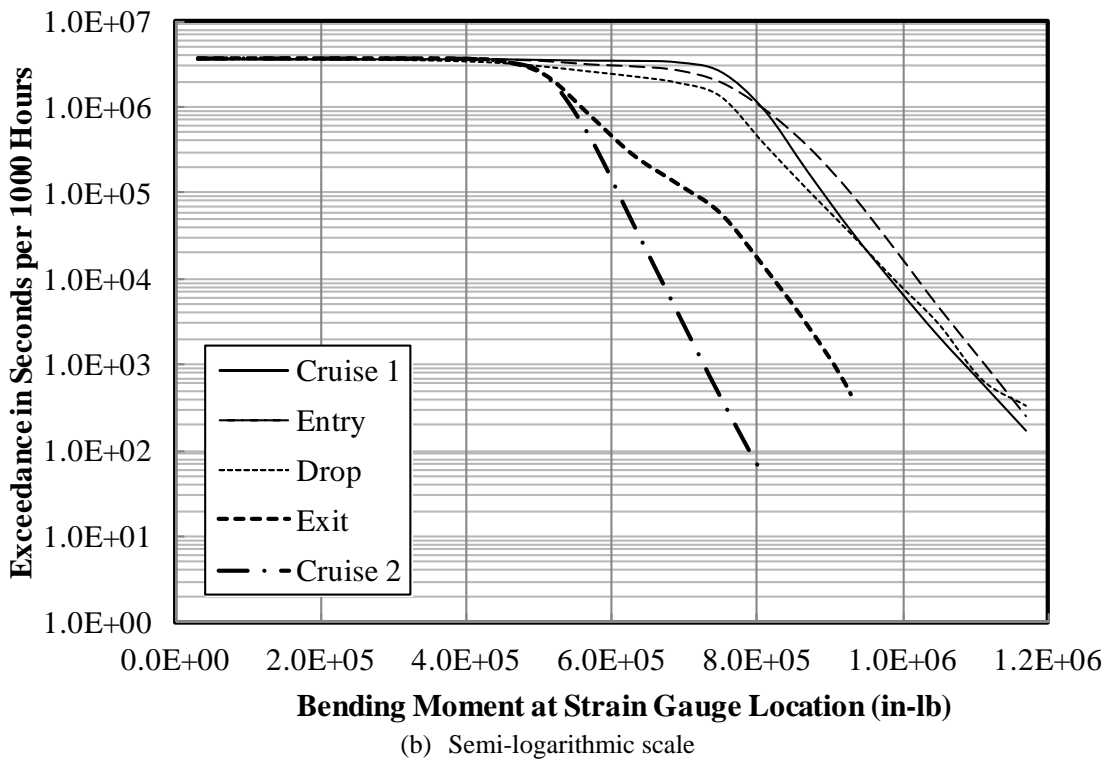
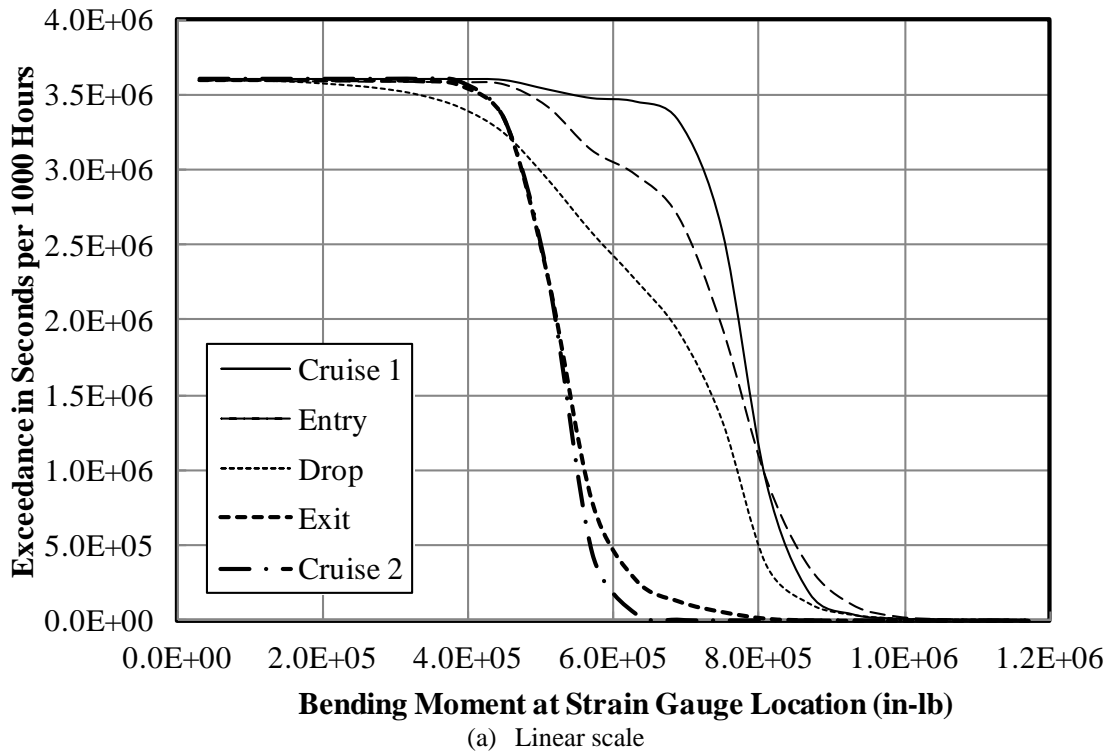


**Figure B-38. Exceedance in seconds of maximum bending moment per 1000 hours—Aircraft 1**

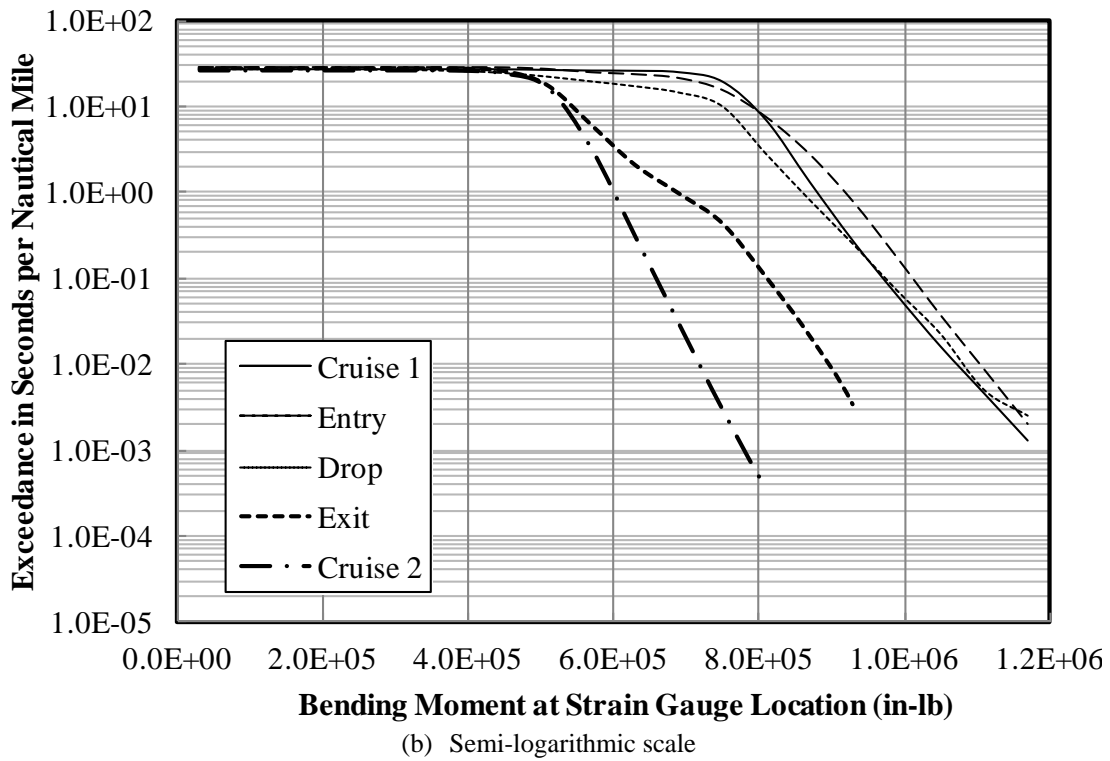
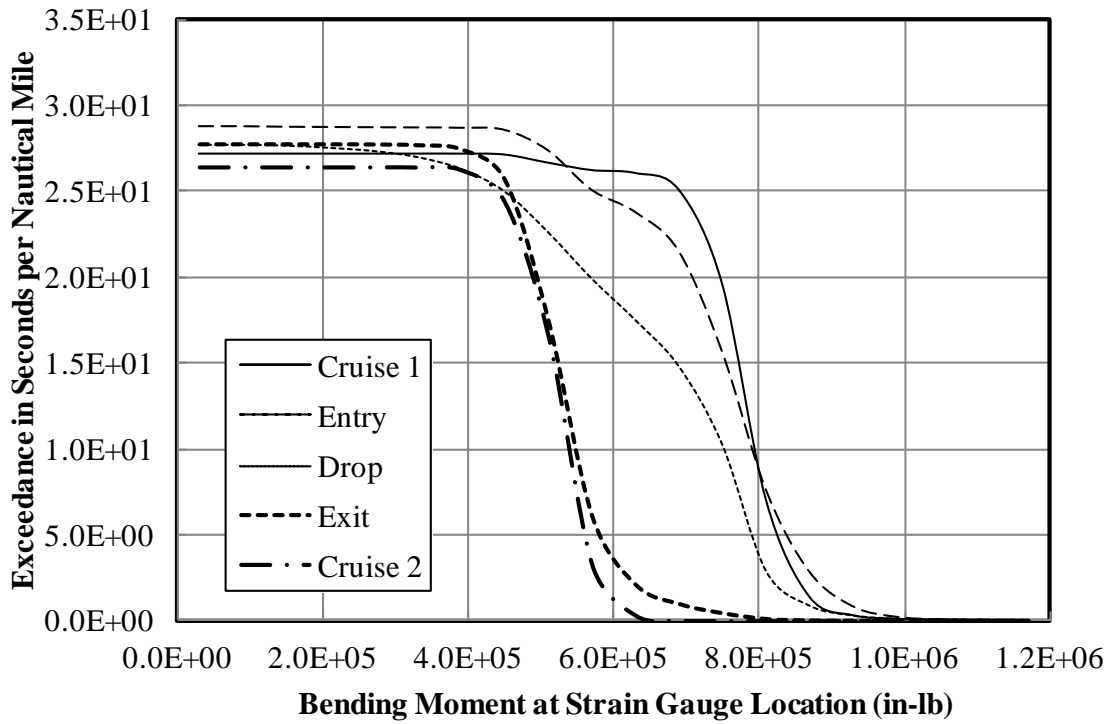
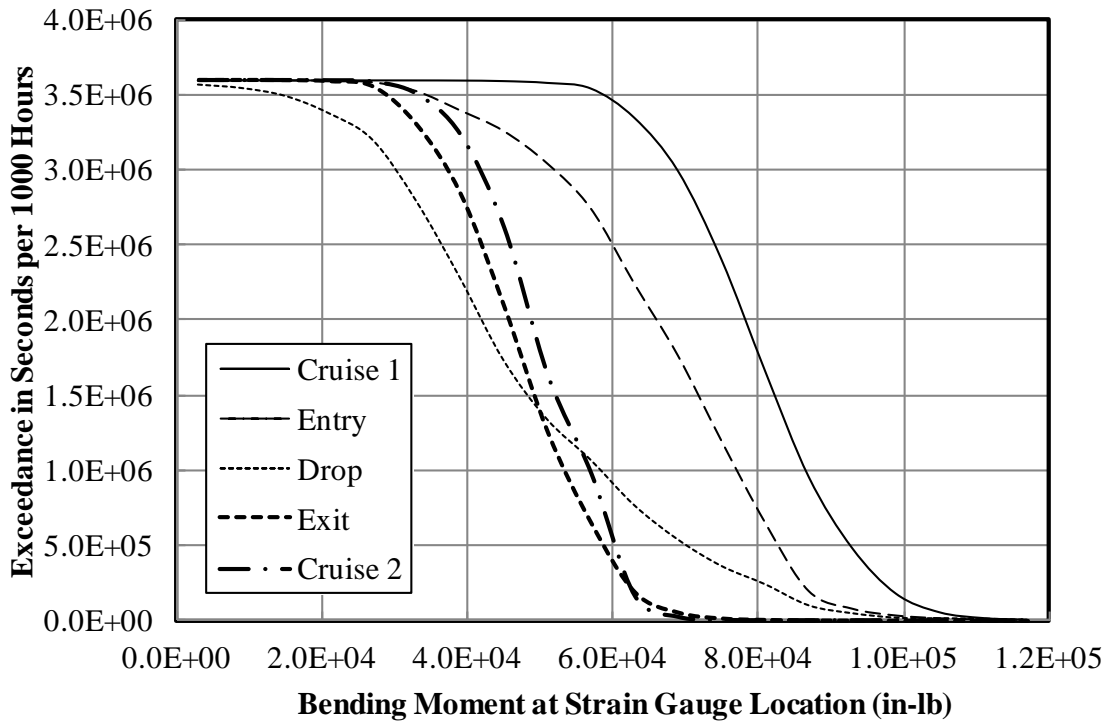
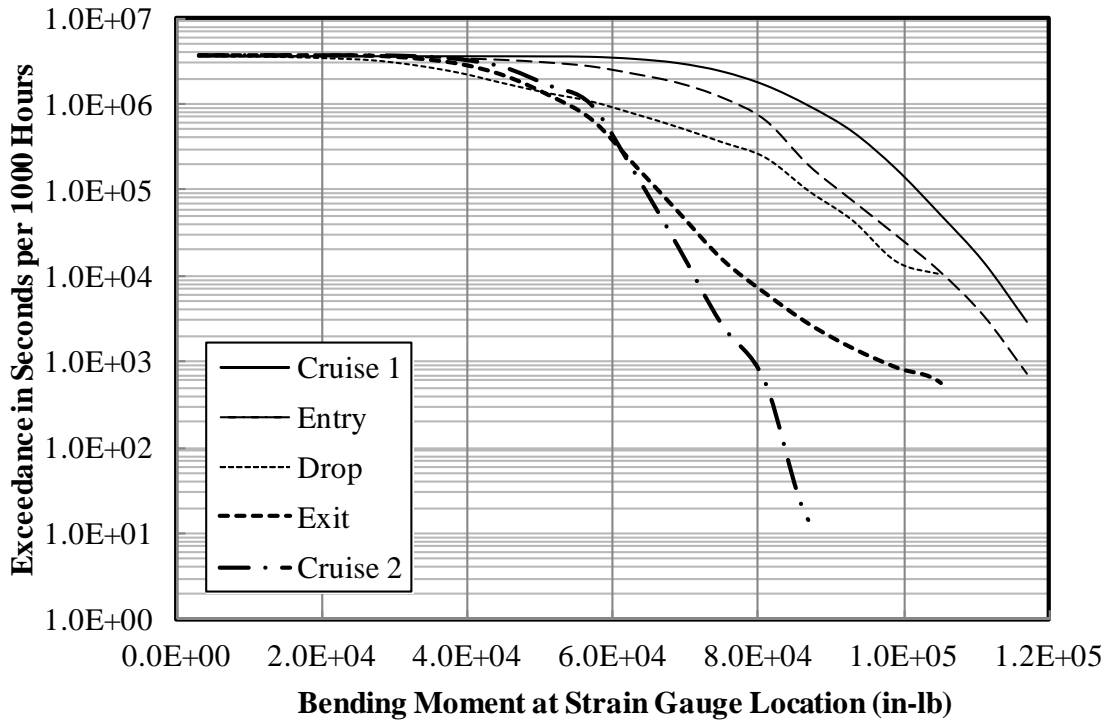


**Figure B-39. Exceedance in seconds of maximum bending moment per nautical mile— Aircraft 1**

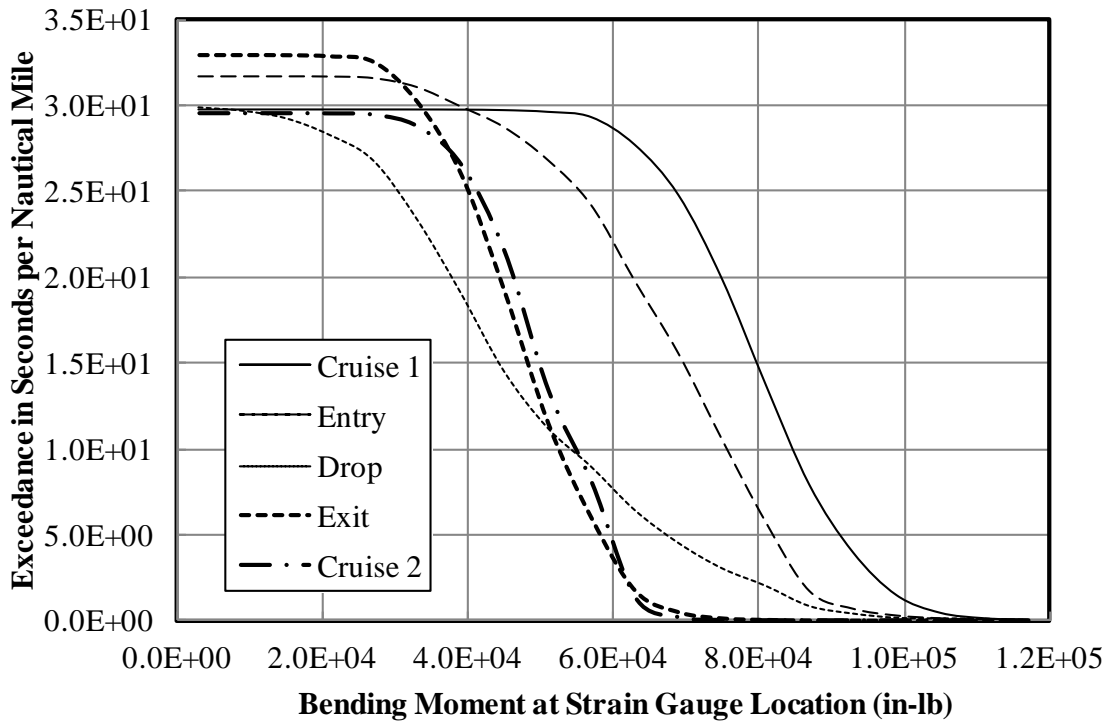


(a) Linear scale

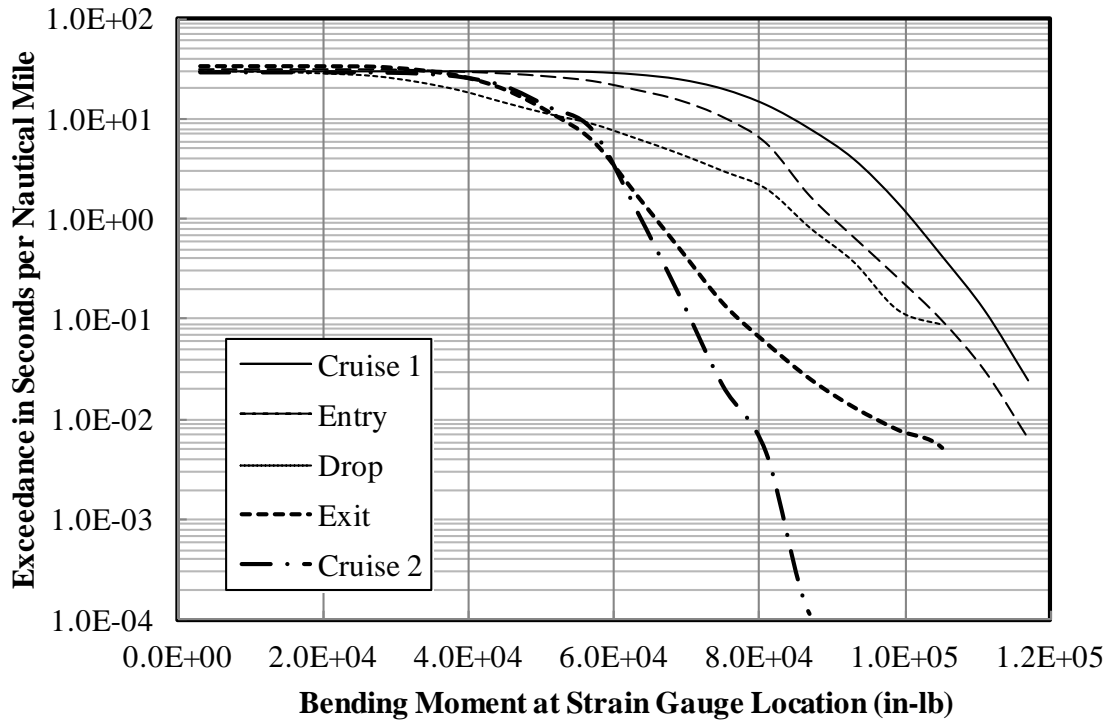


(b) Semi-logarithmic scale

**Figure B-40. Exceedance in seconds of maximum bending moment per 1000 hours—  
Aircraft 3**

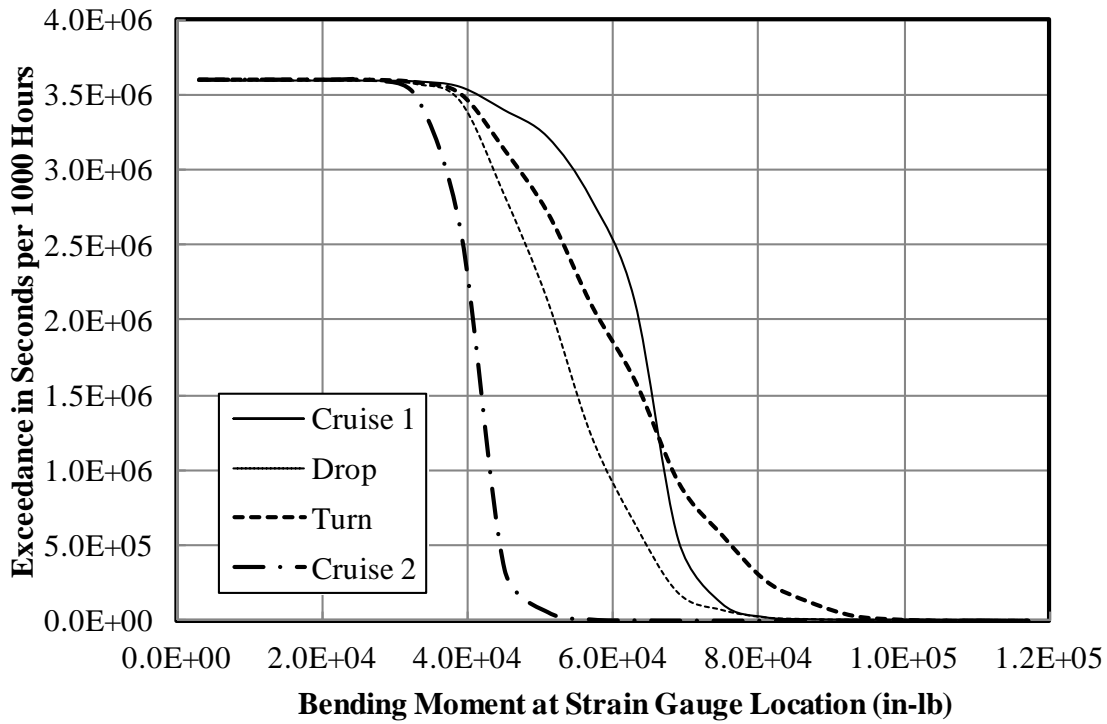


(a) Linear scale

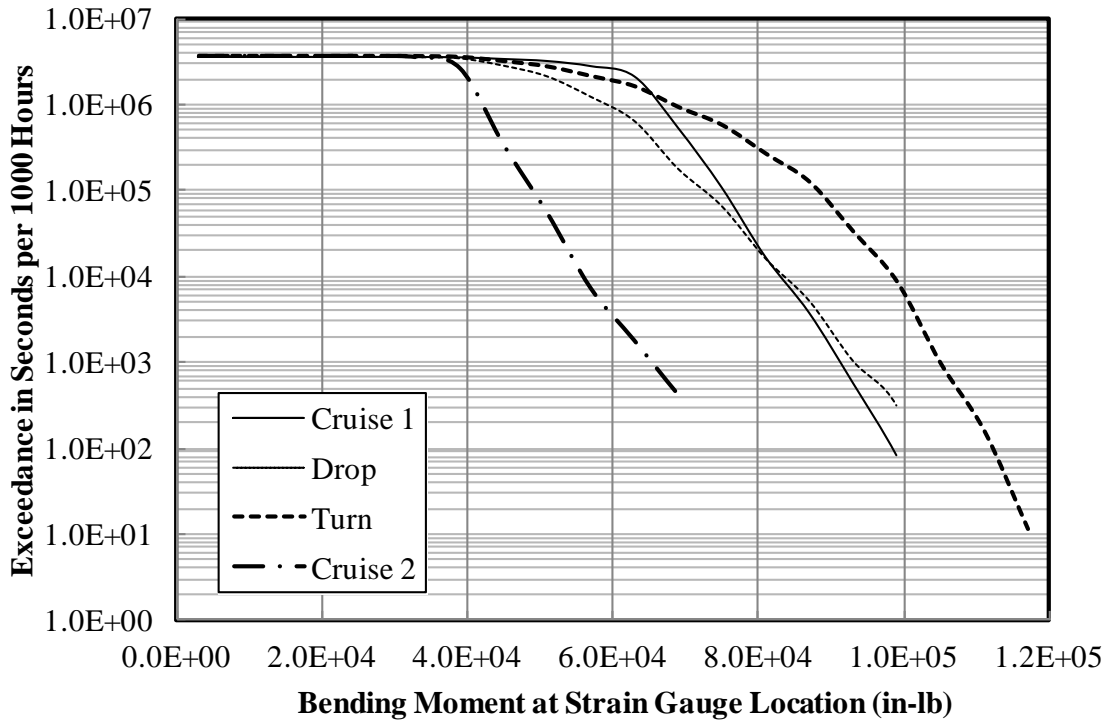


(b) Semi-logarithmic scale

**Figure B-41. Exceedance in seconds of maximum bending moment per nautical mile—  
Aircraft 3**



(a) Linear scale



(b) Semi-logarithmic scale

**Figure B-42. Exceedance in seconds of maximum bending moment per 1000 hours—  
Aircraft 4**

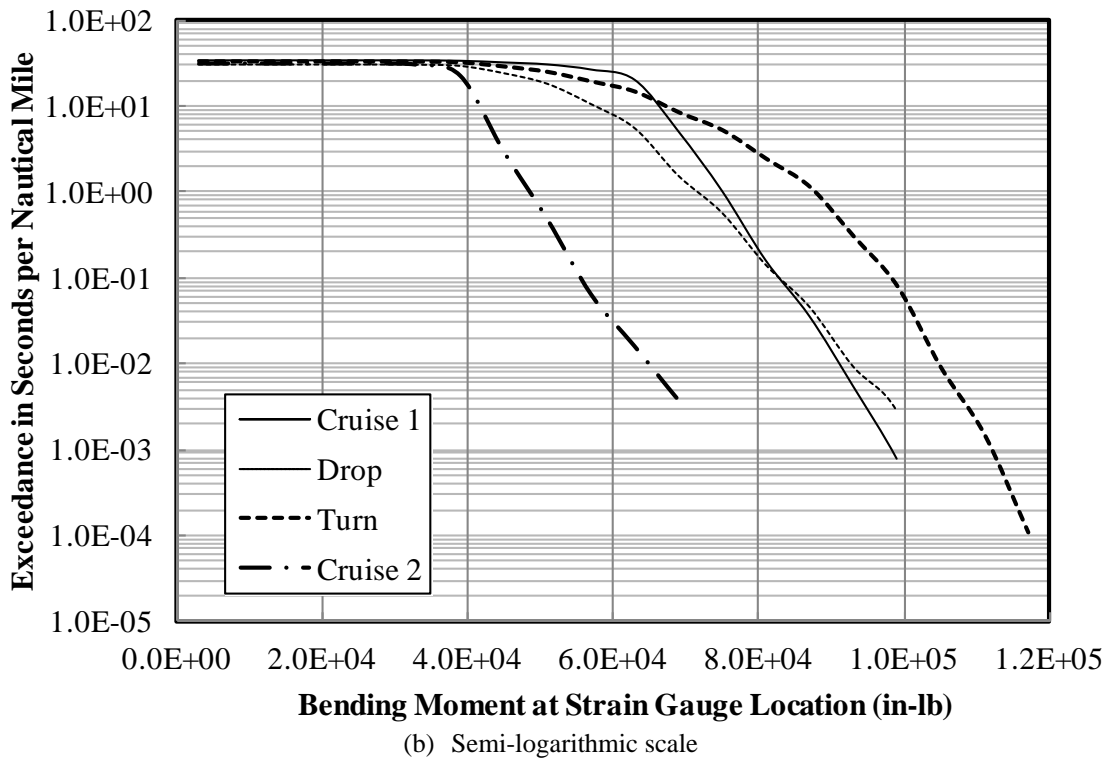
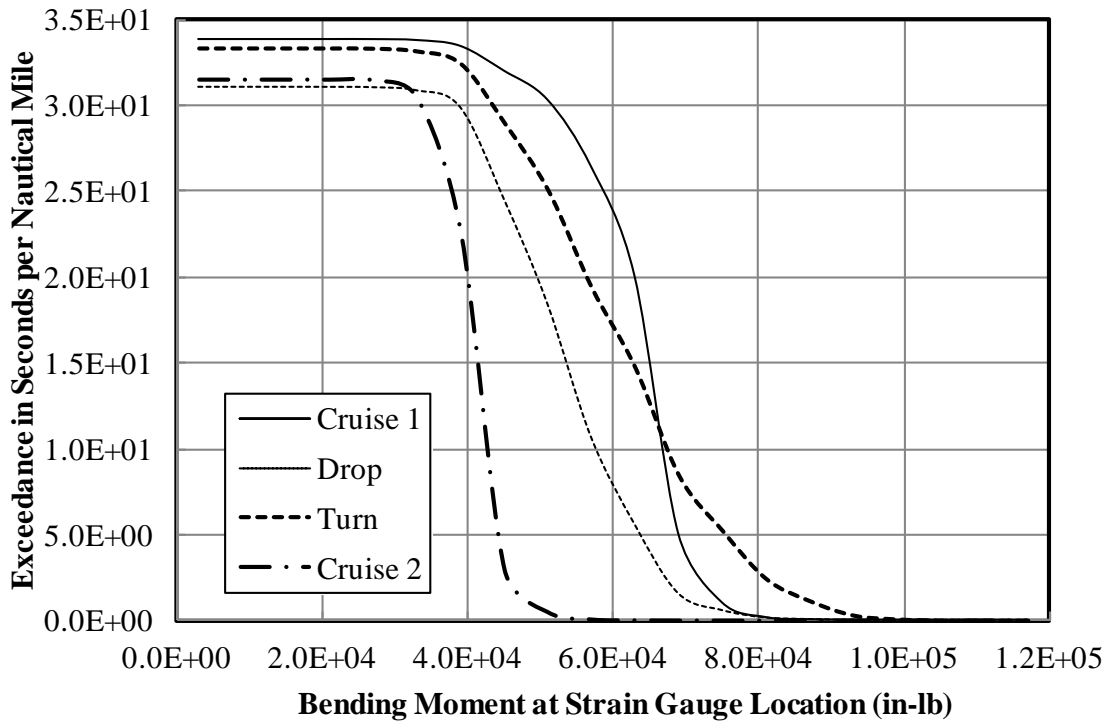


**Figure B-43. Exceedance in seconds of maximum bending moment per nautical mile—  
Aircraft 4**